Bio-based polyamide and poly(hydroxy urethane) coating resins : synthesis, characterization, and properties

Document status and date:
Published: 18/11/2015

Document Version:
Publisher's PDF, also known as Version of Record (includes final page, issue and volume numbers)

Please check the document version of this publication:

• A submitted manuscript is the version of the article upon submission and before peer-review. There can be important differences between the submitted version and the official published version of record. People interested in the research are advised to contact the author for the final version of the publication, or visit the DOI to the publisher's website.
• The final author version and the galley proof are versions of the publication after peer review.
• The final published version features the final layout of the paper including the volume, issue and page numbers.

Link to publication

Download date: 17. Nov. 2023

Bio-based polyamide and poly(hydroxy urethane) coating resins:

synthesis, characterization and properties

Juliën L.J. van Velthoven

Bio-based polyamide and poly(hydroxy urethane) coating resins

Synthesis, characterization, and properties

PROEFSCHRIFT

ter verkrijging van de graad van doctor aan de Technische Universiteit Eindhoven, op gezag van de rector magnificus prof.dr.ir. F.P.T. Baaijens, voor een commissie aangewezen door het College voor Promoties, in het openbaar te verdedigen op woensdag 18 november 2015 om 16:00 uur

door

Juliën Lambertus Jozephus van Velthoven

geboren te Boxtel

Dit proefschrift is goedgekeurd door de promotoren en de samenstelling van de promotiecommissie is als volgt:

voorzitter:	prof.dr.ir. J.C. Schouten
1e promotor:	prof.dr. J. Meuldijk
copromotor:	dr.ir. B.A.J. Noordover
leden:	prof.dr. H. Cramail (Université de Bordeaux)
	prof.dr. K.U. Loos (Rijksuniversiteit Groningen)
	prof.dr. R.A.T.M. van Benthem
	dr.ir. A.R.A. Palmans
adviseur:	dr. D.S. van Es (Wageningen UR Food & Biobased Research)

Het onderzoek of ontwerp dat in dit proefschrift wordt beschreven is uitgevoerd in overeenstemming met de TU/e Gedragscode Wetenschapsbeoefening

Table of contents

Coatings from bio-based amorphous polyamides

Poly(hydroxy urethane)s based on diglycerol dicarbonate

Glossary

^{1}H-NMR		proton nuclear magnetic resonance spectroscopy
^{13}C-NMR		carbon-13 nuclear magnetic resonance spectroscopy
α		alfa elongation, bearing a secondary hydroxyl
β		beta elongation, bearing a primary hydroxyl
δ	[ppm]	chemical shift
ΔH_c	[J g^{-1}]	enthalpic heat of crystallization
ΔH_m	[J g^{-1}]	enthalpic heat of melting
γ	[-]	strain
ω	[rad s^{-1}]	angular frequency
AmV	[mmol g^{-1}]	amine value
AV	[mmol g^{-1}]	acid value
BDA		butane-1,4-diamine
CA		citric anhydride
CDCl$_3$		deuterated chloroform
cryoSEM		cryogenic scanning electron microscopy
cryoTEM		cryogenic transmission electron microscopy
CV	[mmol g^{-1}]	carbonate value
D	[m]	particle diameter
$Đ$	[-]	dispersity index
DGC		diglycerol dicarbonate
DLS		dynamic light scattering
DMAc		*N,N*-dimethylacetamide
DMF		*N,N*-dimethylformamide
DMPA		dimethylolpropionic acid (2,2-bis(hydroxymethyl)propionic acid)
DMSO		dimethylsulfoxide
DP	[-]	degree of polymerization
DSC		differential scanning calorimetry
η	[mPa s]	viscosity
$\eta^\star$	[mPa s]	complex viscosity
FAD		dimerized fatty acid
FDA		dimerized fatty acid diamine
FT-IR		Fourier transform infrared spectroscopy
G'	[Pa]	elastic modulus
G''	[Pa]	loss modulus
gCOSY		gradient correlation spectroscopy
gHMBC		gradient heteronuclear multiple-bond correlation spectroscopy

gHSQC		gradient heteronuclear single-quantum coherence spectroscopy
HFIP		1,1,1,3,3,3-hexafluoro-2-propanol
IIDA		isoididediamine
		(2,5-diamino-2,5-dideoxy-1,4-3,6-dianhydroiditol)
m	[g]	mass
M_n	[g mol^{-1}]	number-average molecular weight
NDA		nonane-1,9-diamine
NMP		*N*-methylpyrrolidone
NMR		nuclear magnetic resonance spectroscopy
p	[Pa]	pressure
PA		pimelic acid (heptanedioic acid)
p_c	[-]	critical point of conversion, gel point
PDA		pentane-1,5-diamine
PHU		poly(hydroxy urethane)
PMMA		polymethylmethacrylate
$pOHV$	[mmol g^{-1}]	hydroxyl value for primary hydroxyls
Primid (XL-552)		*N,N,N',N'*-tetrakis(2-hydroxyethyl) adipamide
PS		polystyrene
PSD	[-]	particle size distribution
PUD		polyurethane dispersion
r	[-]	stoichiometric ratio
SA		succinic anhydride
SEC		size exclusion chromatography
SNR	[-]	signal-to-noise ratio
$sOHV$	[mmol g^{-1}]	hydroxyl value for secondary hydroxyls
tan δ	[-]	phase angle, calculated from G"/G'
T	[°C]	temperature
T_c	[°C]	crystallization temperature
TEA		triethylamine
T_g	[°C]	glass transition temperature
TGA		thermal gravimetric analysis
TGIC		tris(2,3-epoxypropyl) isocyanurate
T_m	[°C]	melting temperature
TMS		tetramethylsilane
VOC		volatile organic compounds
X_{feed}	[-]	chemical composition of the feed
WAXD		wide angle X-ray diffraction

Summary

'Bio-based polyamide and poly(hydroxy urethane) coating resins: synthesis, characterization and properties'

The demand for polymeric materials based on renewable resources is increasing. This doctoral thesis is focused on the development of novel bio-based coating resins for application in environmentally benign powder coatings and water-borne coatings.

Resins used in powder coatings should be amorphous polymers with a number-average molecular weight (M_n) value below 6,000 g mol^{-1}, and have a glass transition temperature (T_g) exceeding 50 °C. The strategy chosen is based on the hydrolytic stability and chain stiffness of polyamides. Normally, polyamides are highly crystalline materials. However, by blending odd- and even-numbered monomers and by incorporating rigid monomers, amorphous resins with a sufficiently high T_g can be prepared.

Pimelic acid, which has an odd number of carbon atoms (7), was reacted with mixtures of 1,4-butane diamine (**BDA**) and the rigid isoidide diamine (**IIDA**) to produce partially bio-based polyamides with the potential to become fully bio-based. Neat polyamide-4,7 had a T_g value of 65 °C, but the polymer was highly crystalline. When increasing the **IIDA** content, simultaneously the M_n value decreased from 5,000 to 1,000 g mol^{-1}, the crystallinity completely vanished and the T_g value increased to 102 °C for fully **IIDA**-based polyamides. Optimization of the polymerization procedure provided amorphous polyamides with M_n values of approximately 3,000 g mol^{-1} and T_g values of 65 to 70 °C. These polyamides have been cured with β-hydroxyalkylamides and epoxides onto aluminum panels. The coatings had excellent solvent resistance against acetone but poor resistance against ethanol. The coatings displayed good toughness upon deformation.

Bio-based isocyanate-free polyurethanes for water-borne polyurethane dispersions were synthesized using diglycerol dicarbonate and aliphatic diamines. The synthesis was performed without solvent and catalyst at moderate temperatures. Reaction of the five-membered cyclic carbonate group with primary amines proceeded

readily and polymers with M_n values up to 15,000 g mol^{-1} could be obtained. NMR spectroscopy has been applied to determine the composition and stereochemistry of the resulting polymers. DSC analysis of the poly(hydroxy urethane)s (PHU) indicates that amorphous polymers are obtained, regardless of the diamine used. This finding is attributed to the presence of both primary and secondary hydroxyl groups, which are formed randomly along the polymer backbone during the ring-opening of the cyclic carbonate.

PHUs based on fatty acid diamine (**FDA**) and **BDA** in a molar ratio of 3:7 were synthesized to be applied in water-borne dispersions. The hydroxyl groups present along the PHU backbone were reacted with succinic anhydride to provide pendent carboxylic acid groups. Triethylamine was added to neutralize the carboxylic acid groups, facilitating anionic stabilization of the aqueous dispersions. This method resulted in stable PHU dispersions with solid contents up to 20 wt%. These dispersions displayed particle sizes ranging from 200 nm to several micrometers and zeta potential values near -40 mV in the *pH* range between 6 and 8. Over time, the ester bonds of the pendent carboxylic acid groups hydrolyzed, releasing succinic acid from the particles and hence reducing the ionic stabilization. Electron microscopy images indicated that besides the targeted solid polymer particles, separation of **FDA**- and **BDA**-rich phases led to dissolved polymers and bilayer structures.

In summary, bio-based polyamides as well as bio-based non-isocyanate polyurethanes have been synthesized successfully and carefully characterized. These polymers are promising materials to replace currently applied coatings resins based on fossil raw materials.

Summary

Samenvatting

'Biobased polyamide en poly(hydroxy urethaan) verfharsen: synthese, karakterisering en eigenschappen'

Er is een toenemende vraag naar polymere materialen die worden geproduceerd uit duurzame natuurlijke grondstoffen. Dit proefschrift richt zich op de ontwikkeling van biobased binderharsen die toegepast kunnen worden in poederlakken en watergedragen verf. Deze coatingmethoden zijn beiden minder belastend zijn voor het milieu dan traditionele verven op basis van organische oplosmiddelen.

De harsen die gebruikt worden in poedercoatings zijn veelal amorfe polymeren met een lage molaire massa (minder dan 6000 g mol⁻¹) en een glasovergangstemperatuur (T_g) die hoger is dan 50 °C. Om aan deze eisen te voldoen is gekozen voor polyamides. Deze zijn redelijk bestand tegen hydrolyse en hebben een stijve polymeerketen. Polyamides zijn vaak zeer kristallijne materialen. Door gebruik te maken van monomeren met een oneven aantal koolstofatomen alsmede starre monomeren, kunnen amorfe harsen worden geproduceerd met een T_g die hoog genoeg is.

Om gedeeltelijk biobased polyamides te produceren zijn syntheses uitgevoerd met pimelinezuur, dat een oneven aantal koolstofatomen (7) heeft, en een mengsel van 1,4-butaandiamine (**BDA**) en het stijve isoididediamine (**IIDA**). In de toekomst kunnen deze monomeren en daarmee de polyamides, waarschijnlijk volledig duurzaam worden geproduceerd. Zuiver polyamide-4,7 heeft een T_g waarde van 65 °C. Dit polymeer heeft echter een zeer hoge kristalliniteit. Door **IIDA** aan de samenstelling van het polymeer toe te voegen ging de molaire massa weliswaar omlaag van 5000 naar 1000 g mol⁻¹, maar tegelijkertijd verdween de kristalliniteit en ging de T_g waarde omhoog tot een maximum van 102 °C. Optimalisatie van de synthese resulteerde in amorfe polyamides met een molaire massa van ongeveer 3000 g mol⁻¹ en T_g waarden tussen 65 en 70 °C. Met deze polymeren werden coatings gemaakt op aluminium plaatjes door reactie met β-hydroxyalkylamides of met epoxides. De resulterende coatings waren uitstekend bestand tegen aceton maar werden op één coating na allemaal door ethanol aangetast. De coatings waren taai bij deformatie.

Biobased polyurethanen voor watergedragen verven werden geproduceerd zonder gebruik te maken van isocyanaten. Hiervoor werden bij relatief lage temperaturen reacties uitgevoerd met diglycerol dicarbonaat en diamines zonder gebruik te maken van oplosmiddelen of katalysatoren. Deze reacties resulteerden in polymeren met molaire massas van 15.000 g mol^{-1}. De chemische samenstelling en de stereochemie van deze poly(hydroxy urethanen) (PHU) werden vastgesteld met behulp van NMR spectroscopie. Thermische analyses lieten zien dat alle polymeren amorf waren, ongeacht de diamines gebruikt in de synthese. Dit wordt toegedicht aan de aanwezigheid van twee structurele elementen die willekeurig verspreid zijn over de lengte van de polymeerketens. Deze vormen zich tijdens de polymerisatie, als gevolg van de openen van de ringen in het diglycerol dicarbonaat monomeer.

Er zijn PHU gemaakt die zowel vetzuurdiamine (**FDA**) als **BDA** bevatten in een molverhouding van 3:7. Vrije zuurgroepen werden geïntroduceerd door barnsteenzuuranhydride met deze PHU te laten reageren. Deze groepen werden vervolgens geneutraliseerd met triethylamine. Hierdoor werd elektrostatische repulsie tussen de deeltjes in een olie-in-water dispersie mogelijk. Met deze PHU werden colloïdaal stabiele dispersies gemaakt met een vastestofgehalte tot 20 gew%. De deeltjesgroottes in de dispersies varieerden van 200 nanometer tot enkele micrometers. De ζ-potentiaal waarden waren rond de -40 millivolt bij *pH* waarden tussen 6 en 8. De esterbindingen die de zuurgroepen met de polymeren verbonden splitsten langzaam door hydrolyse met water. Zodoende kon het hierdoor gevormde barnsteenzuur uit de polymeerdeeltjes naar de waterfase diffunderen. Daardoor werd de elektrostatische stabilisatie minder goed voor oudere dispersies. Elektronenmicroscopie onthulde dat naast de beoogde vaste polymeerdeeltjes er ook andere structuren waren gevormd. Fasenscheiding van **FDA** en **BDA** tijdens de synthese zorgde ervoor dat zich ook hydrofiele polymeren vormden die oplosten in het water, en amfifiele polymeren die bilagen vormden.

We kunnen concluderen dat zowel biobased polyamides als biobased isocyanaatvrije polyurethanen zijn geproduceerd en zorgvuldig geanalyseerd. Deze polymeren zijn veelbelovende materialen om de huidige harsen op basis van fossiele grondstoffen te vervangen.

XIV

Chapter 1

Introduction

1.1 Polyamides and polyurethanes

1.1.1 Polyamides

Polyamides (PAs) are an important class of polymers, which can be found in a broad range of products: automotive applications, electrical insulation, machinery, consumer goods, textiles & sportswear, ropes, films, packaging, and coatings. By definition, PAs are polymer chains in which the repeating units are connected by amide bonds. They are produced by Nature in the form of polypeptides, or synthetically by mankind. Polypeptides are based on amino acids and are linear chains. They constitute the basis of natural materials such as hair, wool, and collagen. Polypeptides can also fold in a specific orientation to form proteins, which are the advanced polymers necessary for life to exist. Proteins obtain their functionality from the structures into which they fold. Intramolecular interactions create secondary and tertiary structures, while intermolecular interactions lead to specific aggregation between proteins to form quaternary structures. A well-known example is hemoglobin for oxygen transport in the blood. To achieve these functional structures, Nature produces PAs with a high degree of complexity and precision from more than 20 different building blocks.[1] Synthetic PAs display much less chain complexity. The commercially most important PAs are made from just one monomer (PA 6) or two different monomers (PA 66). Nylon 66 (or PA 66) is the first example of a man-made PA, synthesized by the group of Carothers at DuPont in 1935.[2] Nowadays, the commercial name Nylon is used for linear aliphatic PAs, the numerical addition (66) indicates the number of carbon atoms in the diamine residue (6) followed by the number of carbon atoms in the diacid residue (6). Polyamides synthesized from amino- and carboxylic acid-functional monomers,
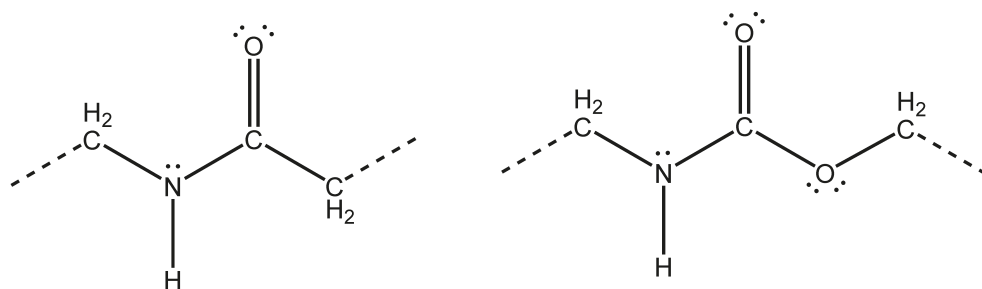
Figure 1.1 Amide bond (*left*) and urethane bond (*right*).
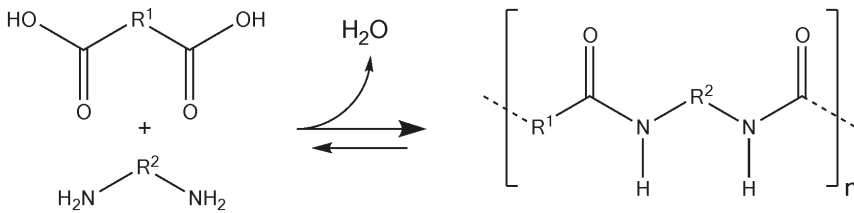
Figure 1.2 Polyamide synthesis from dicarboxylic acids and diamines.

e.g. PA 6 from caprolactam, only have one number that indicates the number of carbon atoms in the monomer residue.

The amide bond, as shown in Figure 1.1, provides characteristic properties to PAs. The C-N bond displays a pseudo double bond character as the nitrogen can donate an electron to the π-orbital to form a transition state with a double bond. Therefore, the amide bond can be considered to be a rigid bond. Another typical feature of amide bonds is the presence of both a hydrogen bond donor (N-H) and a hydrogen bond acceptor (C=O). As a result, amide bonds can form hydrogen bonds between polymer chains which are responsible for much stronger interactions between the chains. Because of these strong interactions, PAs are typically semi-crystalline materials, with high melting enthalpies and melting temperatures (T_m).

PAs can be synthesized through a condensation reaction as shown in Figure 1.2. When a carboxylic acid group and an amine group come into contact with each other, they can form the amide bond with the simultaneous release of a molecule of water. This reaction is an equilibrium reaction with K ≈ 10, indicating that at equilibrium there is roughly a ten-fold amount of amide groups compared to the carboxylic acid and amine groups. Polyamides are significantly more hydrolytically stable than polyesters (K ≈ 1). Besides amide synthesis from carboxylic acid groups, transamidation reactions can be performed through the reaction of an amine with an ester groups to form amide bonds, releasing an alcohol as condensate. For this reaction, the presence of a catalyst is usually required. To achieve high molecular weight PAs, the condensate has to be removed because of the equilibrium. This is commonly achieved by reducing the pressure towards the end of the reaction when the temperature is already high to maintain a polymer melt. Increasing the surface area of the melt aids the removal of the condensate.

1.1.2   Polyurethanes

Polyurethanes (PUs) have been reported first by Bayer in 1947.[3] PUs show a large similarity with polyamides. The repeat units are connected by urethane groups, which are also called carbamates. The urethane bond possesses an additional oxygen atom compared to the amide bond, as can be seen in Figure 1.1. The urethane group is also capable of forming hydrogen bonds, thus strengthening the interchain interactions. The additional oxygen atom in the urethane bond does cause some differences in properties. PUs are slightly less chemically resistant than PAs, yet PUs show more flexibility compared to a similar PA structure. PUs are generally prepared by reacting diisocyanates with diols (Figure 1.3). Commercial PUs are commonly based on a rigid aromatic diisocyanate combined with a flexible diol. This combination leads to the formation of rigid polymer segments that have a tendency to aggregate and/or crystallize (the so-called hard segments), and the formation of amorphous, flexible segments (the so-called soft segments). The combination of these segments in the polymer constitutes a thermoplastic material. Physical cross-links arising from the interaction between the hard segments give these materials their coherence and resistance against deformation (*i.e.* modulus), whereas the soft segments provide flexibility over a large temperature range. Upon heating, the hard segments dissociate and the polymer can be shaped through processing. During subsequent cooling, the hard segments reaggregate and/or recrystallize and the original morphology is recovered. Due to this unique property, a rubbery material is obtained which can be processed in the melt. Due to their diverse properties, PUs have applications as soft and rigid foams, adhesives, coatings, and elastomers.
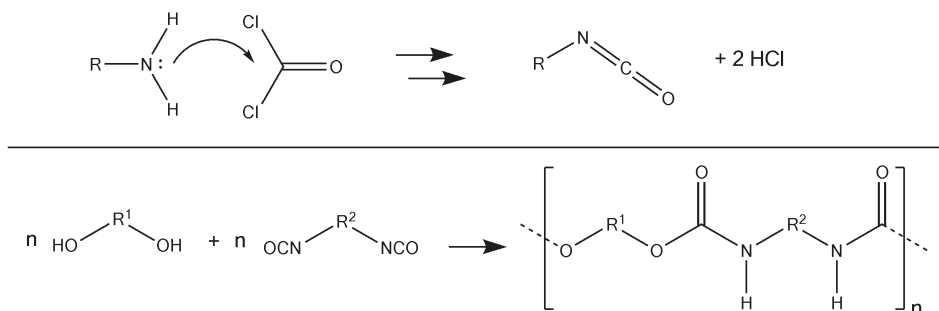
Figure 1.3   *Top*: **synthesis of isocyanates from an amine and phosgene.** *Bottom*: **Polyurethane synthesis from diisocyanates and diols.**

1.1.3 *Isocyanate-free synthetic routes to PUs*

Commonly accepted as the biggest issue in polyurethane technology is the use of isocyanates. Isocyanates are produced from the reaction between amines and highly toxic phosgene (Figure 1.3).[4] In addition to the hazardous production process, isocyanates themselves pose serious health risks. Besides short term effects like problematic breathing and skin and mucous membrane irritation, isocyanates are strongly sensitizing and long term exposure causes severe medical disorders, *e.g.* respiratory diseases. Note that isocyanates are potentially carcinogenic.[5] Furthermore, isocyanates are moisture sensitive. They react with water to form a carbamic acid which dissociates into an amine group and a CO_2 molecule. The amine will then react with another isocyanate to form an urea bond. Sufficient exposure to water will therefore decrease the isocyanate functionality and ultimately render a useless product.

Several pathways have been developed throughout the years to avoid the use of isocyanates, yet none of the published pathways is currently used for the large scale production of non-isocyanate polyurethanes (NIPU). Although carbamates
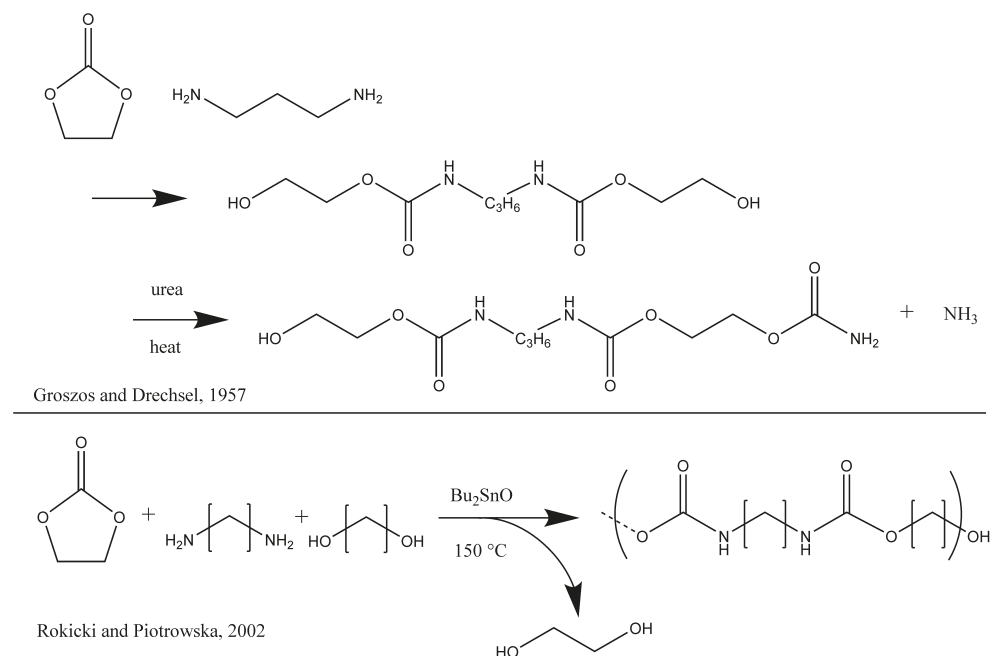
Figure 1.4 *Top*: The reaction of ethylene carbonate with diamine and the subsequent reaction of the polyol with urea by Groszos and Drechsel.[7] *Bottom*: Variation of final polymerization by Rokicki and Piotrowska.[8]

have already been prepared in a non-isocyanate fashion by Leopold and Paquin in the early 1930s[6], the first patent describing NIPUs dates 26 years later, see Groszos and Drechsel (Figure 1.4).[7] This non-isocyanate method uses the reaction between ethylene carbonate and a diamine to form a biscarbamate polyol which is extended by reaction with urea. Rokicki *et al*. published a very similar route using Bu_2SnO as catalyst for the final transurethanization reaction.[8]

At Union Carbide Corporation, another class of NIPU was developed by Whelan *et al*.[9] Cyclic carbonates are reacted with diamines to form poly(hydroxy urethane)s (PHUs). In the 1990s, this reaction regained much attention by the work of Endo *et al*.[10] These authors used bifunctional cyclic carbonates to produce a wide range of NIPUs (Figure 1.5 and Table 1.1).

The group of Höcker developed two cyclic monomer routes: one involves the use of cyclic urea and cyclic carbonate, the other starts from cyclic urethanes.[11–14] This elegant route provides high molecular weight polymers. The cyclic urethane was synthesized from amino alcohols with diphenyl carbonate.

Sharma *et al*. reported a very similar pathway to that used by the group of Höcker for the synthesis of NIPUs.[15–18] They synthesized a monomer bearing hydroxyl- and amino-functionality from caprolactone and a diamine, or from caprolactam and an amino alcohol. Using diphenyl carbonate, they converted the amine to a urethane with one phenyl end-group. The polymerization is performed with $Bu_2Sn(OCH_3)_2$ either on purified monomer or sequentially in a one-pot synthesis with removal of phenol.

Deepa and Jayakannan reported another similar route but using dimethyl carbonate. An aliphatic diamine is converted under strong basic conditions to its diurethane equivalent.[19] The diurethane could then be polymerized using a transurethane melt process with diols, catalyzed by titanium(IV) butoxide and removal of methanol. Number-average molecular weight (M_n) values up to 20,000 g mol^{-1} were obtained. Dimethyl carbonate could potentially be obtained from biomass and is therefore a good alternative to diphenyl carbonate.[20]

The use of carbonylbiscaprolactam (CBC) for the synthesis of urethane and urea groups was reported by Maier[21,22] CBC is reacted with hydroxyl groups without a catalyst, or in presence of the catalysts NaOMe or $Zr(OC_3H_7)_4$. Two competing reactions,
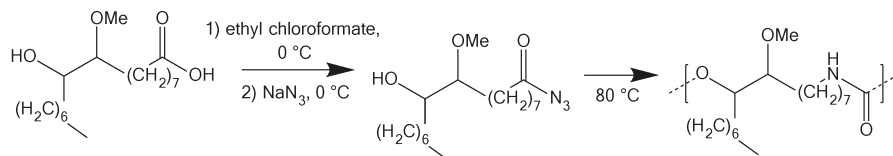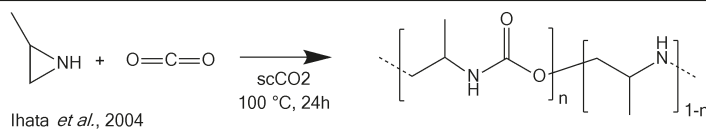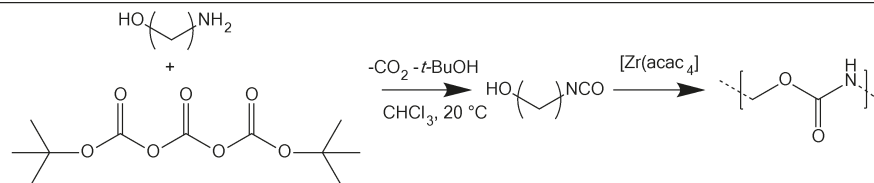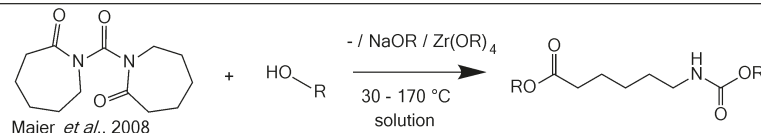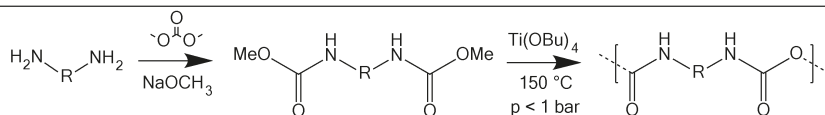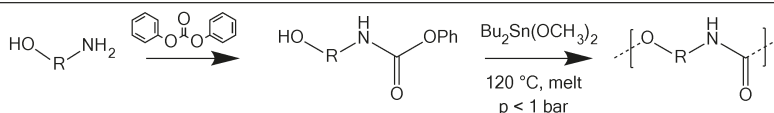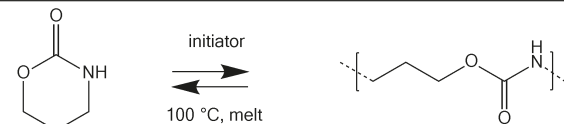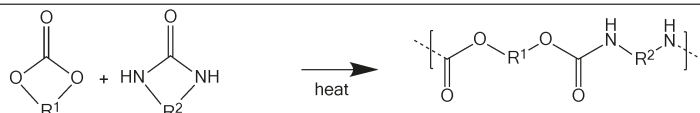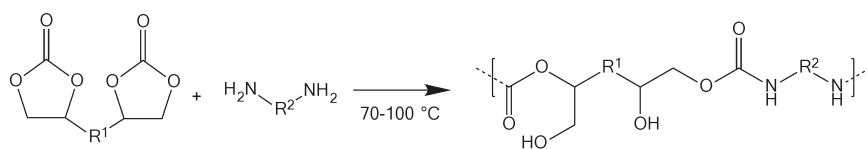
Figure 1.5   NIPU reactions: Kihara and Endo[10]; Schmitz[11]; Neffgen[12–14]; Sharma[15–17]; Deepa and Jayakannan[19]; Maier[21]; Versteegen[23]; Ihata[24]; More and Palaskar[25–27].

ring-opening and ring-elimination, lead to the formation of five different products. The study focused on the effects of the catalyst and the reaction temperature on the ratio of these products. The research by Maier *et al.* can yield NIPU by either driving the reaction towards poly(ester urethane)s, or the sequential addition of amine- and hydroxyl-functional monomers to synthesize caprolactam-blocked isocyanates in the first step and polymerize these in the second step.

Although strictly speaking not a NIPU, the route postulated by Versteegen *et al.* is a good option as the starting compounds are safe. The reaction of an amino alcohol with di-tert-dibutyl tricarbonate yields an *in-situ* isocyanate group which can be polymerized with the remaining hydroxyl. In this route, the exposure to isocyanates is very limited.[23]

An interesting route utilizes CO_2 as monomer. Ihata *et al.* investigated the reaction of CO_2 with aziridines under supercritical conditions to limit the inherent homopolymerization of the aziridine.[24] These authors managed to increase the amount of urethane links for this reaction from 30% to 74% with respect to the amine links originating from the homopolymerization.

More and Palaskar produced NIPUs from fatty acid materials.[25–27] Both routes use a self-condensation approach of acyl azide with hydroxyl groups. Palaskar reports the use of the double bond in methyl oleate for epoxidation and subsequent ring-opening with methanol to yield a methoxy group and an alcohol. More uses thiol-ene chemistry with 2-mercaptoethanol to introduce the hydroxyl functionality. Subsequently, the ester bond is hydrolyzed and the resulting carboxylic acid is converted to the acyl azide by ethyl chloroformate and sodium azide treatment. The NIPUs can then be prepared in solution or bulk at moderate temperatures of 60 to 80 °C. A point of attention is the use of chloroformates and azides, both are harmful chemicals.

Another route is to prepare urethane-bearing monomers and to couple these monomers through other types of chemistry. Calle *et al.* prepared such a urethane-based monomer using chloroformates and subsequently used thiol-ene chemistry to polymerize poly(thioether urethane)s.[28] Again, the use of chloroformates is undesirable.

1.1.4   Poly(hydroxy urethane)s
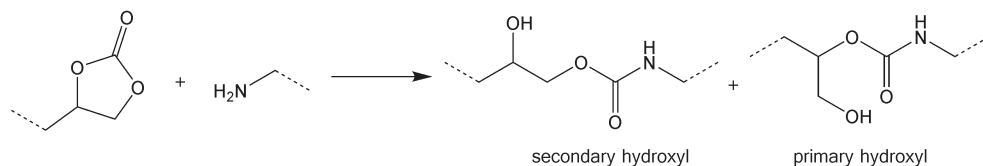
Figure 1.6 **Formation of primary and secondary hydroxyl groups in poly(hydroxy urethane)s by the reaction of a cyclic carbonate and an amine**

The reaction between bifunctional cyclic carbonates and a diamine results in poly(hydroxy urethane)s as shown in Figure 1.6. These polymers bear an additional
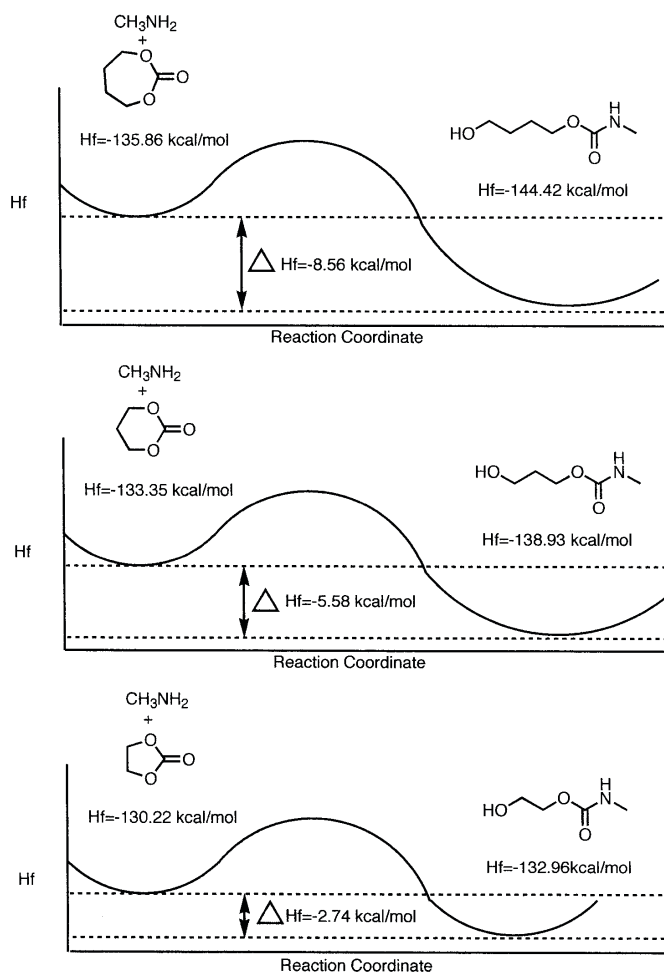
Figure 1.7 **Heat of formation for the reactants and products of the reactions of seven-, six-, and five-membered cyclic carbonates with methylamine. Reprinted from reference[35] with permission of the copyright owner.**
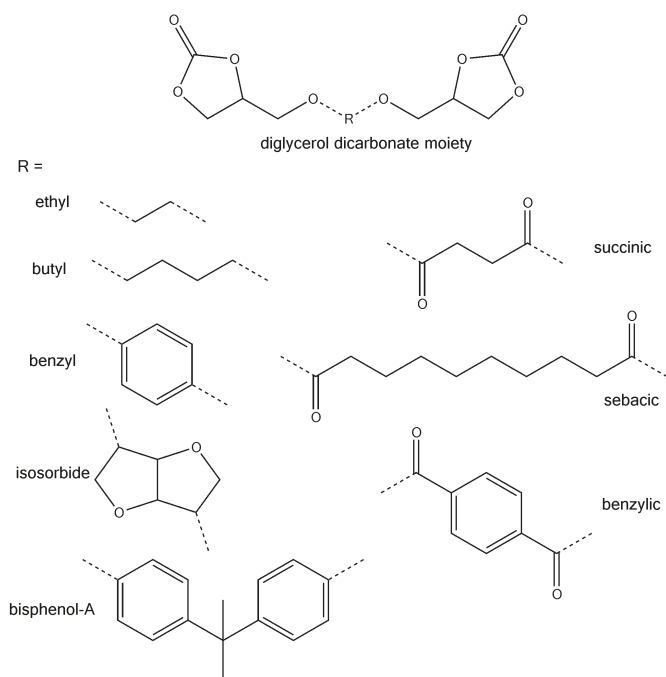
Figure 1.8   Glycerol dicarbonate based structures as used in Table 1.1.

hydroxyl group adjacent to the formed urethane, which may be a primary or a secondary hydroxyl group. Tomita *et al.* performed an investigation of the parameters influencing the formation of the primary, or the secondary hydroxyl group.[29] Predominantly the secondary hydroxyl group is formed. Temperature did not have an influence, more bulky amines and more polar solvents appear to slightly shift the ratio towards more primary hydroxyl formation. The presence of the hydroxyl groups is claimed to increase the chemical and hydrolytic stabilities of the resulting PHUs.[30,31] Furthermore, the hydroxyl groups will increase the polarity of the polymer chain, which may improve its solubility in more polar solvents.

The reaction has been reported for five-, six-, and seven-membered cyclic carbonates. Furthermore, both primary and secondary amines are being used.[32] In a study performed by the group of Endo, the reaction rates for six-membered cyclic carbonates were determined to be 30 to 60 times higher than those for five-membered rings.[33] These authors attributed the increased reaction rate to the higher ring strain of the six-membered carbonate. The results were verified experimentally, and also the hypothesis was extended to seven-membered cyclic carbonates.[34,35] Using PM3

Table 1.1 Glycerol carbonate based PHUs with different short spacers with ether- or ester-linkage. The structures are shown in Figure 1.9.

Spacer	Solvent	T_r °C	t h	Catalyst	M_n kg mol^{-1}	Đ	T_g °C	Ref.
none	bulk	100	10 min		n.d.	n.d.	n.d.	9
ethyl	bulk	80	2:20		25.4 – 30.2	1.18 – 1.22	-2 – 9	134
butyl	DMAc	70 – 100	24		18.0 – 21.0	1.42 – 1.57	n.d.	10
butyl	water	70	24		n.d.	n.d.	n.d.	39
benzyl	DMAc	70 – 100	24		27.0	1.55 – 1.63	n.d.	10
isosorbide	n.a.	20	n.a.	Yes, not reported	n.d.	n.d.	n.d.	31
diisosorbide	n.a.	20	n.a.	Yes, not reported	7.8 – 8.6	2.55 – 6.34	-8 – 59	31
triisosorbide	n.a.	20	n.a.	Yes, not reported	n.d.	n.d.	n.d.	31
bisphenol-A	DMSO	70 – 100	24	*none* / water / MeOH / EtOAc / 4Å molecular sieves	21.0 – 28.0	1.64 – 2.06	n.d.	10
bisphenol-A	DMAc	70 – 100	24		13.0 – 28.0	1.39 – 2.16	n.d.	10
bisphenol-A	DMAc	100	50		23.0	1.58	n.d.	10
bisphenol-A	DMF	20	72		6.3 – 13.2	1.52 – 1.8	3 – 29	135
bisphenol-A	DMSO	30	30 d		n.d.	n.d.	n.d.	29
bisphenol-A	water	50 – 100	24		0.5 – 4.2	1.03 – 2.16	n.d.	39
bisphenol-A	water	50 – 60	48		3.9 – 4.4	1.9	n.d.	39
bisphenol-A	water	70 – 100	24		2.0 – 2.1	1.14 – 1.88	n.d.	39
bisphenol-A	DMSO	30	20	TBD	53.4	1.38	n.d.	40
bisphenol-A	DMSO	30 – 80		none	5.4 – 20.1	1.17 – 1.39	n.d.	40
succinic	DMAc	70 – 100	24		22.0 – 28.0	1.66 – 2.04	n.d.	10
sebacic	bulk	75	96		6.0 – 9.0	2.4 – 3.1	-22 – (-14)	71
benzylic	DMF	75 – 120	48		8.0 – 20.0	1.9 – 2.5	41 – 48	136
benzylic	DMF	75			3.1 – 18.0	1.5 – 2.4	4 – 72	137

Hamiltonian modeling, the ring-strain energy of butyl-1,4-carbonate was calculated to be 12.5 kJ mol^{-1} larger than that of propyl-1,3-carbonate, which was 11.9 kJ mol^{-1} larger than that of ethylene-1,2-carbonate (see Figure 1.7).

He *et al.* published work in which they exploit this rate difference.[36] A coupler was synthesized with both a five-membered and a six-membered cyclic carbonate. Amines were functionalized with the five-membered moiety by selectively reacting the amine with the six-membered side of their 5,6-coupler. Combining this method with sequential feed of diamines, alternating PHU copolymers could be produced.

Most literature reporting five-membered cyclic carbonates use monomers based on two glycerol carbonate moieties linked by a diester or dioxy spacer. The polymer properties are summarized in Table 1.1 and the corresponding dicarbonate monomers are shown in Figure 1.8. Most polymers are based on the bisphenol-A spacer. However, in the last decade the use of bisphenol-A has been reconsidered for a number of applications as it may cause health issues, *e.g.* when used in food packaging.[37,38] Most reactions of dicyclic carbonates with diamines are performed in high-boiling polar solvents at reaction temperatures between 20 and 100 °C while reaction times tend to be in the order of days instead of hours. For most PHUs, M_n values up to 20,000 g mol^{-1} are achieved with dispersity ($Đ$) values between 1 and 2. The reported use of water as a solvent is interesting as it is environmentally benign. Unfortunately, molar masses were reported to be much lower than those obtained in other, organic solvents.[39]

Only one reference shows the successful use of a catalyst. Lambeth and Henderson could obtain significantly higher M_n values using 1,5,7-triazabicyclo[4.4.0]dec-5-ene (TBD) as a catalyst at 30 °C (M_n = 53.4 kg mol^{-1}) compared to the M_n values obtained using the same conditions in the absence of TBD (M_n = 5.4 - 20.1 kg mol^{-1}).[40] Note that, these M_n values are the highest reported for all polymers in Table 1.1.

Besides relatively small monomers, also examples have been published in which macromonomers have been end functionalized with glycerol carbonate.[41–44] The subsequent chain-extension of these functionalized macromonomers with amines yielded polymers with M_n values up to 68,000 g mol^{-1}.

Fatty acid-based materials have also been utilized for the production of dicyclic dicarbonates and their use in PHUs.[45–47] The group of Cramail synthesized a diamide

monomer from *ω*-unsaturated fatty acids and a diamine.[48] The double bond was converted by epoxidation and subsequent carbonation with CO_2 to terminal cyclic carbonates. Oils also have been extensively investigated for carbonation to *e.g.* carbonated soy bean oil (CSBO).[45–47,49,50] However, the use of oils implies a significant limitation for NIPUs. The functionality of these carbonated oils is significantly higher than 2, which will induce network formation.

Bähr *et al.* reported a very interesting monomer based on limonene.[51] Using a limonene-based dicyclic dicarbonate, materials were produced with glass transition temperature (T_g) values up to 70 °C. However, very low molecular weights based on SEC were reported, while FT-IR indicates that all carbonates have reacted. Possibly, the choice for a SEC system running on THF as the eluent was not optimal, as most other research groups use systems running on DMF or DMAc.

Another interesting route to NIPUs is by linking cyclic carbonate-functional molecules with thiol-ene chemistry.[30,34,35]

1.2 Bio-based polymers

For the last two decades, the interest for bio-based polymers increased noticeably. Estimates on remaining fossil resources vary considerably, yet it cannot be denied that this feedstock is finite. Furthermore, crude oil is predominantly used as fuel while the Earth's energy consumption increases. As a consequence, feedstock prices will continue to increase, making the exploitation of renewable resources to produce energy carriers and chemicals, including monomers, a necessity. In some cases, these renewable monomers can be drop-in replacements such as ethylene produced from bioethanol.[52–54] However, the production of commodity chemicals from biomass is not necessarily atom efficient and does not take advantage of the range of functionalities Nature has to offer. Introducing these functionalities starting from conventional petrochemicals is not trivial and requires a number of synthetic steps, resulting in lower atom efficiency and lower yields compared to renewable monomers. Therefore, natural compounds should be used with minimal alteration to provide monomers which give rise to novel polymers with differentiated properties.

1.2.1 Polymers from fats and oils

The list of polymers produced from biomass is long, so this section is limited to polymers that use similar monomers or polymerization chemistries as described in this thesis.[49,54–58]

One of the largest sources of renewable raw materials are plant oils.[59,60] A plant oil is a triacylglyceride: it is a triester of glycerol with three fatty acids which may differ from each other. Each plant species produces its own composition of different fatty acids.[57] Despite the structural differences, the fatty acids have several functional groups that can be used for the production of polymers. They all contain either a carboxylic acid or alkyl ester, and most have an internal double bond. Some contain additional functional groups such as hydroxyl (ricinoleic acid) or epoxy groups (vernolic acid). Especially the double bonds have already been used for a long time in varnishes and drying oils.[55] In more recent examples, the double bond is epoxidized and either ring opened to form hydroxyl or ether groups[27], or the epoxy is converted to a five-membered cyclic carbonate.[48,61] When two fatty acids are combined using a diamine or diol prior to the epoxidation/carbonation, they can be reacted with diamines to form PHUs. This approach has also been reported for unmodified plant oils such as soy bean oil to form networks with urethane linkages.[45–47,62–64]

Cyclic carbonates can also be synthesized from the fatty ester group. The group of Cramail describes the conversion of the ester group in methyl undecenoate to a diol and the subsequent conversion to a six-membered cyclic carbonate.[65] This pathway is very interesting, as six-membered cyclic carbonates are more reactive than their five-membered counterparts. Furthermore, in this specific case, no constitutional isomers are formed upon reaction with diamines. In addition, it leaves the double bonds intact to couple and form dimers.

Fatty acids have also been dimerized and trimerized, and commercialized under the trade names Empol® and Pripol™. These can easily be reacted with diols
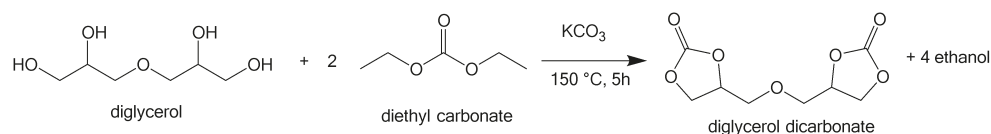
Figure 1.9 **Synthesis of diglycerol dicarbonate from diglycerol and diethyl carbonate.[9]**

to form polyesters or with diamines to synthesize polyamides.[66–70] Recently, Croda developed a diamine functional monomer based on dimerized fatty acid under the name Priamine™. During the last two years, articles have been published that use this monomer in NIPU synthesis.[48,71,72]

Glycerol is an abundant bio-based monomer which is produced as a major side product (>10 wt%) of the biodiesel industry.[58,73,74] It originates from the plant oils discussed earlier. Glycerol can be dimerized to the tetrafunctional polyol diglycerol and subsequently used in polymerization reactions.[75–77]

Furthermore, diglycerol can be converted to diglycerol dicarbonate through the reaction with a dialkyl carbonate, forming five-membered cyclic carbonate groups as shown in Figure 1.9.[9] The resulting diglycerol dicarbonate can be used in NIPU synthesis.[78]

1.2.2   *Polymers from sugar alcohols*

Carbohydrates are an abundant source of bio-based feedstock. Examples include starch, cellulose, and sugars. It has to be noted that this source of raw materials has a large overlap with the food industry. Cellulose is a polysaccharide that is not digestible by humans and therefore not a direct food source. However, it can be depolymerized to yield D-glucose (dextrose) which is edible.[79,80] Still, it is considered to be an acceptable source for bio-based materials.

Of all the monomers which can be derived from sugars, research has mainly focused on two monomers and their derivatives. These monomers are 2,5-furandicarboxylic acid, which is ultimately derived from fructose with hydroxymethylfurfural as intermediate, and isosorbide which is produced from glucose. Isosorbide has
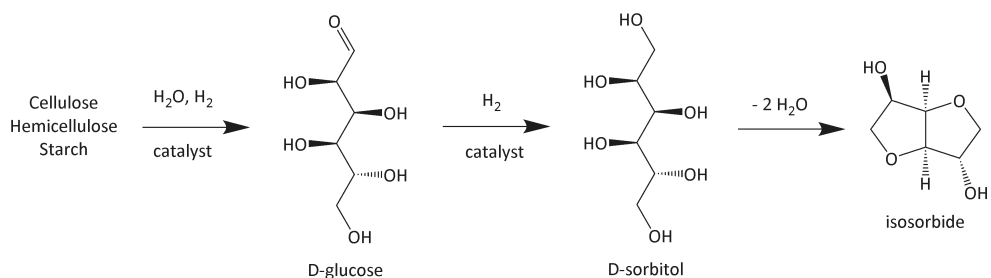
Figure 1.10   Production of isosorbide from starch.[84]
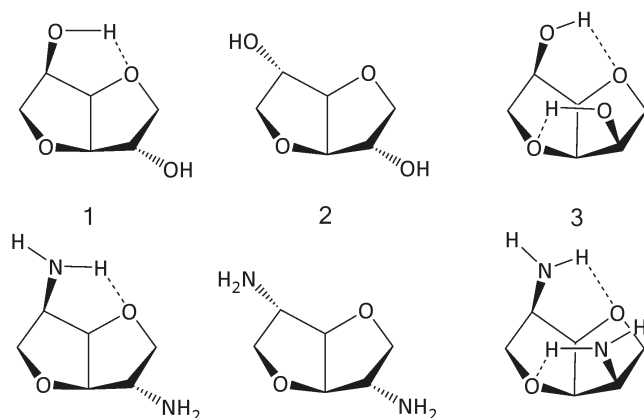
Figure 1.11   **Structures of isosorbide (1), isoidide (2), and isomannide (3) and their diamine derivatives.**

stereoisomers: isoidide and isomannide which are produced from fructose and mannose, respectively (see Figure 1.10).[81–85] Isomannide was the first of these compounds to be synthesized in 1875, while isosorbide followed in 1946.[81,86] The hydroxyl group can form an intramolecular hydrogen bond with the ether oxygen atom when it is in the endo-position (see Figure 1.11).[87] This may reduce the reactivity of the endo-hydroxyl in polyester synthesis[88] but no differences are observed when *e.g.* isosorbide is reacted with isocyanates.[89,90]

Isosorbide has been used in the synthesis of polyurethanes and polyesters.[88,91,92] Interesting derivatives of isohexides are the diamine analogues of isosorbide, isoidide, and isomannide (see Figure 1.11).[93–95] Despite the fact that their first synthesis was described in 1946, they haven't been used extensively so far. Still, these molecules are interesting as monomers for polymer production due to their rigidity and amine functionality.[84] Thiem reported their use in polyamide synthesis by interfacial polycondensation.[82] All three isomers were reacted with both aliphatic and aromatic diacid chlorides. During these reactions a reduced activity of the isomannide-based diamine was observed as compared to its two stereoisomers. T_g values were between 50 and 130 °C, and melting points between 120 and 180 °C for polyamides based on aliphatic diacid chlorides, and around 280 °C for polyamides based on aromatic diacid chlorides. No melting and crystallization enthalpies were reported.

Jasinska *et al.* reported the use of bulk polycondensation to react isoidide

diamine with sebacic acid, followed by solid state polymerization (SSP) of the formed prepolymers.[96,97] Later, the same authors reported the synthesis of polyamides based on isosorbide diamine with sebacic and brassylic acid.[98] The bulk reaction resulted in low molecular weight polymers with M_n values ranging from 4,200 to 5,600 g mol^{-1}. Note that the isohexide-based homopolymers could not be subjected to SSP, due to the low melting point of these polymers. When the isohexide diamines were copolymerized with butane-1,4-diamine, SSP became possible and M_n values in the order of 20,000 g mol^{-1} were achieved. Isoidide diamine was found to be more stable at higher temperatures than isosorbide diamine, while the crystallinity of both polymers was limited.

1.3   Coating systems

Coatings are designed to provide decoration and protection to increase product life. The extended lifetime results in a reduced use of raw materials which is good for the environment. However, coatings nowadays are mostly produced from fossil-based feedstock. Crude oil is a depleting source, and not sustainable for the production of coating materials. Therefore, bio-based macromolecular alternatives such as the examples described in the previous section are becoming a necessity. Ideally, these bio-based polymers will be employed in environmentally-friendly coating systems. Systems with low VOC emissions include water-borne, high-solids, and powder coatings.[99]

1.3.1   Cured systems

Curable coating systems are based on low molecular weight polymers that are cross-linked to form a network. These coatings can be one-component or two-component systems.[100] Two-component (2K) coatings are mixed just prior to application on a substrate as the reactive groups generally can react at room temperature. For one-component systems, the reactive groups are already mixed but the reaction is inhibited to prevent undesired cross-linking during storage. The cross-linking is usually activated by heat or irradiation. UV-curable systems contain unsaturations along

Table 1.2   Advantages and disadvantages of high solids *vs*. powder coatings

High solids	Powder coating
Advantages	
Low film thickness	No VOC emission
Color matching is easy	Safe for painter
Large surfaces possible	Fast curing in 20 minutes
	Recycling of unused powder paint
Disadvantages	
Still VOC emissions	Careful preparation to avoid paint defects
High viscosity of the paint	T_g has to be higher than storage temperature
	Color matching and changes are difficult
	Suitability of substrate material and shape

the resin backbone, which can be cross-linked radically. Thermosetting coatings use chemical reactions between different functional groups, *e.g.* (blocked) isocyanates with hydroxyl groups, or between carboxylic acid and epoxy groups. Blocked isocyanates are inactive at room temperature and require heat to remove a small molecule to yield the active isocyanate.[101]

Paint systems that are currently on the market often have a solids content above 60 wt% in an organic solvent (high solids) or entirely eliminate the use of solvents (powder coatings).[99] High solids paints are viscous liquid systems which can be applied with conventional application equipment. Powder coating application requires ovens and *e.g.* electrostatic powder application or fluidized bed equipment.[99] The application of powder coatings emits almost no solvents but can release blocking agents if used. Curing of the paint requires energy. The differences between high solids paints and powder coatings are listed in Table 1.2.

Standard commercial powder coatings contain six main ingredients: a resin, a curing agent, additives and post-extrusion additives, tint pigments, and fillers.[102] The resin and the curing agent react to form a cross-linked network and hence make up the coating. The resin and curing agent are a properly designed couple, their curing chemistry has to match. Polyesters are cured with *β*-hydroxyalkylamides or epoxy-based crosslinkers, and epoxy-terminated resins are cross-linked with dicyandiamides.

A few bio-based alternatives exist to replace isophthalic and terephthalic acid, important monomers in polyester resins. The main options are 2,5-furandicarboxylic

acid or synthesizing these monomers from bio-ethylene. These monomers are aromatic and provide rigidity to the polymer chain of the resin. This rigidity is necessary to combine a high glass transition temperature with a low molecular mass while having an amorphous polymer, requirements of a good powder coating resin. Note that epoxy resins are mainly based on bisphenols, also aromatic compounds.

Thermo-setting powder coatings are not suitable for all substrates. The object has to be cured in an oven, therefore the material has to be stable at elevated temperatures of up to 220 °C. However, research on the development of low-temperature curing systems has been performed.[103] This enables the technique to be applied to temperature-sensitive materials, *e.g.* wood.

1.3.2 Water-borne coatings

Instead of reducing the amount of solvents in paint, organic solvents can be replaced altogether by environmentally friendly alternatives. Water is naturally abundant and the most environmentally friendly carrier. Over the years, many different water-borne systems have been developed or adapted from solvent-borne systems: alkyds, acrylic latexes, acrylic-epoxy hybrids, acrylic epoxies, and polyurethane dispersions.[104,105] Still, none of these systems have zero VOC emissions as they require additives or co-solvents to form a good coating upon drying. They can be air-dried, or force-dried to enhance the evaporation of the water. For some systems, such as alkyds and acrylics, formulations have been developed that can form a thermally cross-linked network.

Polyurethane dispersions are a promising coating system:

+ The coatings are tough films after drying and can be applied to a wide range of rigid and flexible substrates.
+ They require very little additives and therefore have a very low VOC emission.
+ Polyurethane dispersions have excellent gloss and color.
+ Upon drying there is no chemical change which provides a long lifetime.
- Like other water-borne systems, drying time depends on the environmental conditions.
- Compared to solvent-borne paints, they have low solids content and require multiple layers.

- The interlayer adhesion requires more care as the dried layer does not redissolve in the wet layer.

Polyurethane dispersions

Polyurethane dispersions (PUDs) consist of polyurethane particles suspended in water.[105–107] To provide colloidal stability, the polyurethanes often bear an internal emulsifier. Most often, dimethylol propionic acid (DMPA) is used as stabilizer.[108] Four major processes exist to form PUDs: the acetone process, the prepolymer mixing process (Figure 1.12), the melt dispersion process, and the ketamine and ketazine processes. In the acetone process, the chain extension of the isocyanate end-capped prepolymer with a diamine is performed in solution in an organic solvent such as acetone. Dispersion into water is done after the chain extension reaction. In the prepolymer process, first the low viscosity polymers are dispersed into water
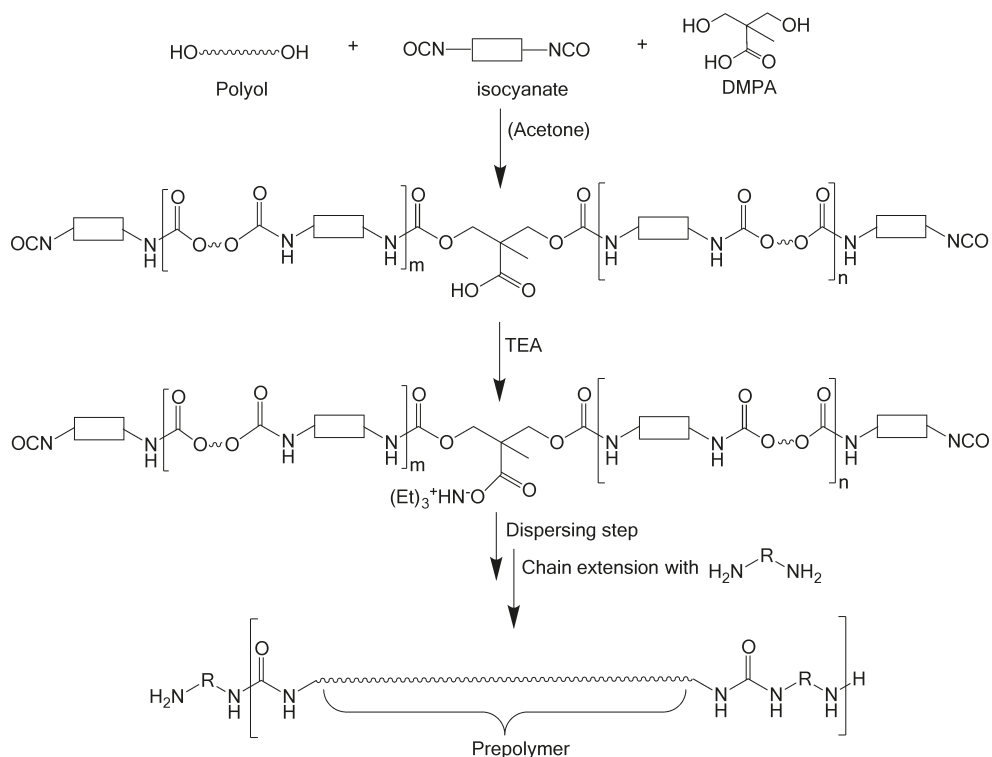
Figure 1.12 **Synthesis of polyurethane dispersions based on a prepolymer mixing process.**[109]
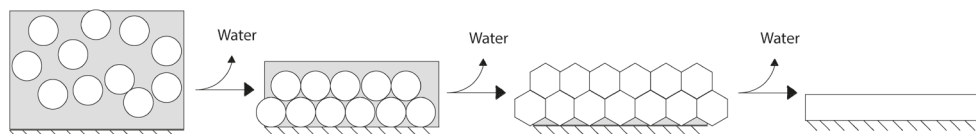
Figure 1.13 **Idealized picture of the drying and film formation of a water-borne dispersion to form a coating.**

and diamine chain extension occurs in the dispersed phase. As water reacts with isocyanates, the stoichiometry between isocyanate and diamine is usually off-balance. In the melt dispersion process, the isocyanate-functional polymers are reacted with ammonia or urea to achieve terminal urea or biuret groups. These can be readily dispersed at high temperature and chain extended with formaldehyde. The ketimine and ketazine processes are variations on the prepolymer mixing process. Diamines or hydrazines are reacted with ketones to form the ketimines and ketazines which are non-reactive with isocyanates. Upon dispersing the ketimines or ketazines together with the prepolymers, reaction with water removes the ketone and the diamines or hydrazine that form can react with the isocyanate to chain extend the prepolymers.[109]

The polyurethane coating is formed by evaporation of the water as shown in Figure 1.13.[110] In the ideal case, the particles will deform as more water evaporates, creating large pressures between the particles. Reptation of the polymer chains will lead to interdiffusion of the polymers to form the final coating. In practice, the original particles will not completely disappear.

Most of the efforts to produce environmentally friendly PUDs are based on replacing the polyol by bio-based alternatives (see Figure 1.12). Examples like soy bean oil[111], linseed oil[112], fish oil[113], castor oil[107,112,114], and cardanol[115] have been reported in combination with IPDI as the diisocyanate. The group of Larock reported several systems based on soy bean oil. They've synthesized cationic dispersions using N-methyl diethanolamine for its antibacterial properties.[116] Isosorbide was incorporated to increase the T_g value[117], and radical polymerization was applied to graft onto dispersions made from acrylated soybean oil with TDI. Xu synthesized a bio-based tricarboxylic acid from rosin and fumaric acid, which was polymerized with diethylene glycol to form a polyol bearing one free carboxylic acid group on the rosin.[118]

The use of bio-based isocyanates to produce fully bio-based PUDs has been reported. Fu *et al*. synthesized a diisocyanate from castor oil-derived undecylenic acid using thiol-ene chemistry and a Curtius rearrangement.[119] The produced diisocyanate was reacted with castor oil to produce the polyurethane resin. Note that the chemicals used to convert the carboxylic acid into the isocyanate group (thionyl chloride and sodium azide) are not bio-based and toxic. The group of Koning reported the use of two commercial diisocyanates produced from biomass.[89,120–122] One was an isocyanate functionalized dimerized fatty acid, and the other was the ethyl ester of L-lysine diisocyanate. Most likely these compounds are synthesized using the aforementioned Curtius rearrangement or the Schmidt reaction which uses hydrazoic acid to form isocyanates from a carboxylic acid. These isocyanates were reacted with isosorbide and DMPA to yield stable PUDs.

Increasing the renewable content of the polyurethanes is a positive development. However, the conversion of biomass to the isocyanates is based on chemistry that is environmentally unfriendly as well as hazardous. Therefore, the use of non-isocyanate poly(hydroxy urethane)s for PUDs would be a desired alternative. The dispersing of NIPUs has been reported by Blank and by Tramontano.[123–125] The polymers were synthesized by reacting propyl-1,2-carbonate with hexane-1,6-diamine and transesterification with a polyester polyol.[126] Despite the low molecular weights obtained ($M < 5000$ g mol^{-1}), the dispersions showed excellent properties in dispersing both organic as inorganic pigments. They were superior to their conventional polyurethane counterparts.

1.4 Objective and approach

This dissertation describes the synthesis, characterization and application as coating resins of several polyamides and non-isocyanate polyurethanes. These polymers are based on the compounds shown in Figure 1.14. These monomers can be produced from biomass although **BDA**, **PDA**, and **PA** are currently still synthesized through petrochemical routes.[9,66,71,127–132] Bio-based **BDA** and **PDA** are announced to be commercially available in the coming years.
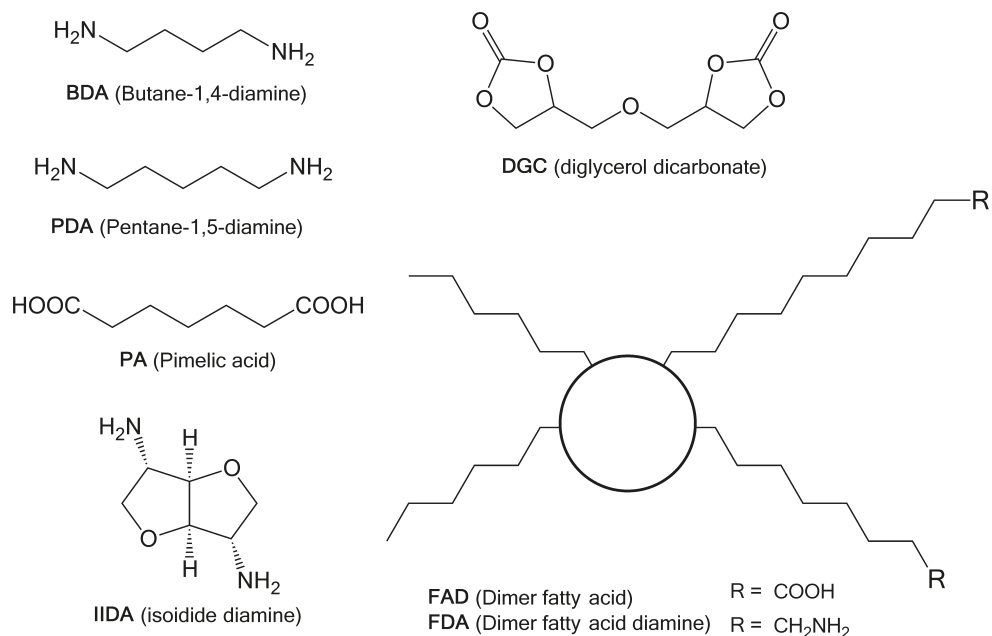
Figure 1.14 **Structures of the monomers used in the work described in this dissertation that can be obtained from biomass.**

The synthesis of bio-based polyamides and their properties will be evaluated in Chapter 2. The polyamides reported are intended for application as powder coating resins. Two distinct properties which these resins typically display are that they are amorphous, and that they have a glass transition temperature (T_g) exceeding 50 °C. To design amorphous polyamides, fatty acid materials can be used in combination with the odd-numbered monomers to decrease chain regularity in polyamides which is known to reduce crystallinity in polymers.[133] To achieve the target of the increased T_g, **IIDA** will be introduced to increase chain stiffness.

In Chapter 3, the polyamides that are developed in the work described in Chapter 2 are optimized and mixed with standard cross-linkers. The behavior of these mixtures will be analyzed using rheology and DSC techniques. The data obtained will be used to choose the conditions of solvent-borne coating tests. The mixtures of polyamide with cross-linker are applied to aluminum test panels. The mixtures are cured and the final coatings are tested for their performance using standardized industrially relevant methods, *e.g.* pencil hardness, reverse impact, and solvent resistance.

The synthesis of novel non-isocyanate polyurethanes is reported in Chapter 4.

These polyurethanes are synthesized from renewable diglycerol dicarbonate together with a diamine. Various renewable diamines are used to produce a range of properties which may be suitable for a dispersion application. The poly(hydroxy urethane)s will be characterized on composition, structure, and thermal behavior.

Chapter 5 describes the dispersing of poly(hydroxy urethane)s in water. The polyurethanes are synthesized according to the procedure described in Chapter 4. Covalently bound carboxylic acid functionality will be introduced for ionic stabilization of the polymer particles. The dispersions will be analyzed on particle size and colloidal stability as a function of carboxylic acid content and the degree of neutralization.

The major conclusions of the dissertation are summarized in Chapter 6. These results will be compared with the current industrial standards. The feasibility of the methods used, and their limitations, are discussed. On basis of this assessment, recommendations for the coatings industry will be made.

1.5 References

(1)   Berg, J. M.; Tymoczko, J. L.; Stryer, L. Biochemistry, 5th ed.; W.H. Freeman and Co.: New York, 2002.

(2)   Carothers, W. H. Linear condensation polymers, US2071250, 1937.

(3)   Bayer, O. Angew. Chemie 1947, 59 (9), 257–272.

(4)   Six, C.; Richter, F. In Ullmann's Encyclopedia of Industrial Chemistry; 2003.

(5)   Occupational Safety & Health Administration. Isocyanates https://www.osha.gov/SLTC/isocyanates/ (accessed Nov 7, 2014).

(6)   Paquin, M.; Richard, L. Urea derivative of the 1.3-butylene-glycol and process of preparing them. US1817992, 1931.

(7)   Groszos, S. J.; Drechsel, E. K. Method of preparing a polyurethane. US2802022, 1957.

(8)   Rokicki, G.; Piotrowska, A. Polymer 2002, 43 (10), 2927–2935.

(9)   Whelan Jr., J. M.; Hill, M.; Cotter, R. J. Multiple cyclic carbonate polymers. US3072613, 1963.

(10)   Kihara, N.; Endo, T. J. Polym. Sci. Part A: Polym. Chem. 1993, 31 (11), 2765–2773.

(11)   Schmitz, F.; Keul, H.; Höcker, H. Polymer 1998, 39 (14), 3179–3186.

(12)   Neffgen, S.; Kušan, J.; Fey, T.; Keul, H.; Höcker, H. Macromol. Chem. Phys. 2000, 201 (16), 2108–2114.

(13)   Neffgen, S.; Keul, H.; Höcker, H. Macromolecules 1997, 30 (5), 1289–1297.

(14)   Kušan, J.; Keul, H.; Höcker, H. Macromolecules 2001, 34 (3), 389–395.

(15)   Sharma, B.; Keul, H.; Höcker, H.; Loontjens, T.; Benthem, R. van. Polymer 2005, 46 (6), 1775–1783.

(16) Sharma, B.; Ubaghs, L.; Keul, H.; Höcker, H.; Loontjens, T.; Benthem, R. Van. Polymer 2004, 45 (16), 5427–5440.

(17) Ubaghs, L.; Sharma, B.; Keul, H.; Höcker, H.; Loontjens, T.; Benthem, R. Van; Ubaghs, L.; Keul, H.; Höcker, H.; Loontjens, T.; Benthem, R. Van. e-Polymers 2003, 68.

(18) Sharma, B.; Ubaghs, L.; Keul, H.; Höcker, H.; Loontjens, T.; Van Benthem, R. Macromol. Chem. Phys. 2004, 205 (11), 1536–1546.

(19) Deepa, P.; Jayakannan, M. J. Polym. Sci. Part A: Polym. Chem. 2008, 46 (7), 2445–2458.

(20) Delledonne, D.; Rivetti, F.; Romano, U. Appl. Catal. A Gen. 2001, 221 (1-2), 241–251.

(21) Maier, S.; Loontjens, T.; Scholtens, B.; Mülhaupt, R. Angew. Chemie - Int. Ed. 2003, 42 (41), 5094–5097.

(22) Maier, S.; Loontjens, T.; Scholtens, B.; Mülhaupt, R. Macromolecules 2003, 36 (13), 4727–4734.

(23) Versteegen, R. M.; Sijbesma, R. P.; Meijer, E. W. Angew. Chem. Int. Ed. Engl. 1999, 38 (19), 2917–2919.

(24) Ihata, O.; Kayaki, Y.; Ikariya, T. Angew. Chem. Int. Ed. Engl. 2004, 43 (6), 717–719.

(25) More, A. S.; Gadenne, B.; Alfos, C.; Cramail, H. Polym. Chem. 2012, 3 (6), 1594.

(26) More, A. S.; Maisonneuve, L.; Lebarbé, T.; Gadenne, B.; Alfos, C.; Cramail, H. Eur. J. Lipid Sci. Technol. 2013, 115 (1), 61–75.

(27) Palaskar, D. V.; Boyer, A.; Cloutet, E.; Alfos, C.; Cramail, H. Biomacromolecules 2010, 11 (5), 1202–1211.

(28) Calle, M.; Lligadas, G.; Ronda, J. C.; Galià, M.; Cádiz, V. J. Polym. Sci. Part A: Polym. Chem. 2014, 52 (21), 3017–3025.

(29) Tomita, H.; Sanda, F.; Endo, T. J. Polym. Sci. Part A: Polym. Chem. 2001, 39 (6), 851–859.

(30) Benyahya, S.; Desroches, M.; Auvergne, R.; Carlotti, S.; Caillol, S.; Boutevin, B. Polym. Chem. 2011, 2 (11), 2661–2667.

(31) Besse, V.; Auvergne, R.; Carlotti, S.; Boutevin, G.; Otazaghine, B.; Caillol, S.; Pascault, J.-P.; Boutevin, B. React. Funct. Polym. 2013, 73 (3), 588–594.

(32) Camara, F.; Benyahya, S.; Besse, V.; Boutevin, G.; Auvergne, R.; Boutevin, B.; Caillol, S. Eur. Polym. J. 2014, 55, 17–26.

(33) Tomita, H.; Sanda, F.; Endo, T. J. Polym. Sci. Part A: Polym. Chem. 2001, 39 (1), 162–168.

(34) Tomita, H.; Sanda, F.; Endo, T. J. Polym. Sci. Part A: Polym. Chem. 2001, 39 (6), 860–867.

(35) Tomita, H.; Sanda, F.; Endo, T. J. Polym. Sci. Part A: Polym. Chem. 2001, 39 (23), 4091–4100.

(36) He, Y.; Keul, H.; Möller, M. React. Funct. Polym. 2011, 71 (2), 175–186.

(37) European Food Safety Authority. Bisphenol A http://www.efsa.europa.eu/en/topics/topic/bisphenol.htm (accessed Nov 11, 2014).

(38) Center for Food Safety and Applied Nutrition. Food Additives & Ingredients - Bisphenol A (BPA) http://www.fda.gov/food/ingredientspackaginglabeling/foodadditivesingredients/ucm166145.htm (accessed Nov 11, 2014).

(39) Ochiai, B.; Satoh, Y.; Endo, T. Green Chem. 2005, 7 (11), 765–767.

(40) Lambeth, R. H.; Henderson, T. J. Polymer 2013, 54 (21), 5568–5573.

(41) Helou, M.; Carpentier, J.-F.; Guillaume, S. M. Green Chem. 2011, 13 (2), 266–271.

(42) Annunziata, L.; Diallo, A. K.; Fouquay, S.; Michaud, G.; Simon, F.; Brusson, J.-M.; Carpentier, J.-F.; Guillaume, S. M. Green Chem. 2014, 16 (4), 1947–1956.

(43) Annunziata, L.; Fouquay, S.; Michaud, G.; Simon, F.; Guillaume, S. M.; Carpentier, J.-F. Polym. Chem. 2013, 4 (5), 1313.

(44) Diallo, A. K.; Annunziata, L.; Fouquay, S.; Michaud, G.; Simon, F.; Brusson, J.-M.; Guillaume, S. M.; Carpentier, J.-F. Polym. Chem. 2014, 5 (7), 2583.

(45) Bähr, M.; Mülhaupt, R. Green Chem. 2012, 14 (2), 483–489.

(46) Javni, I.; Hong, D. P.; Petrović, Z. S. J. Appl. Polym. Sci. 2008, 108 (6), 3867–3875.

(47) Javni, I.; Hong, D. P.; Petrović, Z. S. J. Appl. Polym. Sci. 2013, 128 (1), 566–571.

(48) Maisonneuve, L.; More, A. S.; Foltran, S.; Alfos, C.; Robert, F.; Landais, Y.; Tassaing, T.; Grau, E.; Cramail, H. RSC Adv. 2014, 4 (49), 25795–25803.

(49) Biermann, U.; Bornscheuer, U.; Meier, M. A. R.; Metzger, J. O.; Schäfer, H. J. Angew. Chem. Int. Ed. Engl. 2011, 50 (17), 3854–3871.

(50) Kathalewar, M. S.; Joshi, P. B.; Sabnis, A. S.; Malshe, V. C. RSC Adv. 2013, 3 (13), 4110.

(51) Bähr, M.; Bitto, A.; Mülhaupt, R. Green Chem, 2012, 14 (5), 1447–1454.

(52) Morschbacker, A. Polym. Rev. 2009, 49 (2), 79–84.

(53) Mathers, R. T. J. Polym. Sci. Part A: Polym. Chem. 2012, 50 (1), 1–15.

(54) Chen, G.-Q.; Patel, M. K. Chem. Rev. 2012, 112 (4), 2082–2099.

(55) Williams, C.; Hillmyer, M. Polym. Rev. 2008, 48 (1), 1–10.

(56) Nayak, P. L. J. Macromol. Sci. Part C Polym. Rev. 2000, 40 (1), 1–21.

(57) Montero de Espinosa, L.; Meier, M. A. R. Eur. Polym. J. 2011, 47 (5), 837–852.

(58) Corma, A.; Iborra, S.; Velty, A. Chem. Rev. 2007, 107 (6), 2411–2502.

(59) Meier, M. A. R.; Metzger, J. O.; Schubert, U. S. Chem. Soc. Rev. 2007, 36 (11), 1788.

(60) Meier, M. A. R. Macromol. Rapid Commun. 2011, 32 (17), 1297–1298.

(61) Cramail, H.; Boyer, A.; Cloutet, E.; Gadenne, B. Précurseurs biscarbonates, leur procédé de préparation et leurs utilisations. WO2011/061452, May 26, 2011.

(62) Tamami, B.; Sohn, S.; Wilkes, G. L. J. Appl. Polym. Sci. 2004, 92 (2), 883–891.

(63) Wilkes, G. L.; Sohn, S.; Tamami, B. Nonisocyanate polyurethane materials, and their preparation from epoxidized soybean oils and related epoxidized vegetable oils, incorporation of carbon dioxide into soybean oil, and carbonation of vegetable oils. US7045577, 2004.

(64) Lee, A.; Deng, Y. Eur. Polym. J. 2015, 63, 67–73.

(65) Maisonneuve, L.; Wirotius, A.-L.; Alfos, C.; Grau, E.; Cramail, H. Polym. Chem. 2014, 5 (21), 6142–6147.

(66) Hablot, E.; Donnio, B.; Bouquey, M.; Avérous, L. Polymer 2010, 51 (25), 5895–5902.

(67) Vedanayagam, H. S.; Kale, V. Polymer 1992, 33 (16), 3495–3499.

(68) Fan, X. D.; Deng, Y.; Waterhouse, J.; Pfromm, P. J. Appl. Polym. Sci. 1998, 68 (2), 305–314.

(69) Deng, Y.; Fan, X. D.; Waterhouse, J. J. Appl. Polym. Sci. 1998, 73 (6), 1081–1088.

(70) Kale, V.; Vedanayagam, H. S.; Devi, K. S.; Rao, S. V.; Lakshminarayana, G.; Rao, M. B. J. Appl. Polym. Sci. 1988, 36 (7), 1517–1524.

(71) Carré, C.; Bonnet, L.; Avérous, L. RSC Adv. 2014, 4, 54018–54025.

(72) Cornille, A.; Dworakowska, S.; Bogdal, D.; Boutevin, B.; Caillol, S. Eur. Polym. J. 2015, 66, 129–138.

(73) Zhou, C.-H.; Beltramini, J. N.; Fan, Y.-X.; Lu, G. Q. Chem. Soc. Rev. 2008, 37 (3), 527–549.

(74) Chiu, C.-W.; Dasari, M. A.; Suppes, G. J.; Sutterlin, W. R. AIChE J. 2006, 52 (10), 3543–3548.

(75) Medeiros, M. A.; Araujo, M. H.; Augusti, R.; de Oliveira, L. C. A.; Lago, R. M. J. Braz. Chem. Soc. 2009, 20 (9), 1667–1673.

(76) Dakshinamoorthy, D.; Weinstock, A. K.; Damodaran, K.; Iwig, D. F.; Mathers, R. T. ChemSusChem 2014, 7 (10), 2923–2929.

(77)   Zhang, H.; Grinstaff, M. W. Macromol. Rapid Commun. 2014, 35, 1906–1924.

(78)   Jerome, F.; de Sousa, R.; Barrault, J.; Pouilloux, Y. Method for preparing dithiocarbamates in particular from polyols of the glycerol type. US20120264941, 2012.

(79)   Klemm, D.; Philipp, B.; Heinze, T.; Heinze, U.; Wagenknecht, W. Comprehensive Cellulose Chemistry; Wiley-VCH Verlag GmbH & Co. KGaA: Weinheim, FRG, 1998; Vol. 1.

(80)   Klemm, D.; Heublein, B.; Fink, H. P.; Bohn, A. Angew. Chemie - Int. Ed. 2005, 44 (22), 3358–3393.

(81)   Montgomery, R.; Wiggins, L. F. J. Chem. Soc. 1946, 390–393.

(82)   Thiem, J.; Bachmann, F. Die Makromol. Chemie 1991, 192 (9), 2163–2182.

(83)   Kricheldorf, H. R. J. Macromol. Sci. Part C Polym. Rev. 1997, 37 (4), 599–631.

(84)   Fenouillot, F.; Rousseau, A.; Colomines, G.; Saint-Loup, R.; Pascault, J.-P. Prog. Polym. Sci. 2010, 35 (5), 578–622.

(85)   Gandini, A. Macromolecules 2008, 41 (24), 9491–9504.

(86)   Bouchardat, M. G. Ann. Chim. Phys. 1875, No. 6, 100–135.

(87)   Jacquet, F.; Audinos, R.; Delmas, M.; Gaset, A. Biomass 1985, 6 (3), 193–209.

(88)   Noordover, B. A. J.; van Staalduinen, V. G.; Duchateau, R.; Koning, C. E.; van Benthem, R. A. T. M.; Mak, M.; Heise, A.; Frissen, A. E.; van Haveren, J. Biomacromolecules 2006, 7 (12), 3406–3416.

(89)   Li, Y.; Noordover, B. A. J.; van Benthem, R. A. T. M.; Koning, C. E. ACS Sustain. Chem. Eng. 2014, 2 (4), 788–797.

(90)   Cognet-Georjon, E.; Méchin, F.; Pascault, J.-P. Macromol. Chem. Phys. 1995, 196 (11), 3733–3751.

(91)   Braun, D.; Bergmann, M. J. für Prakt. Chemie/Chemiker-Zeitung 1992, 334 (4), 298–310.

(92)   Noordover, B. A. J.; Heise, A.; Malanowski, P.; Senatore, D.; Mak, M.; Molhoek, L.; Duchateau, R.; Koning, C. E.; van Benthem, R. A. T. M. Prog. Org. Coatings 2009, 65 (2), 187–196.

(93)   Montgomery, R.; Wiggins, L. F. J. Chem. Soc. 1946, 393–396.

(94)   Thiyagarajan, S.; Gootjes, L.; Vogelzang, W.; Wu, J.; van Haveren, J.; van Es, D. S. Tetrahedron 2011, 67 (2), 383–389.

(95)   Thiyagarajan, S.; Gootjes, L.; Vogelzang, W.; van Haveren, J.; Lutz, M.; van Es, D. S. ChemSusChem 2011, 4 (12), 1823–1829.

(96)   Jasinska, L.; Villani, M.; Wu, J.; van Es, D. S.; Klop, E.; Rastogi, S.; Koning, C. E. Macromolecules 2011, 44 (9), 3458–3466.

(97)   Jasinska-Walc, L.; Villani, M.; Dudenko, D.; van Asselen, O.; Klop, E.; Rastogi, S.; Hansen, M. R.; Koning, C. E. Macromolecules 2012, 45 (6), 2796–2808.

(98)   Jasinska-Walc, L.; Dudenko, D.; Rozanski, A.; Thiyagarajan, S.; Sowinski, P.; van Es, D.; Shu, J.; Hansen, M. R.; Koning, C. E. Macromolecules 2012, 45 (14), 5653–5666.

(99)   Weiss, K. D. Prog. Polym. Sci. 1997, 22 (2), 203–245.

(100) Meier-Westhues, U. Polyurethanes: Coatings, Adhesives and Sealants; Vincentz Network GmbH & Co KG: Hannover, 2007.

(101) Delebecq, E.; Pascault, J.-P.; Boutevin, B.; Ganachaud, F. Chem. Rev. 2013, 113 (1), 80–118.

(102) What's in a Powder Coating - AkzoNobel Powder Coatings https://www.akzonobel.com/ powder/guide_to_powder_coatings/whats_in_a_powder_coating/ (accessed May 21, 2015).

(103) Wuzella, G.; Kandelbauer, A.; Mahendran, A. R.; Teischinger, A. Prog. Org. Coatings 2011, 70 (4), 186–191.

(104) Joseph, R. Met. Finish. 2010, 108 (11-12), 90–99.

(105) Athawale, V. D.; Nimbalkar, R. V. J. Am. Oil Chem. Soc. 2010, 88 (2), 159–185.

(106) Kim, B. K.; Lee, J. C. J. Polym. Sci. Part A: Polym. Chem. 1996, 34 (6), 1095–1104.

(107) Rix, E.; Ceglia, G.; Bajt, J.; Chollet, G.; Heroguez, V.; Grau, E.; Cramail, H. Polym. Chem. 2015, 6, 213–217.

(108) Hourston, D. J.; Williams, G. D.; Satguru, R.; Padget, J. C.; Pears, D. J. Appl. Polym. Sci. 1999, 74 (3), 556–566.

(109) Kim, B. K. Colloid Polym. Sci. 1996, 274 (7), 599–611.

(110) Winnik, M. A.; Wang, Y. C.; Haley, F. J. Coat. Technol. 1992, 64 (811), 51–61.

(111) Oh, J. K.; Anderson, J.; Erdem, B.; Drumright, R.; Meyers, G. Prog. Org. Coatings 2011, 72 (3), 253–259.

(112) Chen, R.; Zhang, C.; Kessler, M. R. RSC Adv. 2014, 4 (67), 35476–35483.

(113) Athawale, V. D.; Nimbalkar, R. V. J. Dispers. Sci. Technol. 2011, 32 (7), 1014–1022.

(114) Madbouly, S. A.; Otaigbe, J. U.; Nanda, A. K.; Wicks, D. A. Macromolecules 2005, 38 (9), 4014–4023.

(115) Patel, C. J.; Mannari, V. Prog. Org. Coatings 2014, 77 (5), 997–1006.

(116) Lu, Y.; Larock, R. C. Prog. Org. Coatings 2010, 69 (1), 31–37.

(117) Xia, Y.; Larock, R. C. ChemSusChem 2011, 4 (3), 386–391.

(118) Xu, X.; Song, Z.; Shang, S.; Cui, S.; Rao, X. Polym. Int. 2011, 60 (10), 1521–1526.

(119) Fu, C.; Zheng, Z.; Yang, Z.; Chen, Y.; Shen, L. Prog. Org. Coatings 2014, 77 (1), 53–60.

(120) Li, Y.; Noordover, B. A. J.; van Benthem, R. A. T. M.; Koning, C. E. Eur. Polym. J. 2014, 52, 12–22.

(121) Li, Y.; Noordover, B. A. J.; van Benthem, R. A. T. M.; Koning, C. E. Eur. Polym. J. 2014, 59, 8–18.

(122) Li, Y. Bio-based poly(urethane urea) dispersions : chemistry, colloidal stabilization and properties, Eindhoven, University of Technology, 2014.

(123) Tramontano, V. J.; Thomas, M. E.; Coughlin, R. D. Technology for Waterborne Coatings; Glass, J. E., Ed.; ACS Symposium Series; American Chemical Society: Washington, DC, 1997; Vol. 663.

(124) Blank, W. J. Prog. Org. Coatings 1992, 20 (3-4), 235–259.

(125) Blank, W. J. Formulating Polyurethane Dispersions; Norwalk, CT, 1996.

(126) Blank, W. J. In Proceedings of the 17th Water-Borne and Higher Solids Coatings Symposium; University of Southern Mississippi: New Orleans, LA USA, 1990; pp 279–291.

(127) Schneider, J.; Wendisch, V. F. Appl. Microbiol. Biotechnol. 2010, 88 (4), 859–868.

(128) Tateno, T.; Okada, Y.; Tsuchidate, T.; Tanaka, T.; Fukuda, H.; Kondo, A. Appl. Microbiol. Biotechnol. 2009, 82 (1), 115–121.

(129) Ogata, K.; Tochikura, T.; Osugi, M.; Shojiro Iwahara. Agric. Biol. Chem. 1966, 30 (2), 176–180.

(130) Zhang, W.-W.; Yang, M.-M.; Li, H.; Wang, D. Electron. J. Biotechnol. 2011, 14 (6).

(131) Wiggins, L. F. J. Chem. Soc. 1946, 384–388.

(132) Scott, E.; Peter, F.; Sanders, J. Appl. Microbiol. Biotechnol. 2007, 75 (4), 751–762.

(133) Rulkens, R.; Koning, C. E. In Polymer Science: A Comprehensive Reference; Matyjaszewski, K., Möller, M., Eds.; Elsevier, 2012, 431–467.

(134) Sheng, X.; Ren, G.; Qin, Y.; Chen, X.; Wang, X.; Wang, F. Green Chem. 2015, 17 (1), 373–379.

(135) Steblyanko, A.; Choi, W.; Sanda, F.; Endo, T. J. Polym. Sci. Part A: Polym. Chem. 2000, 38 (13), 2375–2380.

(136)   Benyahya, S.; Boutevin, B.; Caillol, S.; Lapinte, V.; Habas, J.-P. Polym. Int. 2012, 61 (6), 918–925.

(137)   Benyahya, S.; Habas, J.-P.; Auvergne, R.; Lapinte, V.; Caillol, S. Polym. Int. 2012, 61 (11), 1666–1674.

2

Chapter 2

Polyamides from fatty acid- and isoidide-based monomers

*The aim of this work is to synthesize amorphous polyamides from renewable monomers derived from vegetable oils and sugars. By making use of both odd- and even-numbered monomers to hamper intermolecular hydrogen bonding, combined with either the incorporation of dimerized fatty acid monomers or isoidide diamine (**IIDA**) produced from fructose, the crystallization of the polyamides was suppressed considerably. Polyamides based on the dimerized fatty acid showed T_g values below 10 °C. The introduction of the isoidide-based diamine enhanced the rigidity of the polymer backbone, which enabled the synthesis of amorphous polyamides with T_g values up to 100 °C. For both series incomplete reaction has been observed as both end groups, i.e. amine and carboxylic acid, were detected in ^{1}H-NMR. This results in M_n values from ^{1}H-NMR for the fatty acid-based series in the range of 4,700 to 21,000 g mol^{-1}. The M_n values measured by SEC for the **IIDA**-based were in the range of 3,000 to 10,700 g mol^{-1}. The broad range of T_g values found for these materials in combination with their relatively low molecular weights and the corresponding large amount of reactive end-groups make them suitable for application in coatings, composites, or soft-touch surfaces.*

2.1 Introduction

In recent years, the interest for bio-based polymers increased noticeably. Estimates on remaining fossil resources vary considerably, yet it cannot be denied that this feedstock is finite. Furthermore, crude oil is predominantly used as fuel while the global energy consumption is growing. This will lead to a continuously increase of feedstock prices, making exploration and exploitation of renewable resources to produce energy and chemicals, including monomers, a necessity. In some instances, these renewable monomers can be drop-in replacements such as ethylene produced from bioethanol.[1] However, such conversions are not necessarily atom efficient and do not take advantage of the range of functionalities Nature has to offer. Introducing these functionalities starting from conventional petrochemicals is not trivial and requires a number of synthetic steps, resulting in a lower atom efficiency and lower yields compared to renewable monomers. Therefore, natural compounds should be used with only minor or preferably no alteration to provide monomers which may give rise to novel polymers with differentiated properties.

Amorphous polyamides are uncommon but they may have applications in coatings, composites, or soft-touch materials. However, the preparation of bio-based, amorphous polyamides is a challenge. Some examples of bio-based, amorphous polyesters are known, including isosorbide- and furandicarboxylic acid-based polymers.[2-5] Suppression of crystallinity in polyamides is mostly accomplished by combining appropriate monomers, *e.g.* non-linear bicyclic diamines with longer chain diacids or by enforcing kinks in the polymer chains.[6,7] Polyamides obtain their good solvent resistance, hydrolytic stability, and mechanical strength from the amide linkage. It displays hydrogen bonding as each amide linkage contains a H-bond donor as well as an acceptor, and its pseudo-double bond character provides rigidity to the polymer main chain. However, due to the fact that linear polyamides easily form hydrogen bonds, it is hard to prepare materials having a low degree of crystallinity and reduced melting temperatures (T_m) to obtain a good flow behavior in the melt at acceptable processing temperatures.

In this chapter, the synthesis of two series of renewable amorphous polyamides

is described, one from fatty acid- and one from sugar-based monomers. The selected approach to achieve amorphous polymers is based on the hampering of the regular organization of the polymer chains. To prevent H-bonds from forming, it is necessary to perturb the alignment of the amide bonds in adjacent polyamide chains. This can be achieved by mixing odd- and even-numbered monomers, resulting in the misalignment of the repeating units.[8–10] Because of the molecular structure of the monomers used, a broad range of T_g values is expected for these polyamides. Dimerized fatty acid (Pripol™ 1009, Scheme 2.1) has been previously reported to yield polyamides with reduced crystallinity.[11] The presence of non-functional side chains or bulky, asymmetric chain elements in the fatty acid monomer prevents the alignment of chains. In the work reported in this paper, the steric effects of the monomer will be combined with the introduction of odd-numbered diamines in the polyamide backbone. The second series is based on isoidide diamine (see Scheme 2.2 for its structure).[12,13] Previous studies indicated that the cocrystallization of polyamide chains containing isoidide diamine (**IIDA**) with chains containing butane-1,4-diamine (**BDA**), which has the same number of carbon atoms in the main chain, is limited.[14,15] Similar to the other series, an odd-numbered dicarboxylic acid is introduced in an attempt to prepare fully amorphous polyamides based on isoidide diamine. The use of the more rigid isoidide diamine is likely to increase the T_g of the polymer significantly compared to the fatty acid series.[16] Besides using renewable monomers, synthesis in the melt was selected as it is an industrially relevant technology and limits the use of solvents and harmful chemicals, as would be required in *e.g.* biphasic acid chloride-based synthesis.

In summary, the aim of this work is to design amorphous polyamides with tunable T_g values, to establish appropriate synthetic routes to prepare these materials and to study their thermal and morphological properties.

2.2 Materials and methods

2.2.1 Materials

The reactants pimelic acid (**PA**, 98%), butane-1,4-diamine (**BDA**, 99%) and pentane-1,5-diamine (**PDA**, ≥ 97%) were purchased from Sigma-Aldrich. Pripol™

1009 (**FAD**, 98.7% dicarboxylic acid, 1% tricarboxylic acid) was kindly supplied by Croda. 2,5-diamino-2,5-dideoxy-1,4-3,6-dianhydroiditol (isoidide diamine, **IIDA**, ≥ 95%) was synthesized by Wageningen UR Food and Biobased Research.[17,18] Solvents were obtained from Biosolve in AR grade. Deuterated solvents for NMR spectroscopy were purchased from Cambridge Isotope Laboratories, Inc. All chemicals were used as received without further purification.

2.2.2 Methods

NMR spectroscopy

^{1}H-NMR spectroscopy measurements were performed on an Agilent 400-MR NMR system in DMSO-d_6. Data was acquired using VnmrJ3 software. Chemical shifts are reported in ppm relative to tetramethylsilane (TMS). The number-average molecular weight (M_n) values of the NIPUs were calculated using the integral values of repeating units and end-groups:

$$M_n = \sum_{i=0}^{n} \frac{\left(\dfrac{I_{rep,i}}{H_i} \right)}{A} M_{rep,i} + \sum_{i=0}^{n} \frac{\left(\dfrac{I_{end,i}}{H_i} \right)}{A} M_i$$

Eq-2.1

with:

$$A = \sum_{i=0}^{n} \frac{I_{end,i}}{H_i}$$

Eq-2.2

In which I_{end} is the integral value belonging to an end-group, I_{rep} belongs to the integral value of a repeating unit, and H the number of protons represented by that integral ($H_{PA} = 2$, $H_{BDA} = 2$, $H_{PDA} = 2$, $H_{IIDA} = 1$). The left part of the formula calculates the molecular weight (M) contribution of the repeat units, the right side the M contribution of the end-groups. For this reaction, the molecular mass of the repeat unit of monomer i ($M_{rep,i}$) is chosen to be the mass of the original monomer minus 34 for dicarboxylic acid monomers, and minus 2 for diamines. The normalization factor (A) is solely based on the end-groups as a telechelic polymer chain can be considered as one complete monomer (end-group monomer) extended with repeat units.

34

TGA

Thermogravimetric analysis (TGA) was performed on a TA Q500 instrument (TA Instruments). Samples with a typical mass of 5 to 10 mg were heated at a rate of 10 °C min^{-1} to 600 °C in an N$_2$ atmosphere.

DSC

Differential Scanning Calorimetry (DSC) was performed on a TA Q100 DSC. Approximately 5 mg of dried polymer (60 °C overnight at reduced pressure) was accurately weighed and sealed into an hermetically closed aluminum pan. Temperature profiles were measured from at least 50 °C below T_g to 50 °C above T_m and consisted of two heating runs and one cooling run, at a heating/cooling rate of 10 °C min^{-1}. TA Universal Analysis software was used for data acquisition and analysis. The value for the T_g was determined from the inflection point of the curve during the second heating run.

FTIR

IR measurements were performed on a Varian Excalibur 3100 FT-IR Spectrometer, equipped with a diamond Specac Golden Gate attenuated total reflection (ATR) setup over a spectral range of 4000 to 650 cm^{-1} with a resolution of 4 cm^{-1}. 100 scans were signal-averaged and the resulting spectra were analyzed using Varian Resolutions Pro software.

SEC

Size-exclusion chromatography (SEC) was measured on a system equipped with a Waters 1515 Isocratic HPLC pump, a Waters 2414 refractive index detector (40 °C), a Waters 2707 autosampler, a PSS PFG guard column followed by 2 PFG-linear-XL (7 μm, 8x300 mm) columns in series at 40 °C. 1,1,1,3,3,3-Hexafluoroisopropanol (HFIP, Biosolve) with potassium trifluoro acetate (20 mmol L^{-1}) was used as eluent at a flow rate of 0.8 mL min^{-1}. The molecular weights were calculated against poly(methyl methacrylate) standards (Polymer Laboratories, M_p = 580 g mol^{-1} up to M_p = 7.1·10^6 g mol^{-1}). Samples were prepared in the eluent at a concentration of 2-3 mg mL^{-1}.

WAXD

The WAXD measurements were carried out with a Rigaku D/Max-B diffractometer, using Cu K$_\alpha$ radiation at 40 kV and 30 mA. WAXD samples were prepared by pasting

the precipitated polyamide powder onto a cover glass using a small amount of grease. WAXD patterns were obtained by step scans from $2\theta = 3°$ to $50°$ with a step size of $0.01°$ and an acquisition time of 5 s per step.

2.2.3   Synthetic procedures

Procedure to prepare polyamides based on fatty acid dimer

A series of polyamides was synthesized from the fatty acid dimer dicarboxylic acid (**FAD**) Pripol™ 1009 and different ratios of butane-1,4-diamine (**BDA**) and pentane-1,5-diamine (**PDA**). The molar ratio of the diamines is indicated by the nomenclature **FAD-BDA$_x$PDA$_y$** where $x + y = 100$, the relative amount of **FAD** is 100 in all cases.
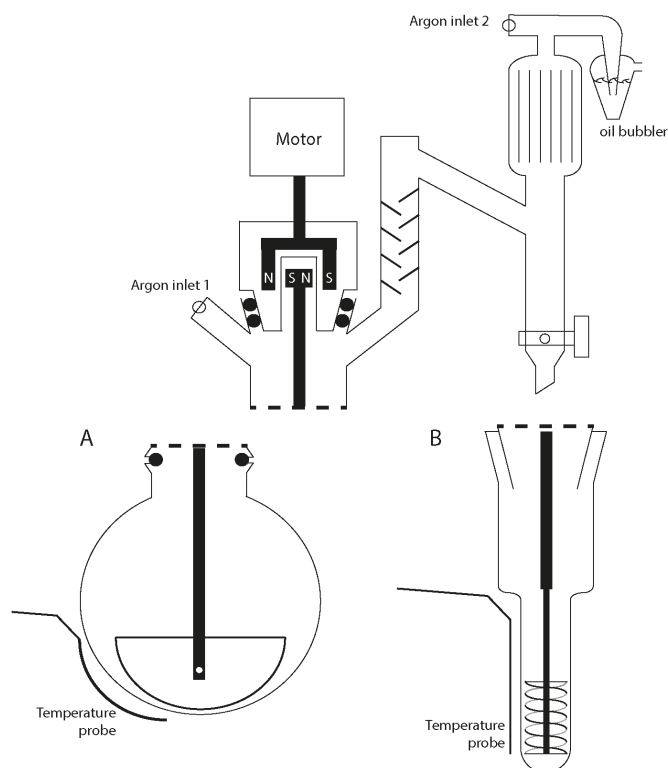
Figure 2.1   Reactor setups for the synthesis of polyamide resins. A magnetic coupling is fitted to ensure low pressure capabilities. A facilitates a half-moon stirrer and B a helical ribbon impeller. Properties of the double helical ribbon impeller: diameter 13 mm, ribbon width 2 mm, shaft diameter 3 mm, length 30 mm, pitch 1 rotation/10 mm, stainless steel.

Polyamides were synthesized using the following typical procedure as is described here for the polyamide **FAD**-**BDA**$_{100}$**PDA**$_0$. The reactants **FAD** (23.10 g, 40.9 mmol) and **BDA** (3.79 g, 43.0 mmol) were weighed and transferred to a glass round bottom reactor equipped with a mechanical 'half-moon' stirrer, an argon inlet and a distillation setup (see Figure 2.1). The mixture was stirred to form a highly viscous liquid salt within minutes after the start of the process. The salt was heated until a clear melt with a low viscosity was achieved and kept at this temperature ($100 \leq T \leq 120$ °C) for 20 minutes. The reaction mixture was gradually heated to ensure a clear melt until the final reaction temperature of 250 °C was reached in 4 hours. After an additional 30 minutes, the reaction mixture was stirred under reduced pressure ($p = 0.7$ hPa) for 30 minutes. The reaction product was transferred from the reactor to a storage container.

Procedure to prepare polyamides containing isoidide diamine

A series of polyamides was synthesized from pimelic acid (**PA**, heptanedioic acid) and different ratios of isoidide diamine (**IIDA**) and butane-1,4-diamine (**BDA**). The molar ratio of the diamines is indicated by the nomenclature **PA-II**$_x$**BDA**$_y$ where x + y = 100, the relative amount of **PA** is 100 in all cases.

Polyamides containing isoidide diamine were synthesized using the following typical procedure. **PA** (2.00 g, 12.5 mmol) and the diamines (12.5 mmol) were dissolved in methanol in a closed reactor equipped with a helical ribbon impeller, a nitrogen inlet and a distillation setup (see Figure 2.1). Evaporation of the solvent at 120 °C provided a clear liquid melt, which was gradually heated to 230 °C (270 °C for **PA-II**$_0$**BDA**$_{100}$). At this temperature the melt was stirred at reduced pressure ($p = 1.0$ hPa) for 30 minutes after which the product was discharged in the liquid state.

2.3 Polyamides based on fatty acid

The synthesis of amorphous polyamides is targeted by using the dimerized fatty acid (**FAD**) Pripol™ 1009. The non-linear structure of **FAD** was combined with mixtures of odd- and even-numbered diamines to hinder crystallization of the resulting polyamides.
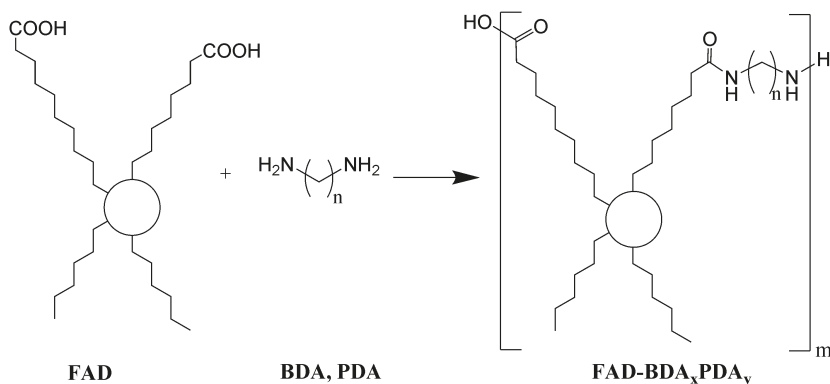
Scheme 2.1 Synthesis of copolyamides **FAD-BDA**$_x$**PDA**$_y$ based on fatty acid dimer (circles indicate structural uncertainty, as **FAD** consists of a mixture of several different but structurally comparable compounds, of which most contain 36 carbon atoms; note that at least 98.7% of the compound is dicarboxylic acid-functional, butane-1,4-diamine (**BDA**, n = 4) and pentane-1,5-diamine (**PDA**, n = 5)).

2.3.1 Synthesis and chemical structure

FAD was reacted with **BDA** and/or **PDA** in a non-catalyzed melt polymerization (Scheme 2.1). Melt synthesis was applied to limit the environmental impact of the synthesis of the desired polyamides. Acid chlorides or dimethyl ester-based synthetic routes produce more harmful condensates and require more synthetic steps and/or work-up for the monomers used in this study. The removal of a homogeneous catalyst after synthesis requires solvents so the reaction was performed in the absence of catalysts. The ^{1}H-NMR measurements, see Figure 2.2, were performed to analyze the molecular compositions and to calculate the number-average molecular weights (M_n)

Table 2.1 Number average molecular weights and compositions of **FAD**-based polyamides determined by ^{1}H-NMR.

Polymer	^{1}H-NMR[a]			
	X_{feed}[b]	$X_{copolymer}$[b]	M_n	DP_n[c]
			g mol^{-1}	
FAD-BDA$_{100}$PDA$_0$	100 / 105.1 / 0	100 / 83.5 / 0	4,700	14.3
FAD-BDA$_{75}$PDA$_{25}$	100 / 82.6 / 27.6	100 / 76.5 / 25.6	10,400	33.9
FAD-BDA$_{50}$PDA$_{50}$	100 / 53.8 / 54.0	100 / 49.3 / 49.1	21,000	67.0
FAD-BDA$_{25}$PDA$_{75}$	100 / 27.6 / 81.9	100 / 25.4 / 76.4	8,300	26.7
FAD-BDA$_0$PDA$_{100}$	100 / 0 / 111.4	100 / 0 / 98.9	12,400	41.1

[a] Number-averaged molecular weight and composition determined by ^{1}H-NMR in CDCl$_3$; [b] Molar ratio of **FAD / BDA / PDA**; [c] Degree of polymerization
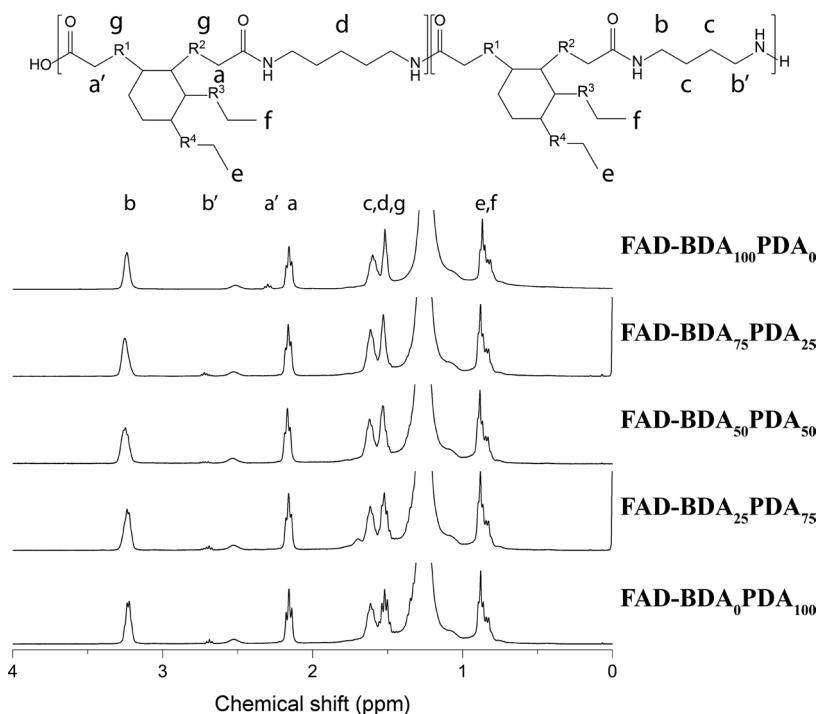
Figure 2.2 ^{1}H-NMR spectra of copolyamides **FAD-BDA$_{100}$PDA$_0$**, **FAD-BDA$_{75}$PDA$_{25}$**, **FAD-BDA$_{50}$PDA$_{50}$**, **FAD-BDA$_{25}$PDA$_{75}$** and **FAD-BDA$_0$PDA$_{100}$** in CDCl$_3$. R1, R2, R3, and R4 are linear alkyl chains of (CH$_2$)$_x$ with $1 \leq x \leq 6$, depending on the feedstock used to prepare **FAD**.

by using the ratio of monomer residues in the polyamide main chain and monomer residues present as end-groups. The resulting molecular weights and compositions of the synthesized polyamides are collected in Table 2.1. In the ^{1}H-NMR spectra, the dominant peak of the long alkyl residues at $\delta = 1.3$ ppm causes a poorly corrected baseline. This results in an overestimation of up to 10 mol% of the amount of **FAD** in the sample. Note that the amount of **FAD** in the sample cannot be accurately quantified.

The syntheses were carried out with a 5 to 10 mol% excess of the diamines, to correct for the evaporation of these volatile compounds. The compositions of the copolyamides, as determined by NMR, indeed indicate that there is a 10 mol% difference between the amount of diamine in the feed and the amount built into the polyamides for most of the polymers, when normalized for **FAD**. This is most noticeable in **FAD-BDA$_{100}$PDA$_0$**, see Table 2.1, where this diamine evaporation

resulted in an excess of carboxylic acid groups in the polymer product whilst the monomer feed contained an excess of diamine (*i.e.* **BDA**). Therefore, this polymer has the lowest molecular weight of the series. In the copolyamides, the losses of both diamines are proportional to the feed ratio, indicating that **BDA** and **PDA** evaporated to a similar extent. As expected, these losses affect the molecular weights, as for larger deviations from stoichiometric balances lower M_n values are calculated from the NMR spectra. The M_n values calculated range from 4,700 g mol^{-1} to 21,000 g mol^{-1}. As a rough estimate, for M_n values exceeding 15,000 g mol^{-1} the integration of the end-groups in the ^{1}H-NMR spectrum is less reliable because of a decreasing signal-to-noise ratio (SNR) when less end groups are present per unit of mass. A lower value of SNR increases the integration error dramatically and this may lead to an overestimated value for the M_n of **FAD-BDA$_{50}$PDA$_{50}$**.

Of the solvents used in the various SEC systems available in our laboratory, chloroform was the only eluent capable to dissolve the series of polyamides **FAD-BDA$_x$PDA$_y$** due to the highly apolar **FAD**. Unfortunately, the high column affinity of the fatty acid residue in chloroform at room temperature resulted in severe tailing of the polymer elution, leading to an inaccurate determination of the molar mass from these chromatograms.

2.3.2   Thermal properties of FAD-based polyamides

The thermal stability of the synthesized polyamides has been assessed with TGA

Table 2.2   Crystallization, melting and glass transition temperatures, as well as heat of melting and crystallization of polyamides synthesized from **FAD**, determined by DSC with a temperature ramp of 10 °C min^{-1}.

Polymer	$T_{m,1}$[a] °C	$\Delta H_{m,1}$[a] J g^{-1}	T_c °C	ΔH_c J g^{-1}	$T_{m,2}$[b] °C	$\Delta H_{m,2}$[b] J g^{-1}	T_g[b] °C
FAD-BDA$_{100}$PDA$_0$	57 / 87	27	69	20	89	19	-10
FAD-BDA$_{75}$PDA$_{25}$	55 / 79	24	53	11	57	11	-7
FAD-BDA$_{50}$PDA$_{50}$	53	14	23	0.7	62	4	-1
FAD-BDA$_{25}$PDA$_{75}$	58	10	-	-	62	0.3	-5
FAD-BDA$_0$PDA$_{100}$	64	22	20	1.0	69	9	-3

[a] As determined during the first heating run; [b] As determined during the second heating run.

40
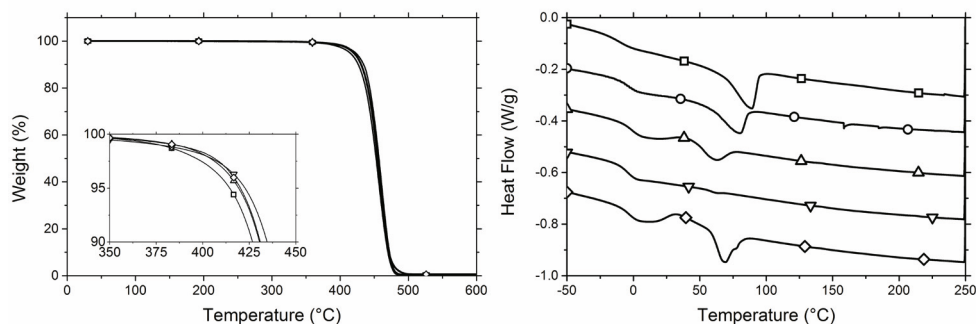
Figure 2.3 TGA (*left*) and DSC (*right,* second heating, exo up) traces of **FAD-BDA$_{100}$ PDA$_0$** (□), **FAD-BDA$_{75}$PDA$_{25}$** (○), **FAD-BDA$_{50}$PDA$_{50}$** (△), **FAD-BDA$_{25}$PDA$_{75}$** (▽) and **FAD-BDA$_0$PDA$_{100}$** (◇) measured at a heating rate of 10 °C min^{-1}. TGA is measured in an N$_2$ atmosphere and the inset shows an expanded view of the region of onset.

as reported in Figure 2.3. For all compositions the onset of degradation is above 300 °C which is sufficient for most common applications. All the studied polyamides show a similar behavior.

DSC was performed to determine the T_g values and the enthalpy of melting of the crystalline phase of the prepared polyamide samples. The DSC traces are shown in Figure 2.3 and the data extracted from these traces are collected in Table 2.2. The samples were dried well above T_g at 60 °C overnight, which most likely led to a certain extent of annealing of the polymers. Annealing during drying leads to a better crystal structure and a higher degree of crystallinity, resulting in a higher melting enthalpy in the first heating run compared to the enthalpy observed in the second heating run. This difference indicates that the cooling rate also affects the degree of crystallinity for this series of polymers. The homopolymers **FAD-BDA$_{100}$PDA$_0$** and **FAD-BDA$_0$PDA$_{100}$** show a limited degree of crystallinity with a $\Delta H_{m,1}$ of 27 and 22 J g^{-1}, respectively. Furthermore, the data in Table 2.2 show that the melting enthalpies (and hence the degrees of crystallinity) for the terpolymers decrease with increasing **PDA** content. Note that **FAD-BDA$_{25}$PDA$_{75}$** has a $\Delta H_{m,1}$ of 10 J g^{-1} and a $\Delta H_{m,2}$ of 0.3 J g^{-1}. No crystallization transition is observed for this composition in the cooling run (performed at 10 °C min^{-1}) of the DSC measurement. Reducing the heating rate to 1 °C min^{-1} increased the $\Delta H_{m,2}$ to 4.3 J g^{-1}, which is still only 43% of $\Delta H_{m,1}$ indicating that at a cooling rate of 1 °C min^{-1} crystallization of this composition
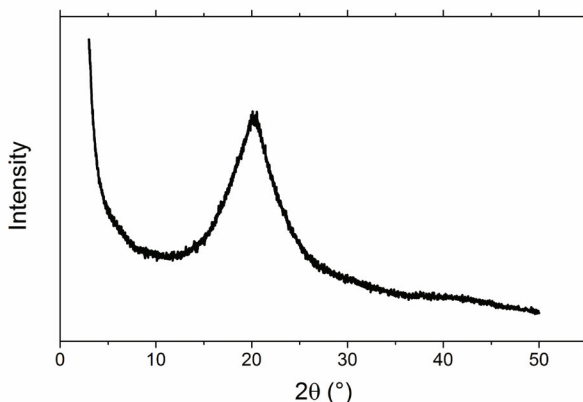
Figure 2.4 **Wide angle X-ray diffraction pattern of FAD-BDA$_{100}$PDA$_0$.**

is still limited and can be increased by annealing. The ratio of diamines in **FAD-BDA$_{25}$PDA$_{75}$** (*i.e.* 3:1 moles odd/moles even) reduces the amount of hydrogen bonds formed and, in combination with the flexibility of the **FAD** residue and the presence of its short side chains, results in the lowest degree of crystallinity approaching an amorphous polyamide. T_g values for this series of polyamides are between -10 °C and 0 °C, see Table 2.2.

The wide angle X-ray diffractogram of **FAD-BDA$_{100}$PDA$_0$** (Figure 2.4) is in agreement with observations from the DSC measurements. The shape of the obtained reflection is very broad with a narrow top, indicating an imperfect crystalline structure. With the series of polyamides **FAD-BDA$_x$PDA$_y$**, it is demonstrated that the mixing of odd- and even-numbered monomers together with the chemical structure of the dimerized fatty acid can be utilized to suppress the crystallinity of fatty acid-based, linear, bio-based polyamides.[8,9] The melting enthalpies of these polymers are negligible, indicating that almost fully amorphous materials have been obtained. Note that the T_g values measured for these compositions are much too low for many engineering applications, but could be suitable for *e.g.* adhesive applications.

2.4 Polyamides containing isoidide diamine

In the previous section, bio-based, low T_g polyamides with strongly reduced crystallinities were presented. The reason for their low T_g values is the flexibility of the

42
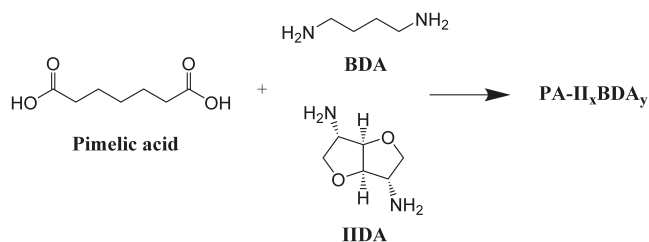
Scheme 2.2   **Synthesis of copolyamides PA-II$_x$BDA$_y$ based on pimelic acid (PA), butane-1,4-diamine (BDA) and isoidide diamine (IIDA).**

long chain **FAD** monomer. In this section, the preparation of bio-based polyamides with much higher T_g values is presented. It was expected that the chain stiffness would be increased upon incorporating a more rigid building block, such as isoidide diamine (**IIDA**, Scheme 2.2). **IIDA** is an aliphatic, bicyclic monomer consisting of two fused anhydro rings.[13] In **IIDA**, the shortest distance between the two amine functionalities is four carbon atoms, which is identical to that of **BDA**. However, previous studies indicated that the cocrystallization of **IIDA**-based polyamides with their **BDA**-based counterparts is limited.[14,15] The positive results of the mixing of odd- and even-numbered monomers will be maintained by using heptanedioic acid (pimelic acid, **PA**) instead of the **FAD** diacid, in an additional effort to reduce chain flexibility while preventing crystallization. Although pimelic acid is not synthesized bio-based, efforts have been made to harvest pimelic acid from bacterial cultures.[19,20]

2.4.1   Synthesis and chemical structure

The synthesis of the polyamides was carried out at a stoichiometric ratio of carboxylic acid and amine reactive groups (Scheme 2.2). The obtained molecular weights and molecular compositions from SEC and NMR techniques are collected in Table 2.3. The polarities of these polyamides are much higher compared to those of the fatty-acid-based series, allowing SEC to be performed using 1,1,1,3,3,3-hexafluoro-2-propanol (HFIP) as the eluent. Unfortunately, there is no good common NMR solvent as not all compositions dissolve in DMSO-d_6 while HFIP-d_2 cannot be used as it has residual solvent signals in the region of interest ($3.0 \leq \delta \leq 4.5$ ppm), hampering molecular weight calculations. A trend linking the fraction of **IIDA** in the feed and the average chain length of the polymers can be observed, see Table 2.3. Higher amounts

Table 2.3 Molecular weights and compositions of **PA**-based polyamides determined by SEC and ^{1}H-NMR.

Polymer	SEC[a]		^{1}H-NMR[b]			
	M_n	Đ	X_{feed}[c]	$X_{copolymer}$[c]	M_n	DP_n
	g mol^{-1}				g mol^{-1}	
PA-II$_{100}$BDA$_0$	3,000	1.3	100 / 99.8 / 0	100 / 91.3 / 0	1,100	7.4
PA-II$_{75}$BDA$_{25}$	3,800	1.5	100 / 75.3 / 24.8	100 / 64.3 / 24.6	1,200	9.6
PA-II$_{50}$BDA$_{50}$	4,800	1.9	100 / 49.8 / 49.9	100 / 43.3 / 46.3	2,000	16
PA-II$_{25}$BDA$_{75}$	6,100	2.0	100 / 25.0 / 75.0	Not soluble		
PA-II$_0$BDA$_{100}$	10,700	2.2	100 / 0 / 100.1	Not soluble		

[a] Number-averaged molecular weights and Đ measured by SEC in HFIP against PMMA standards; [b] Number-averaged molecular weight and composition determined by ^{1}H-NMR in DMSO-d_6; [c] Molar ratio of **PA** / **IIDA** / **BDA**.

of **IIDA** cause a decrease of M_n at constant reaction conditions. The polydispersity index shows a similar trend, indicating lower conversions for compositions with increased **IIDA** contents. The lower M_n and lower Đ upon increasing the **IIDA** fraction in the recipe are caused by two phenomena: the first reason is the lower reactivity of the amine groups of **IIDA** being attached to a secondary carbon atom compared to the amine groups of **BDA**, which are attached to a primary carbon atom. The second reason is the limited thermal stability of the isoidide diamine monomer.[15]
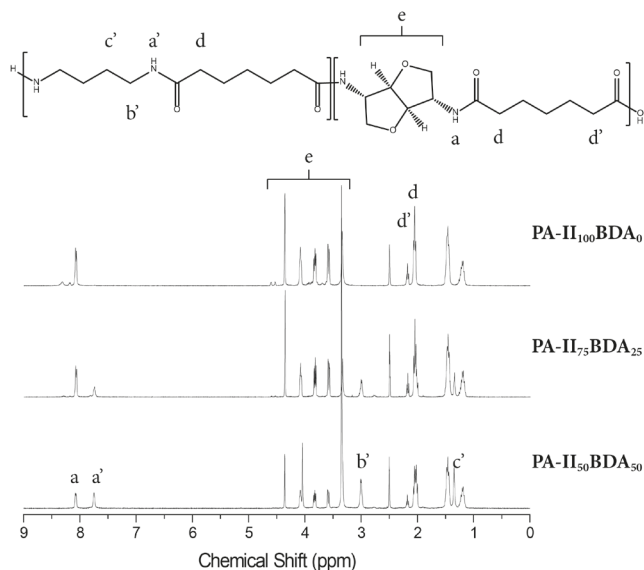
Figure 2.5 ^{1}H-NMR spectra of copolyamides **PA-II$_{100}$BDA$_0$**, **PA-II$_{75}$BDA$_{25}$** and **PA-II$_{50}$BDA$_{50}$** in DMSO-d_6.

Furthermore, SEC measurements yield M_n values of more than a factor of two higher than the M_n values calculated from ^{1}H-NMR spectra for this system. It is a common observation that polyamides show a different hydrodynamic volume than the used PMMA standards depending on the exact chemical composition, leading to miscalculated (*i.e.* overestimated) molecular weights compared to M_n values derived from NMR and titration techniques.[21] Although ^{1}H-NMR results are prone to error caused by the presence of cyclic polyamide chains and by resolution limitations, they are considered to approach the actual M_n more accurately than SEC data. The ^{1}H-NMR spectra in Figure 2.5 predominantly indicate the presence of carboxylic acid end-groups for all compositions (d' in Figure 2.5), verifying the loss of diamines during the synthesis. Obviously, the loss of diamine functionalities can easily be corrected for through the addition of an excess of diamine when targeting higher molecular weights or amine end-groups.

2.4.2   Thermal properties of IIDA-containing polyamides

The synthesized **IIDA**-containing copolyamides were subjected to TGA, see Figure 2.6 The DSC results show a direct link between the composition and the thermal stability. Increasing the **IIDA** content leads to a decrease of the degradation onset temperature from 260 °C for 100% **BDA** to values around 200 °C for 100% **IIDA**. Note that the decreased stability is partly caused by the reduced molecular weights of the
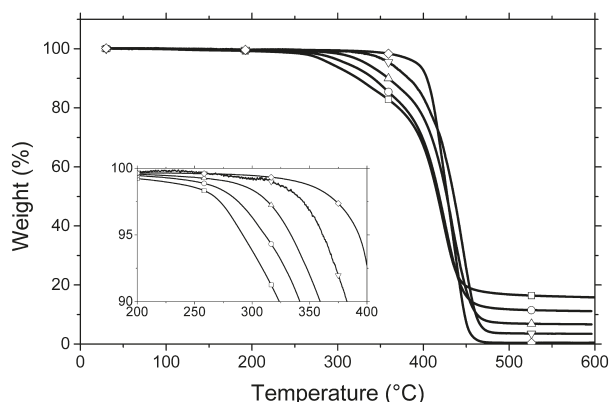
Figure 2.6   TGA traces of **PA-II$_{100}$BDA$_0$** ($\square$), **PA-II$_{75}$BDA$_{25}$** ($\bigcirc$), **PA-II$_{50}$BDA$_{50}$** ($\triangle$), **PA-II$_{25}$BDA$_{75}$** ($\triangledown$) and **PA-II$_0$BDA$_{100}$** ($\diamond$) measured in an N$_2$ atmosphere at a heating rate of 10 °C min^{-1}. The inset shows an expanded view of the region of onset.

Table 2.4 Crystallization, melting and glass transition temperatures, as well as heat of melting and crystallization of polyamides synthesized from **PA**, determined by DSC with a temperature ramp of 10 °C min^{-1}.

Polymer	$T_{m,1}$ [a] °C	$\Delta H_{m,1}$ [a] J g^{-1}	T_c °C	ΔH_c J g^{-1}	$T_{m,2}$ [b] °C	$\Delta H_{m,2}$ [b] J g^{-1}	T_g [b] °C
PA-II$_{100}$BDA$_0$	-	-	-	-	-	-	103
PA-II$_{75}$BDA$_{25}$	124	1.0	-	-	-	-	92
PA-II$_{50}$BDA$_{50}$	120 / 154	3 / 12	-	-	-	-	71
PA-II$_{25}$BDA$_{75}$	118 / 211	4 / 51	155	46	168 / 207	10 / 43	63
PA-II$_0$BDA$_{100}$	252	92	214	81	249	91	64

[a] As determined during the first heating run; [b] As determined during the second heating run.

compositions containing higher contents of **IIDA**. The thermal stability is likely to improve with higher degrees of polymerization. Finally, the polyamides containing larger quantities of **IIDA** showed higher residual masses at the end of the TGA experiments, as was observed previously for these types of polymers.[22]

Information concerning the glass transition temperatures and the enthalpy of melting of the polyamides in this series is obtained from DSC measurements. All samples were dried overnight at 60 °C, which is below the T_g of these **IIDA**-based samples. The results in Figure 2.7 and Figure 2.8 demonstrate that, despite the lower molecular weights obtained, the replacement of **BDA** by **IIDA** increases the T_g from 64 °C to 103 °C, which is significantly higher than the values obtained for the previously described **FAD**-based polyamides. Moreover, **IIDA** reduces both the melting
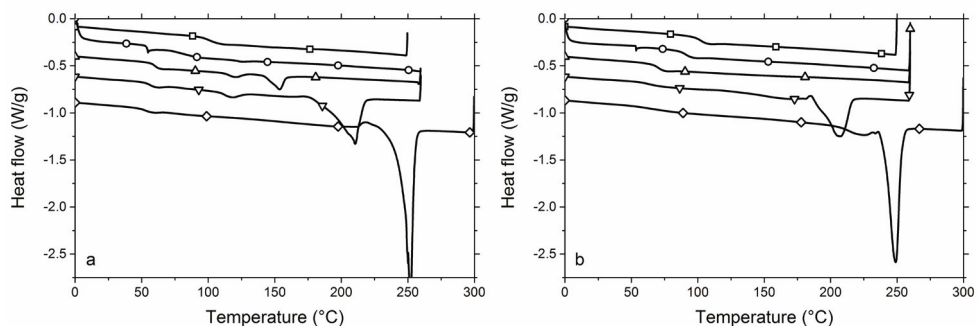
Figure 2.7 DSC melting traces of the first (a) and second (b) heating run of **PA-II$_{100}$BDA$_0$** ($\square$), **PA-II$_{75}$BDA$_{25}$** ($\bigcirc$), **PA-II$_{50}$BDA$_{50}$** ($\triangle$), **PA-II$_{25}$BDA$_{75}$** ($\triangledown$) and **PA-II$_0$BDA$_{100}$** ($\diamond$) recorded at a heating rate of 10 °C min^{-1}. Exo up.
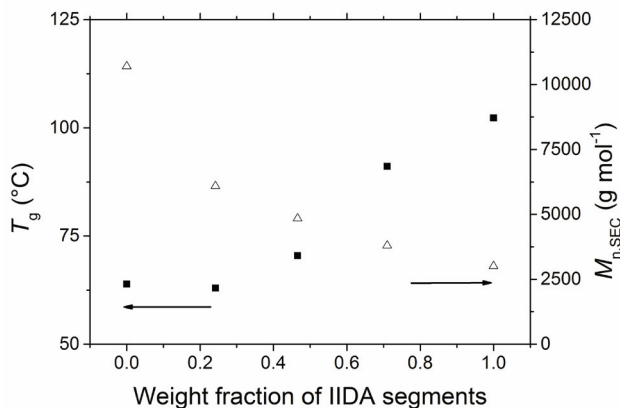
Figure 2.8 **Glass transition temperature (■) and number-averaged molecular weight (△) determined by SEC, as a function of the weight fraction of IIDA residues in the polymers with respect to the total diamine content.**

temperature and the melting enthalpy of the polyamides, see Table 2.4. Polyamides **PA-II$_{50}$BDA$_{50}$**, **PA-II$_{25}$BDA$_{75}$**, **PA-II$_{0}$BDA$_{100}$** show a modest to high melting enthalpy in the first heating run. The latter two compositions maintain their crystallinity during the second heating run while **PA-II$_{50}$BDA$_{50}$** does not crystallize from the melt at the used cooling rate, which indicates that some annealing did occur during drying at 60 °C for **PA-II$_{50}$BDA$_{50}$**. For **PA-II$_{100}$BDA$_{0}$**, no melting of a crystalline phase was observed in both the first heating and the second heating run. This indicates that the combination of the rigid **IIDA** and the odd-numbered pimelic acid prevents the formation of a crystalline phase. The reduced degree of crystallinity is also found in the enlarged difference in heat capacity before and after the T_g. This difference is proportional in size to the fraction of the amorphous phase.

Compositions **PA-II$_{50}$BDA$_{50}$**, **PA-II$_{75}$BDA$_{25}$**, **PA-II$_{100}$BDA$_{0}$** show no crystallinity in the second heating DSC trace. These materials have a melting enthalpy of 15 J g^{-1} or lower (see Table 2.4) combined with a maximum melting temperature of 154 °C in the first heating run.

Amorphous polyamides based on the fructose-derived **IIDA** were successfully synthesized. Upon increasing the **IIDA** content, the degree of crystallinity decreased to ultimately yield a fully amorphous polymer. Simultaneously, the T_g values of this series of polyamides increased to 103 °C.

2.5 Conclusions

Amorphous polyamides have been synthesized from both fatty acid- and sugar-based monomers. In both series, misalignment of the hydrogen bond donor and acceptor sites in the polyamide by the combination of odd- and even-numbered monomers proved to be a successful strategy to suppress crystallization. M_n values for the fatty acid-based series **FAD-BDA$_x$PDA$_y$** were between 4,700 and 21,000 g mol^{-1}. In this series, the amorphous character was enhanced by the presence of the side chains present in the **FAD** monomer residues, which resulted in a very low enthalpy of melting of 0.3 J g^{-1} for **FAD-BDA$_{25}$PDA$_{75}$**. The T_g values were in the range of -10 to 0 °C which make the **FAD**-based polyamides suitable for low T_g value applications like adhesives or soft-touch materials.

In the polyamide series **PA-II$_x$BDA$_y$**, the monomer isoidide diamine (**IIDA**) adds rigidity to the polymer chain and hence increases the T_g values of the polyamides up to 103 °C. Simultaneously, it reduces the degree of crystallinity to form a completely amorphous polymer for high fractions of **IIDA**. The M_n values obtained when incorporating **IIDA** are in the range of 1,000 to 2,000 g mol^{-1}, which is too low for engineering materials but could be very useful in thermosetting coating applications.

2.6 References

(1)   Morschbacker, A. Polym. Rev. 2009, 49 (2), 79–84.

(2)   Gioia, C.; Vannini, M.; Marchese, P.; Minesso, A.; Cavalieri, R.; Colonna, M.; Celli, A. Green Chem. 2014, 16 (4), 1807–1815.

(3)   Noordover, B. A. J.; Heise, A.; Malanowski, P.; Senatore, D.; Mak, M.; Molhoek, L.; Duchateau, R.; Koning, C. E.; van Benthem, R. A. T. M. Prog. Org. Coatings 2009, 65 (2), 187–196.

(4)   Gubbels, E.; Jasinska-Walc, L.; Noordover, B. A. J.; Koning, C. E. Eur. Polym. J. 2013, 49 (10), 3188–3198.

(5)   Gubbels, E.; Drijfhout, J. P.; Posthuma-van Tent, C.; Jasinska-Walc, L.; Noordover, B. A. J.; Koning, C. E. Prog. Org. Coatings 2014, 77 (1), 277–284.

(6)   Linemann, A.; Bussi, P.; Blondel, P. Transparent amorphous polyamides based on diamines and on tetradecanedioic acid. US20050272908, 2005.

(7)   Molhoek, L. J.; Kierkels, R. H. M.; Gijsman, P.; Hendrik, J.; Dutman, J. Thermosetting powder paint composition comprising a crosslinker and thermosetting amorphous polyamide. US7893169, 2011.

(8)   Kinoshita, Y. Die Makromol. Chemie 1959, 33 (1), 1–20.

(9)   Villaseñor, P.; Franco, L.; Subirana, J. A.; Puiggalí, J. J. Polym. Sci. Part B Polym. Phys. 1999, 37 (17), 2383–2395.

(10)   Rulkens, R.; Koning, C. E. In Polymer Science: A Comprehensive Reference; Matyjaszewski, K., Möller, M., Eds.; Elsevier, 2012, 431–467.

(11)   Hablot, E.; Donnio, B.; Bouquey, M.; Avérous, L. Polymer. 2010, 51 (25), 5895–5902.

(12)   Montgomery, R.; Wiggins, L. F. J. Chem. Soc. 1946, 393–396.

(13)   Cope, A. C.; Shen, T. Y. J. Am. Chem. Soc. 1956, 78 (13), 3177–3182.

(14)   Jasinska-Walc, L.; Villani, M.; Dudenko, D.; van Asselen, O.; Klop, E.; Rastogi, S.; Hansen, M. R.; Koning, C. E. Macromolecules 2012, 45 (6), 2796–2808.

(15)   Jasinska, L.; Villani, M.; Wu, J.; van Es, D. S.; Klop, E.; Rastogi, S.; Koning, C. E. Macromolecules 2011, 44 (9), 3458–3466.

(16)   Lavilla, C.; Muñoz-Guerra, S. Green Chem. 2013, 15 (1), 144–151.

(17)   Thiyagarajan, S.; Gootjes, L.; Vogelzang, W.; Wu, J.; van Haveren, J.; van Es, D. S. Tetrahedron 2011, 67 (2), 383–389.

(18)   Thiyagarajan, S.; Gootjes, L.; Vogelzang, W.; van Haveren, J.; Lutz, M.; van Es, D. S. ChemSusChem 2011, 4 (12), 1823–1829.

(19)   Zhang, W.-W.; Yang, M.-M.; Li, H.; Wang, D. Electron. J. Biotechnol. 2011, 14 (6).

(20)   Ogata, K.; Tochikura, T.; Osugi, M.; Shojiro Iwahara. Agric. Biol. Chem. 1966, 30 (2), 176–180.

(21)   Laun, S.; Pasch, H.; Longiéras, N.; Degoulet, C. Polymer. 2008, 49 (21), 4502–4509.

(22)   Wu, J. Carbohydrate-based building blocks and step-growth polymers, Eindhoven, University of Technology, 2012.

2

3

Chapter 3

Coatings from bio-based amorphous polyamides

In this chapter, the synthesis of bio-based polyamides for powder coating applications and their evaluation in a solvent-borne coating system are reported. The M_n values of the low-crystalline resins were between 3,000 and 4,000 g mol^{-1} and the resins displayed T_g values from 60 to 80 °C. Both amine and carboxylic acid functionalities (total ~0.6 mmol g^{-1}) were introduced for curing purposes. The resins were cured with triglycidyl isocyanurate (TGIC) and N,N,N',N'-tetrakis(2-hydroxyethyl) adipamide (Primid XL-552). The curing was monitored using a rheometer and the resulting cured samples were analyzed with DSC. A curing temperature of 150 °C proved insufficient to produce a fully cross-linked network. The gel content was less than 25 wt% for systems using Primid and was over 66 wt% for TGIC. The DSC analysis of the cured discs showed that all cured samples were amorphous as is desired for the targeted coating application. However, the resins require a higher curing temperature than 150 °C. Aluminum panels were coated in a solvent-borne approach at 180 °C during 1 hour. Dewetting was observed on all panels. Network formation was adequate as acetone double rubs did not damage the coatings and reverse impact tests did not produce cracks in the coatings. In conclusion, the developed bio-based polyamide resins are promising materials to be used as binder resins in powder coating applications.

3.1 Introduction

A powder coating is a solvent-free coating system. The coating of metal substrates with this technique is the largest market but many other materials like wood can also be coated, because curing can be successfully performed at lower temperatures nowadays. Powder coatings have several clear advantages compared to solvent-based coating systems:[1–5]

- Low emission of volatile organic components,
- Facile, safe application of the coating,
- Very little waste due to reuse of powder overspray,
- The curing process produces a hard, tough and durable coating.

The dry paints which constitute a powder coating, consist of a binder resin, a curing agent, pigments, and additives to enhance properties such as flow and to reduce film imperfections.[6,7] The different components are dispersed into the resin using an extruder. The residence time in the extruder is very short (~30 s) to prevent premature cross-linking, which may occur due to the relatively high temperature needed to facilitate flow of the resin. For appearance, the final coating needs to be amorphous so the binders should have a low degree of crystallinity or should be amorphous.

Powder coating systems also have some disadvantages. The curing agents are reactive compounds which are harmful to people and the environment in several cases. Furthermore, the absence of solvent makes flow and spreading of the paint onto the substrate more difficult than for solvent-based coatings. The time the powder has to flow and level is limited to minutes. Therefore, the melt viscosity needs to be as low as possible. To achieve the lowest melt viscosity, a small amount of semi-crystalline binder may be added to the otherwise amorphous binders.[8] The melting of the crystalline phase gives a sharp decrease in melt viscosity. Also, storage of the powder imposes requirements on the glass transition temperature (T_g) value of the used polymer resin, which has to be significantly higher than ambient temperature. Storage above the T_g of the powder will cause fusion of the particles, decreasing the ability to level well or even completely hamper paint application. Because of the paint storage, the binder T_g value should exceed 60 °C. As a consequence, the resulting
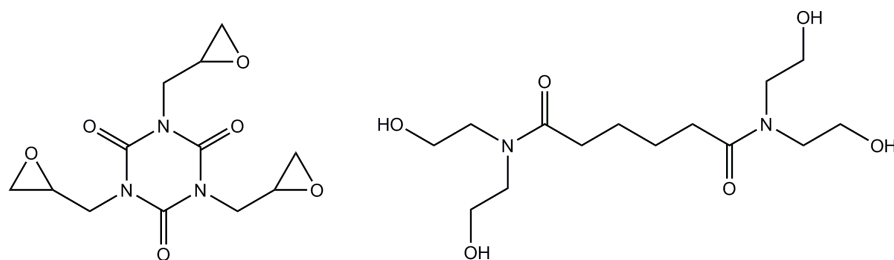
Figure 3.1   **Structures of triglycidyl isocyanurate (TGIC) and *N,N,N',N'*-tetrakis (2-hydroxyethyl) adipamide (Primid XL-552).**

coating will have a T_g value of more than 70 °C due to the curing. This will ensure a stable coating.

Several binder-curing agent combinations exist. One example is where the binders in the powder paint are polyesters with a relatively low molecular weight (M_n = 2,000 – 6,000 g mol^{-1}). These polyesters are often based on bifunctional monomers, *e.g.* terephthalic acid, isophthalic acid, adipic acid, neopentyl glycol, and ethylene glycol.[9–11] These compounds are based on petrochemicals. With depleting oil reserves, efforts are made to replace these starting materials by bio-based alternatives to create more sustainable polyesters.[12–16] The polyester binders can have either hydroxyl- or carboxylic acid-functionality. Fully condensed resins, *i.e.* only one functionality remains on the resin, increase the melt viscosity.[17] Therefore, the polymer synthesis is terminated before complete conversion to prevent either the hydroxyl value (*OHV*) or acid value (*AV*) to become zero. Furthermore, this saves the energy required to remove the last percents of condensate for achieving full conversion. Typical ranges of *OHV* and *AV* are *OHV* < 0.18 mmol g^{-1} and *AV* = 0.53 – 1.52 mmol g^{-1} for carboxylic acid-terminated resins, and *OHV* = 0.45 – 0.98 mmol g^{-1} and *AV* < 0.18 mmol g^{-1} for hydroxyl-terminated resins. Besides telechelic resins, the majority of the commercial resins contains branched structures to increase the functionality and hence, the final cross-link density to improve the coating properties.[18]

The curing agents typically used for bifunctional polyesters must have a functionality greater than two. Triglycidyl isocyanurate (TGIC, Figure 3.1) has been a widely used curing agent for the curing of carboxylic acid-functional resins.[1,7,19–21] Besides carboxylic acids, it can also react with hydroxyl groups and amines (see Scheme 3.1). However, its use in Europe is declining because of its toxicity. For
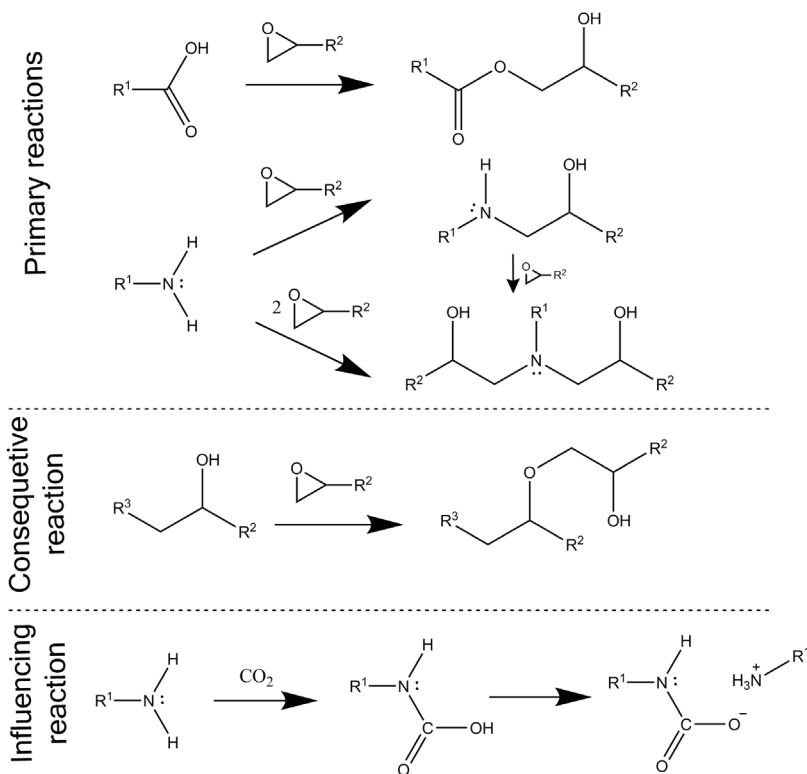
Scheme 3.1   Reactions of the epoxy group in TGIC with polyamides.
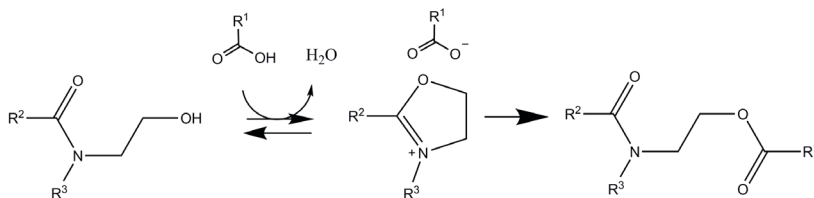
Scheme 3.2   Mechanism of the curing of carboxylic acid-terminated resins using β-hydroxyalkylamides.[23,24]

carboxylic acid-functional resins, β-hydroxyalkylamides have become popular under the tradename Primid (Figure 3.1).[1,2,7,22] These type of curing agents are non-toxic but can only react with carboxylic acid groups through an oxazolinium intermediate (Scheme 3.2). This reaction cannot be catalyzed.[23,24] Furthermore, care has to be taken when preparing thicker coatings as the reaction produces water as a condensate which can cause problems such as bubbling, pinholes, and loss of gloss. This can be prevented by the addition of plasticizers or by reducing the reaction rates.

The powder paint is applied to the substrate and heated to the curing temperature.

Depending on the reactivity of the system, little time is often available for the powder to flow and level before the critical point of gelation (p_c) is reached. At this conversion, an infinite gel has formed and macroscopic rearrangement is no longer possible. This so-called gel point can be calculated using a formula derived from the Flory-Stockmayer Theory:[25,26]

$$p_c = \frac{1}{\sqrt{r \cdot (fe_0 - 1) \cdot (ge_0 - 1)}}$$

Eq-3.1

where r is the ratio of reactive groups, f_{e0} and g_{e0} are the end group averaged functionalities of the resin and the curing agent. For the curing of polyamides, one has to take into account that two epoxy groups can react with the same amine. Therefore, fe0 is not necessarily two for a telechelic polyamide resin but depends on the titration values for carboxylic acid (AV) and amine (AmV). As an example is given a telechelic resin with an $AV = 0.36$ mmol g^{-1} and an $AmV = 0.18$ mmol g^{-1} which will be cured with Primid or TGIC. Cross-linking this resin with TGIC (COOH = A_2, NH$_2$ = A_4, epoxy = B_3) in a ratio of epoxy to end group of 1:1 gives:

6A$_2$ + 3A$_4$ + 8B$_3$ → 24 AB linkages
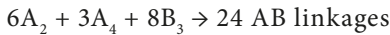
$$r = \frac{\sum_{i=1}^{n} v_i f_{Ai}}{\sum_{i=1}^{n} v_i f_{Bi}} = \frac{6 \cdot 2 + 3 \cdot 4}{8 \cdot 3} = \frac{12 + 12}{24} = \frac{24}{24} = 1$$

In which r ≤1, else B is divided by A,

$$fe_0 = \frac{\sum_{i=1}^{n} v_i f_{Ai}^2}{\sum_{i=1}^{n} v_i f_{Ai}} = \frac{6 \cdot 2^2 + 3 \cdot 4^2}{6 \cdot 2 + 3 \cdot 4} = \frac{24 + 48}{12 + 12} = \frac{72}{24} = 3$$

$$ge_0 = \frac{\sum_{i=1}^{n} v_i f_{Bi}^2}{\sum_{i=1}^{n} v_i f_{Bi}} = \frac{8 \cdot 3^2}{8 \cdot 3} = \frac{72}{24} = 3$$

$$p_c = \frac{1}{\sqrt{r \cdot (fe_0 - 1) \cdot (ge_0 - 1)}} = \frac{1}{\sqrt{1 \cdot (3-1) \cdot (3-1)}} = \frac{1}{\sqrt{4}} = 0.50$$

In which v is the amount of groups that have functionality f_A or f_B. Filling out these

55

equations for cross-linking with Primid in a ratio of hydroxyl to carboxylic acid of 1:1 ($2A_2 + 0A_4 + 1B_4$) gives:

$$p_c = \frac{1}{\sqrt{1 \cdot (2-1) \cdot (4-1)}} = \frac{1}{\sqrt{3}} = 0.58$$

Comparing these two systems, only half the groups have to react for the TGIC-cured system to form an infinite network while this number is 58% when Primid is used as a cross-linker. Note that the actual time that expires before this conversion is reached and the network is set, depends on the reaction kinetics of the reactions involved. To gain more time for given kinetics, the ratio r can be adjusted at the cost of a reduced number of cross-links.

The curing reaction of thermosets can be followed by molecular changes, the disappearance of end groups, the energy required for the reaction, or by measuring material properties. The use of rheological measurements to monitor the extent of cross-linking has been described.[27–31] Upon flow of the powder paint, the viscosity will decrease with increasing temperature. When the curing reaction starts, the viscosity will increase again due to the formed cross-links. This makes rheological measurements a convenient technique to monitor the curing as well as to assess the flow of the powder.

In this chapter, the results obtained in Chapter 2 are used to synthesize and analyze a potentially sugar-based amorphous polyamide, and to test its performance in curing and coating experiments. Before applying the resins to aluminum panels, rheology will be used to analyze the binder-curing agent combination. As mentioned, powder coatings are formulated using additives. To make a fair assessment of the properties of the binders investigated, no formulation with additives like flow agents will be applied.

3.2 Materials and methods

3.2.1 Materials

The reactants pimelic acid (**PA**, 98%), butane-1,4-diamine (**BDA**, 99%), and the cross-linker triglycidyl isocyanurate (TGIC) were purchased from Sigma Aldrich.

N,N,N',N'-tetrakis(2-hydroxyethyl) adipamide (Primid XL-552, 98%) was obtained from Alfa Aesar. 2,5-diamino-2,5-dideoxy-1,4-3,6-dianhydroiditol (isolide diamine, **IIDA**, ≥ 95%) was synthesized by Wageningen UR Food and Biobased Research.[32,33] Solvents were obtained from Biosolve in AR grade. Deuterated solvents for NMR spectroscopy were purchased from Cambridge Isotope Laboratories, Inc. All chemicals were used as received without further purification.

3.2.2 Methods

NMR spectroscopy

^{1}H-NMR (delay time 5s, 32 scans, 90°) and ^{13}C-NMR (delay time 1s, 2000 scans) spectroscopy measurements were performed on a Agilent 400-MR NMR system in DMSO-d_6. Data was acquired using VnmrJ3 software. Chemical shifts are reported in ppm relative to tetramethylsilane (TMS). Number average molecular masses (M_n) were calculated using Eq-2.1. Acid and amine values were calculated by equations Eq-3.3 and Eq-3.4 which were adapted from Eq-3.2 for use with ^{1}H-NMR data:

$$\overline{M_n} = \frac{F}{AV + AmV} \qquad \textbf{Eq-3.2}$$

$$AV = \frac{\overline{F}}{M_n} \cdot \sum_{i=0}^{n} \left[\frac{\left(\dfrac{I_{acid,i}}{H_i} \right)}{\displaystyle\sum_{j=0}^{n} \dfrac{I_{end,j}}{H_j}} \right] \qquad \textbf{Eq-3.3}$$

$$AmV = \frac{\overline{F}}{M_n} \cdot \sum_{i=0}^{n} \left[\frac{\left(\dfrac{I_{amine,i}}{H_i} \right)}{\displaystyle\sum_{j=0}^{n} \dfrac{I_{end,j}}{H_j}} \right] \qquad \textbf{Eq-3.4}$$

in which F is the average functionality (no branching: $F = 2$) and M_n the number average molecular mass of the resin, I_{acid} is the intensity of the protons ($H_{PA} = 2$) next to the free acid end groups, I_{amine} the intensity of the protons ($H_{BDA} = 2$, $H_{IIDA} = 1$) next to the free amine end groups, and I_{end} is the sum of I_{acid} and I_{amine}.

Rheometer

Rheometry experiments were performed with a TA Instruments AR-G2 using plate-plate geometry, angular frequency $\omega = 6.283$ rad s^{-1}, strain $\gamma = 1\%$. Samples were

prepared by mixing 250 mg of resin and cross-linker in a mortar, followed by cold pressing of the mixture to a disc (D = 25 mm, H = 500 nm) at a pressure of 1600 bar. The samples were all subjected to the same temperature profile: heating from 70 to 150 °C at a heating rate of 2 °C min^{-1}, isothermal at 150 °C for 60 minutes, heating to 200 °C with a heating rate of 5 °C min^{-1}, and isothermal at 200 °C for 15 minutes.

DSC

Differential Scanning Calorimetry (DSC) was performed on a TA Q1000 DSC. Approximately 5 mg of polymer or the rheology samples was accurately weighed and sealed into an hermetically closed aluminum pan. Temperature profiles were measured from 0 °C to 250 °C above Tm and consisted of two heating runs and two cooling runs, at a heating/cooling rate of 10 °C min^{-1}. TA Universal Analysis software was used for data acquisition and analysis. The value for the T_g was determined from the inflection point of the curves.

SEC

Size-exclusion chromatography (SEC) was measured on a system equipped with a Waters 1515 Isocratic HPLC pump, a Waters 2414 refractive index detector (40 °C), a Waters 2707 autosampler, a PSS PFG guard column followed by 2 PFG-linear-XL (7 µm, 8x300 mm) columns in series at 40 °C. 1,1,1,3,3,3-Hexafluoroisopropanol (HFIP, Biosolve) with potassium trifluoro acetate (20 mmol L^{-1}) was used as eluent at a flow rate of 0.8 mL min^{-1}. The molecular weights were calculated against poly(methyl methacrylate) standards (Polymer Laboratories, M_p = 580 g mol^{-1} up to M_p = 7.1·10^6 g mol^{-1}). Samples were prepared in the eluent at a concentration of 2-3 mg mL^{-1}.

Panel coating

The coating application procedure for panels was determined by several test panels at different conditions and the rheological results. Samples were prepared in duplicate onto a 15 cm and a 12.5 cm chromated aluminum Q-panel. Half of the large panel and the complete smaller panel have been rubbed using scotch brite to roughen the surface. The panels were cleaned and degreased using *n*-heptane and ethanol. A solution of resin in dimethylacetamide (DMAc, C = 0.16 g/g) was prepared at 150 °C and added to the desired cross-linker (r = 1:1.05 [2·AmV+AV]/[$v·f_{cross-linker}$]). Using a 120 µm doctor blade, a film was applied to panel at 80 °C. The panels were cured for

60 minutes at 180 °C under argon atmosphere.

Coating tests

The coated panels were subjected to several tests. The coating thickness was measured with a VF-DC B639 coating thickness gauge. The panels were rubbed with a cotton cloth drenched in acetone or ethanol for a maximum of 100 double rubs. The pencil hardness was determined using a Erichsen scratch hardness tester model 291 with Hardmuth Koh-I-Noor 1500 pencils. Finally, the panels were subjected to a reverse impact test with a 1 kg weight dropped from 1.00 meter height using a BYK-Gardner PF-5512.

3.2.3   Synthetic procedures

Acid-functional resin A

PA (4.052 g, 25.30 mmol), **BDA** (0.885 g, 10.04 mmol), and **IIDA** (2.203 g, 15.28 mmol) were charged to a closed reactor equipped with a double helical ribbon impeller, an argon inlet at the reactor (1) and a distillation setup with its own argon inlet (2) (see Figure 2.1, reactor B). Approximately 5 mL of methanol was added and only argon inlet 2 was used at a set temperature of 100 °C (reaction temperature didn't exceed 87 °C), to allow for thorough mixing and dimerization of the reactants during the initial phase of the reaction. After 21.5 hours, direct flow of argon gas over the reaction mixture was allowed to remove the methanol from the reaction mixture. After 24 hours the temperature was increased to 130 °C and 30 minutes later argon inlet 2 was used again to prevent loss of **BDA**. After 46 h, the temperature was increased to 170 °C and argon inlet 1 was used to remove the condensate during the remainder of the reaction. The reaction temperature was increased to 230 °C after 49 h. After 51.5 h
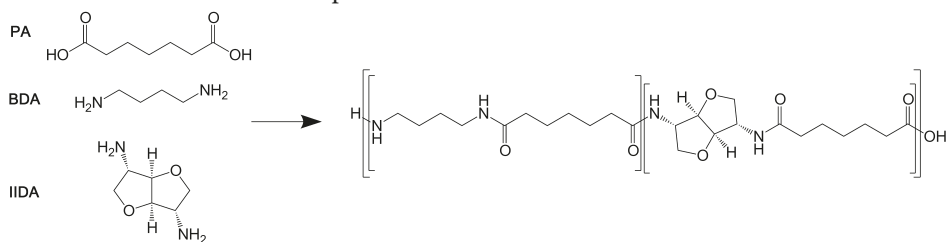
Scheme 3.3   Synthesis of polyamide resins based on pimelic acid (**PA**), butane-1,4-diamine (**BDA**) and isoidide diamine (**IIDA**).

the condensation setup was removed and the pressure in the reactor was decreased to 3.0 hPa during 2.5 h after which the product was discharged in the liquid state. Brittle, light colored, transparent compound (**A**) was obtained with a yield of 3.12 g (50.0 wt% of maximum achievable weight), and two separate fractions with a different composition of monomers (20.6 wt% and 13.9 wt%).

^{1}H-NMR (400 MHz, DMSO-d_6) δ_H (ppm) 8.10 **IIDA** NH (d, 1.1H), 7.77 **BDA** NH (t, 0.8H), 4.36 **IIDA** bridge CH (s, 1.0H), 4.08 **IIDA** CHNH (t, 1.1H), 3.82 **IIDA** *exo*-CH (q, 1.1H), 3.60 **IIDA** *endo*-CH (dd, 1.1H), 3.00 **BDA** CH$_2$NH (d, 1.6H), 2.15 **PA** CH$_2$COOH (t, 0.3H), 2.03 **PA** CH$_2$COOCH (quin, 3.7H), 1.46 **PA** CH$_2$CH$_2$CO (quin, 4.0H), 1.35 **BDA** CH$_2$CH$_2$N (quin, 1.6H), 1.19 **PA** CH$_2$CH$_2$CH$_2$ (m, 2H), ^{13}C-NMR (100 MHz, DMSO-d_6) δ_C (ppm) 172.06, 171.85, 86.04, 71.73, 55.66, 39.52, 38.10, 35.31, 34.94, 30.65, 28.29, 26.67, 25.06, 24.91.

Amine-functional resin B1 and B2

PA (2.995 g, 18.70 mmol), **BDA** (0.690 g, 7.83 mmol), and **IIDA** (1.885 g, 13.07 mmol) were charged to a closed reactor equipped with a double helical ribbon impeller, an argon inlet at the reactor (1) and a distillation setup with its own argon inlet (2) (see Figure 2.1, reactor B). Approximately 5 mL of methanol was added and only argon inlet 2 was used at a set temperature of 100 °C (reaction temperature didn't exceed 71 °C), to allow for thorough mixing and dimerization of the reactants during the initial phase of the reaction. After 69 hours the temperature was increased to 130 °C and to 140 °C 30 minutes later. After 71 hours, direct flow of argon gas over the reaction mixture was allowed to remove the methanol and condensates from the reaction mixture. After 74 h the temperature was increased to 170 °C. The reaction temperature was increased to 230 °C at 76 h. After 77 h the condensation setup was removed and the pressure in the reactor was decreased to 4.0 hPa for 1 h after which the product was discharged in the liquid state. A part of the product was obtained directly from the reactor as a brittle, greenish, transparent compound (**B1**) with a yield of 1.949 g (39.8%).

Part of the product remained in the reactor and was dissolved in 1,1,1,3,3,3-hexafluoroisopropan-2-ol (HFIP). The polymer was precipitated from a

large excess of acetone and was dried after decantation of the solvent mixture. The polymer (**B2**) was obtained as a brittle, gray-colored, opaque solid with a yield of 2.729 g (55.8%).

B1:^{1}H-NMR (400 MHz, DMSO-d_6) δ_H (ppm) 8.09 **IIDA** NH (d, 1.2H), 7.75 **BDA** NH (t, 0.8H), 4.36 **IIDA** bridge CH (s, 1.2H), 4.22 **IIDA** (monomer) bridge CH (s, 0.1H), 4.08 **IIDA** CHNH (t, 1.2H), 3.82 **IIDA** exo-CH (q, 1.1H), 3.60 **IIDA** endo-CH (dd, 1.2H), 3.00 **BDA** CH$_2$NH (d, 1.6H), 2.82 **BDA** CH$_2$NH$_2$ (d, 0.1H), 2.21 **PA** CH$_2$COOH (t, 0.1H), 2.05 **PA** CH$_2$COOCH (quin, 3.9H), 1.46 **PA** CH$_2$CH$_2$CO (quin, 4.0H), 1.35 **BDA** CH$_2$CH$_2$N (quin, 1.6H), 1.19 **PA** CH$_2$CH$_2$CH$_2$ (m, 2H), ^{13}C-NMR (100 MHz, DMSO-d_6) δ_C (ppm) 172.05, 171.84, 86.04, 71.73, 55.66, 39.52, 38.10, 35.29, 34.94, 28.29, 26.67, 25.09, 24.91.

The frequencies of **B2** are identical to **B1** except the ratio between δ_H = 3.00 and 2.82 ppm, and a contamination at δ_H = 5.2 ppm .

3.3 Synthesis of polyamide resins

Based on the results reported in Chapter 2, a composition for a powder coating resin has been chosen with **PA**, **BDA** and **IIDA** in the molar ratio of 100 : 40 : 60. This ratio should produce an amorphous polyamide with an expected T_g value of 70 °C at the targeted molecular weight between 2,000 and 6,000 g mol^{-1}. For these low M_n values, the T_g is strongly dependent on the molecular weight and, consequently, on conversion. The molecular weights achieved in Chapter 2 were on the low side, so the synthetic procedure has been adapted. Reaction times have been increased and also the inlets for inert gas have been used more carefully. An inert atmosphere is maintained throughout the reaction, but especially during the start of the procedure a flow over the melt was avoided to prevent evaporation and subsequent loss of the relatively volatile monomers. Furthermore, the reaction temperature was kept low during the first 24 hours of the reaction to allow for dimerization while limiting monomer evaporation. Both an acid-functional and an amine-functional polyamide resin are described in this chapter.

The polyamides were obtained as brittle compounds. However, the colors of the

3

Figure 3.2 **Polyamide resins A (*left*), B1 (*center*), and B2 (*right*)**

acid- and amine-functional resins differ from each other as shown in Figure 3.2. Most likely the greenish color of **B1** originates from metal ions leached from the impeller. Both **A** and **B1** are highly transparent which indicates that they are amorphous. The precipitation of **B2** yields an opaque material indicating that an ordered phase is present that scatters light at its boundaries with an amorphous phase. The total yield of **A** was 84.5 wt% of maximum achievable weight and that of B was 95.6 wt%. The yields of the polymers were satisfactory, as a synthesis on this small scale usually results in higher losses than at a larger scale.

Polyamide **A** was collected in fractions of different composition. This has two reasons: some monomers had collected in the upper parts of the reactor and may have not experienced the same temperatures as the bulk. This accounts for 16 wt% of the product. A second separate fraction was collected which may be contaminated with glass particles as the reactor broke during the discharge of the polymer. For this reason these fractions haven't been used further. As mentioned in the synthetic procedure, B was collected partly as is from the reactor (**B1**, 40.2 wt% of maximum achievable weight) and partly as precipitated product (**B2**, 55.4 wt%)

3.3.1   Characterization of polyamide resins

The polyamide resins have been analyzed in terms of their molecular weights and compositions using SEC and NMR techniques (see Table 3.1). The acid value (*AV*) and amine value (*AmV*) are important properties of a resin and are commonly determined using end-group titration. Proper end-group titration requires two to three grams of polymer. However, due to the small amount of polyamide synthesized, titration could not be performed and consequently *AV* and *AmV* were calculated from NMR data using Eq-3.2 and Eq-3.3. With optimized NMR measurement settings and data analysis, the resulting error is around 10 %.

Table 3.1 SEC and ¹H-NMR results for polyamide resins A, B1, and B2.

Polymer	SEC[a]		¹H-NMR[b]					
	M_n g mol^{-1}	Đ	X_{feed}[c]	$X_{copolymer}$[c]	M_n g mol^{-1}	DP_n	AV[d] mmol g^{-1}	AmV[d] mmol g^{-1}
A	8030	2.8	100 / 60.4 / 39.7	100 / 51.1 / 34.4	3130	25.1	0.64	0
B1	8760	2.3	100 / 69.9 / 41.9	100 / 62.9 / 41.4	3110	25.2	0.17	0.47
B2	10700	2.1	100 / 69.9 / 41.9	100 / 62.1 / 40.2	3720	30.1	0.13	0.41

*[a] Number-average molecular weight and Đ measured by SEC in HFIP against PMMA standards; [b] Composition, number-average molecular weight, number-average degree of polymerization, and acid and amine values determined by ¹H-NMR in DMSO-d$_6$; [c] Molar ratio of **PA / IIDA / BDA**; [d] Calculated using Eq-3.3 and Eq-3.4*

The results of the SEC measurements (see Table 3.1) indicated that significantly higher M_n values were obtained for polyamides **A**, **B1**, and **B2** compared to the results reported in Chapter 2 which ranged from 3,800 to 4,800 g mol^{-1} for similar compositions, respectively. The dispersity indices reported in Chapter 2 were also much lower (1.5-1.9) than the values obtained for resins **A**, **B1**, and **B2**. The larger Đ values were due to the higher conversions achieved. Figure 3.3 shows the molecular weight distributions for **A**, **B1**, and **B2** which have a similar shape for all three polyamides.

The resins were analyzed using ¹H- and ¹³C-NMR spectroscopy (see Figure 3.4). The resonances have been assigned as in the previous chapter. In contrast to Chapter 2, a signal was observed for the proton next to an amine end-group in **IIDA** (e') at δ = 4.2 ppm. This indicated that the excess amount of **IIDA** used for the synthesis of **B1**
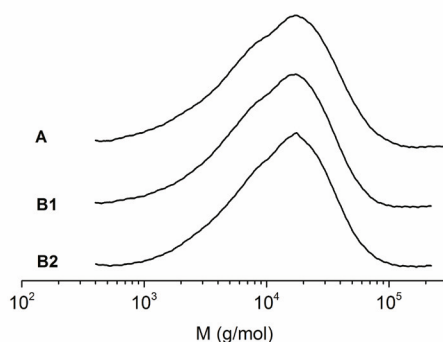
Figure 3.3 SEC traces of resins **A**, **B1**, and **B2** with HFIP as eluent, relative to PMMA standards.

3
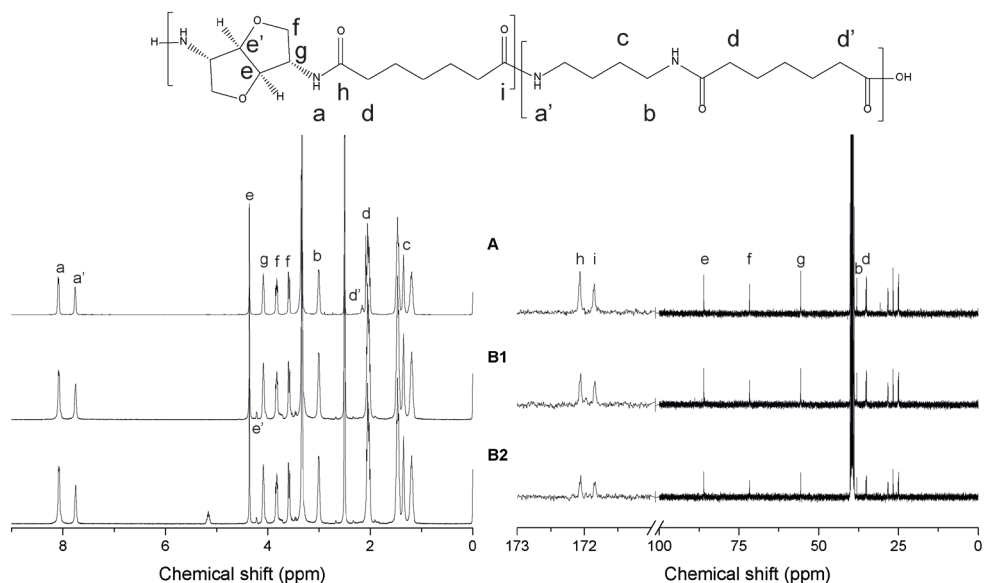
Figure 3.4 ^{1}H- and ^{13}C-NMR spectra and assignment for polyamides A, B1, and B2 recorded in DMSO-d_6.

and **B2** was incorporated and resulted in amine end-groups. End-groups formed by **BDA** accounted for less than 20% of all amine end groups in **B1** and **B2**. The different ratio of end-group signals for **IIDA** and **BDA** with respect to their feed ratio is due to the higher reactivity of the **BDA** amine groups. Therefore, more **BDA** was incorporated into the backbone of the polymers compared to **IIDA**. For **A**, no free amines were observed. For all three compositions, the resonance of the CH$_2$ protons adjacent to unreacted carboxylic acid moieties could be observed at $\delta = 2.2$ ppm, which indicated the presence of carboxylic acid end-groups. In the spectrum of **B2**, a resonance was observed at $\delta = 5.2$ ppm. This signal couldn't be assigned. The ^{13}C-NMR spectra were very clean. All signals could be assigned to the expected polyamide structures.

The data collected in Table 3.1 show that the M_n and DP_n values of **A** and **B1** were very similar, yet the molecular composition differed. As in Chapter 2, a loss of both diamines was observed and this had to be compensated for using the feed ratio to achieve the desired final polymer composition. The calculated AV and AmV are in an suitable range for powder coating resins (target: ~0.50 - 0.70 mmol g^{-1}). The precipitation of **B2** resulted in slightly higher values for M_n and DP_n and lower values for AV and AmV compared to **B1**, which had a very similar composition. This

64
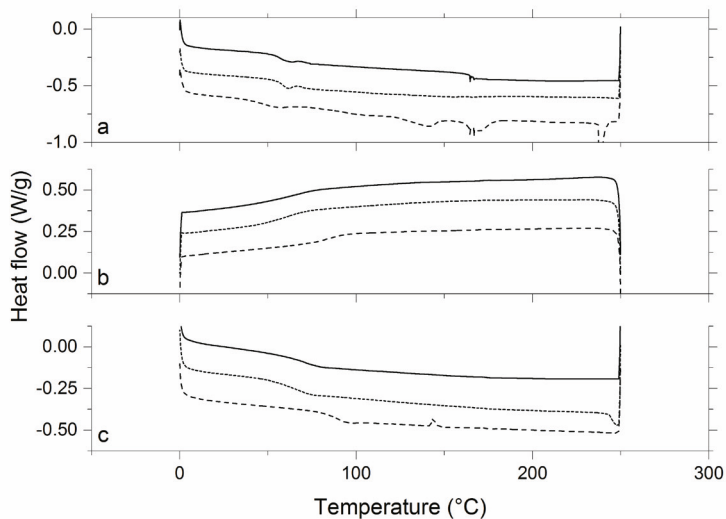
Figure 3.5   DSC thermograms of the (a) first heating, (b) cooling, and (c) second heating run of **A** (solid), **B1** (short dash), and **B2** (long dash), recorded with a temperature ramp of 10 °C min^{-1}. The exotherm is directed upwards and the graphs have been shifted vertically for clarity.

is because the shortest chains in **B2** could remain in solution in the mixture of HFIP (solvent) and acetone (non-solvent, large excess) used for precipitation.

The polyamide resins have been thermally characterized with DSC. The results are reported in Figure 3.5 and Table 3.2. During the first heating run, all three polyamides showed a moderate melting endotherm between 100 and 200 °C with $\Delta H_{m,1}$ ranging from 10 to 17 J g^{-1}. This indicated that some ordered phases were present in the polymers after uncontrolled cooling due to collection of the material from the melt. Furthermore, **B2** showed a sharp melting peak at 238 °C. This can be explained by crystallized short PA-4,7 segments, which together with the observation of an increased ratio of **IIDA** chain ends in ^{1}H-NMR, suggests that the molecular composition was not completely random. The T_g values determined from the first heating trace were between 45 and 55 °C, which is well above room temperature. Therefore, as the polymers had no mobility during storage at room temperature, the first heating run shows the ordering in the polymers obtained from uncontrolled cooling during the discharge of the reactor.

The cooling runs showed no crystallization phenomena for these polyamides, which therefore remained amorphous. In the second heating run, the T_g values showed

65

Table 3.2 Thermal properties of polyamide resins A, B1, and B2 as obtained from DSC with a temperature ramp of 10 °C min^{-1}.

Polymer	$T_{m,1}$[a] °C	$\Delta H_{m,1}$[a] J g^{-1}	$T_{m,2}$[b] °C	$\Delta H_{m,2}$[b] J g^{-1}	T_g[b] °C
A	175	15	-	-	71
B1	151	10	177	2.7	64
B2	141 / 167 / 238	14	-	-	89

[a] As determined during the first heating run; [b] As determined during the second heating run.

some spread despite that the polymers had similar M_n values. The precipitation of **B2** did remove some of the shorter chains which can act as plasticizers. Therefore, it is expected that **B2** had a higher T_g value than **B1**, but the difference was larger than anticipated. This indicated that the molecular weight of **B2** was significantly higher than that of **B1**. The T_g value of **A** was similar to the value expected from the results of Chapter 2. Polyamide **B1** showed an endothermic peak during its second heating run just before reaching 250 °C. Polyamide **B1** continues to melt in the isothermal section of the DSC measurement. The exact origin of this endothermic peak at high temperature is unclear as it was not reproducible. Possibly, some additional reaction occurred.

The characterization of the polyamides indicates that polymers have been synthesized which have suitable M_n values and end-group content for powder coating applications. Especially the extension of the reaction time led to much higher M_n values than obtained for the polymers described in Chapter 2. The thermal characterization with DSC indicated that T_g values were adequate and the degree of crystallinity was low. During the second heating run they were amorphous.

3.4 Curing of the polyamide resins

Ultimately, the polyamides reported in this dissertation are intended to replace petrochemistry-based resins used in powder coatings. Therefore, the synthesized resins were analyzed in terms of their curing behavior with two well-known curing agents: triglycidylisocyanurate (TGIC, a trifunctional epoxy) and *N,N,N',N'*-tetrakis(2-hydroxyethyl) adipamide (Primid XL-552, a tetrafunctional *β*-hydroxy
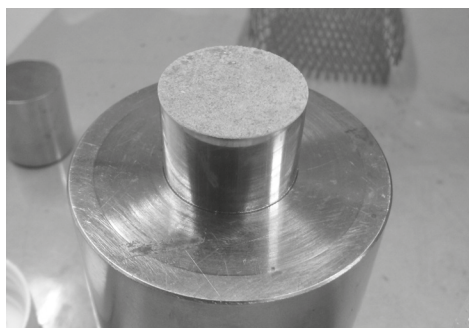
Figure 3.6   Sample disc for rheology after pressing.

alkamide). TGIC is capable of reacting with both acid- and amine-functional resins, while the activated OH-groups of Primid will only react with acid-functionalities. Resin **A** is expected to perform similarly with both cross-linkers, while the resins **B1** and **B2** should in principle form a more dense network with TGIC than with Primid because of the presence of amine groups (see Scheme 3.1 and Scheme 3.2).

3.4.1   *Monitoring the curing reaction in a rheometer*

To follow the curing reactions between the cross-linkers and the resins, a rheometer was used. Sample discs were prepared by cold pressing the resins **A** and **B1** and one of the cross-linkers at high pressure (1600 bar) and room temperature (Figure 3.6). The compositions of the samples are provided in Table 3.3. The higher amine value of **B1** compared to that of **A** (0.47 vs. 0 mmol g^{-1}, respectively) results in a significantly lower point of gelation (p_c) when TGIC was used. The presence of amine groups effectively increased the functionality of the polymer chain (f_{e0}) from 2.0 (with Primid) to 3.7 (with TGIC). This likely resulted in differences in the final cross-link density and hence the toughness and hardness of the final coating. When Primid XL-552 was used, a different phenomenon occurred. While for resin **A** all the end groups (*i.e.* carboxylic acid groups, see Table 3.1) can be fully cross-linked, for polyamide **B1** only the carboxylic acid groups can react, while the amine end groups remain as dangling chain ends (see Scheme 3.2). Because the *AmV* is higher than the *AV*, some chains which will have one amine group and one carboxylic acid group, and a large fraction of the polymers will bear two amine groups at both ends. This results in polymers that will have reacted only once, and chains that were not cross-linked and remained as free chains in the network.

67

Table 3.3 Composition and resulting stoichiometric ratio (*r*) and critical point of gelation (p_c) for rheology samples based on **A** and **B1**.

Experiment	Polymer	*m*	Curing agent	m	*r*	p_c
		mg		mg		
1	**A**	249.87	TGIC	16.51	0.96	0.72
2	**A**	249.68	Primid	13.58	0.94	0.60
3	**B1**	257.39	TGIC	29.94	0.95	0.44
4	**B1**	262.17	Primid	3.93	0.92	0.60

Sample discs were loaded in the rheometer at 70 °C and the curing reaction was followed during a temperature program (see Figure 3.7). Unfortunately, some samples (1 and 2) had defects at the edges which will affect the measurement. The measured viscosities and moduli will be lower than their actual values. An insufficient amount of material remained to prepare new samples, so the results should be considered in a qualitative and not in a quantitative manner. The samples were heated gradually to 150 °C and kept at this temperature for 60 minutes to cure. Subsequently, the temperature was increased to 200 °C to assess the cross-linking in the system.

During heating all samples behaved as solids until roughly 20 min (T = 110 °C), at which point the graph smoothened out. For 1 and 2 (resin **A**), fluctuations were observed in the first fifty minutes of the experiments. Although at different temperatures, both experiments 1 and 2 showed a sudden decrease in the viscosity at 150 °C. It is likely that these were a result from the damaged samples because the samples experience a compressive force by the machine. The samples may flow when the polymers achieve sufficient mobility, which could result in the expulsion of trapped air pockets from the sample. This leads to a volume change in the total sample, which may cause reduced contact between sample and machine. Both samples were submitted to a trial experiment with a similar temperature profile in which this unexpected drop was not observed. After this event, the viscosity increased in time which indicated cross-linking of the resin. At *t* = 80 minutes the viscosity of sample 2 reaches a plateau value of 2,900 Pa·s.

Samples 3 and 4 showed an initial decrease of the viscosity as the polymers achieved mobility. At 136 °C, sample 3 (**B1**+TGIC) showed an increase of the viscosity, indicating that the viscosity increase is dominated by cross-linking. Sample 4 showed a

viscosity decrease until the isothermal section of the measurement at 150 °C, at which point the viscosity started to increase. The viscosities of all the samples increased during the hour at which the temperature was kept at 150 °C. When the temperature was further increased, all samples showed a decrease of the viscosity, indicating that curing wasn't complete. For sample 3, this drop was 25% but the other samples show a decrease of up to two orders of magnitude. Sample 1 cross-linked very fast starting from 175 °C as the viscosity increased 140-fold in 10 minutes. For the samples based on Primid (2 and 4), the viscosity decreased continuously until the isothermal section at 200 °C was reached. From this point on the viscosity increased again but no plateau was reached before the end of the measurement, indicating incomplete curing. It should be noted that the reaction between Primid and the resin produces water as a condensate. Therefore, this water has to diffuse to the edge of the disc where it will be removed by the inert nitrogen gas flow. The increase in the viscosity will hamper the diffusion of water during reaction and hence limit the conversion.

None of the samples achieve complete curing after one hour at 150 °C. TGIC shows much faster curing than Primid XL-552 for both resins. The final values for the complex viscosity are in the same order of magnitude as cured systems based on epoxy-acid and epoxy-amine reactions.[30,34]

Figure 3.8 shows the *G'*, *G"* and *tan δ* of the rheological experiments. When *G"*
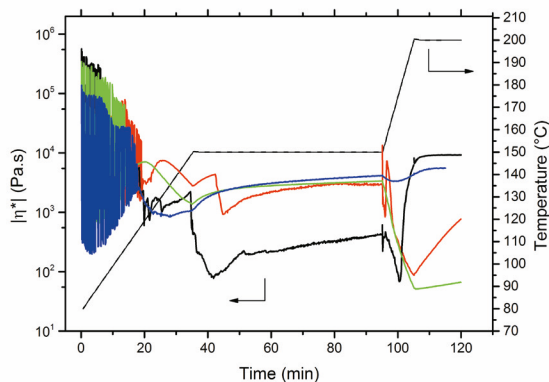
Figure 3.7 **Complex viscosity and temperature profile as functions of time for experiments 1 (black), 2 (red), 3 (blue), and 4 (green) as noted in Table 3.3 with angular frequency ω = 6.283 rad s⁻¹, strain γ = 1%. Note: samples 1 and 2 were not perfectly circular.**
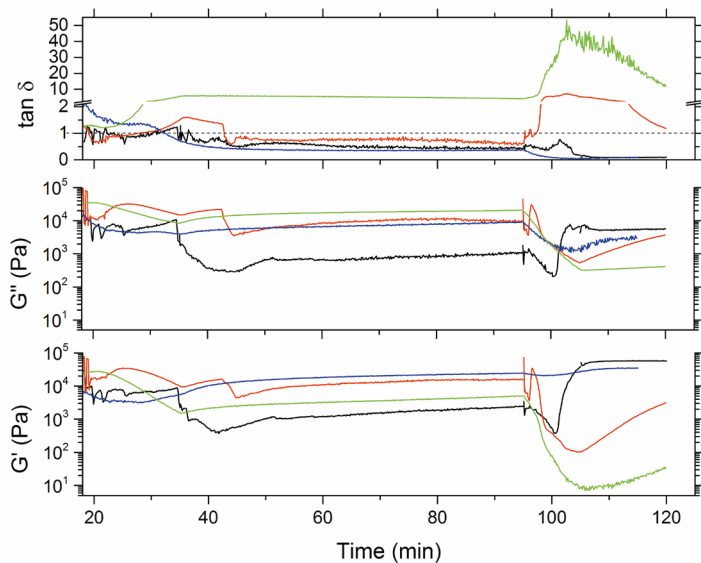
Figure 3.8 *Tan δ*, *G'*, and *G"* as function of time for experiments 1 (black), 2 (red), 3 (blue), and 4 (green) as noted in Table 3.3 with angular frequency *ω* = 6.283 rad s^{-1}, strain *γ* = 1%. Note: samples 1 and 2 were not perfectly round.

is larger than *G'*, the system behaves predominantly as a viscous liquid. At *G'* > *G"*, the system is behaving mostly like an elastic solid. Therefore, at *G'* = *G"*, or *tan δ* = 1, the system transfers from liquid to solid behavior. This point is the crossover point and is regarded as the gel point.[35] Samples 1, 2, and 3 showed *tan δ* < 1 during the isothermal curing at 150 °C and became cross-linked gels. Sample 4 remained a viscous liquid. Upon heating to 200 °C, the *tan δ* of sample 2 increased again to six. This indicated that the system contained thermally labile physical cross-links, in addition to the chemical cross-links. The cross-linker and resin may have formed hydrogen bonds which will break upon further heating. When a temperature of 200 °C is reached, *tan δ* decreases again indicating that the cross-linking reaction continues. The crossover point is almost achieved at the end of the experiment. Sample 4 has *tan δ* > 1 during the entire temperature profile indicating that either no complete curing is possible, or that energy input of this temperature profile is insufficient to bring the reaction to completion. The low ratio of acid to amine end groups (1 : 2.8) is most likely the reason for the lack of gelation. As the *AV* is less than half the *AmV*, fully amine-terminated polymers will reside in the final coating when Primid is used as a curing agent.

Sol-gel analysis of rheometer products

The gel content of the samples has been determined (Table 3.4). Part of the samples have been soaked in DMAc overnight at 110 °C to extract the soluble fraction above T_g. Afterwards, the samples were filtered and dried at p = 4 Pa until constant weight. The remaining solid content of the samples with TGIC were 97 and 66 wt%, respectively. For samples containing Primid, these were 27 and 12 wt%. Clearly, TGIC forms a network which is cross-linked to a higher extent compared to Primid. This observation supports the results obtained from the rheological experiments. The temperature profile used was not suitable to fully cure the Primid-based system and therefore the sol-content was high.

Table 3.4   Gel content of rheology samples

Experiment	Polymer	Curing agent	Sample mg	Gel mg	Gel content wt%
1	**A**	TGIC	48.6	47.0	97
2	**A**	Primid	55.0	15.1	27
3	**B1**	TGIC	91.1	60.2	66
4	**B1**	Primid	56.2	6.7	12

3.4.2   DSC analysis of cured samples

The samples of the rheology measurements have been dried over P_2O_5 at room temperature prior to analysis using DSC (see Figure 3.9). The thermograms are depicted against time to visualize the isothermal sections. The first heating run showed two T_g values (49 – 61 °C and 72 – 87 °C) for all four samples. The presence of two separate T_g values indicates that two phases were present, The first transition at lower temperatures was due to domains of pure resin with unreacted cross-linker. The cross-linker will act as a plasticizer and hence reduce the T_g of the unreacted resin.[17] The second transition was 21 to 35 °C higher and is attributed to the T_g value of the formed network. The T_g of the network is usually higher than that of the resin.

All samples showed an exothermic reaction in the first heating run. For sample 1 (11 J g^{-1}, 178 to 250 °C) and 3 (27 J g^{-1}, 164 to 250 °C) these were rather clear, while for 2 and 3 the curing was observed mostly while the samples were kept isothermal at
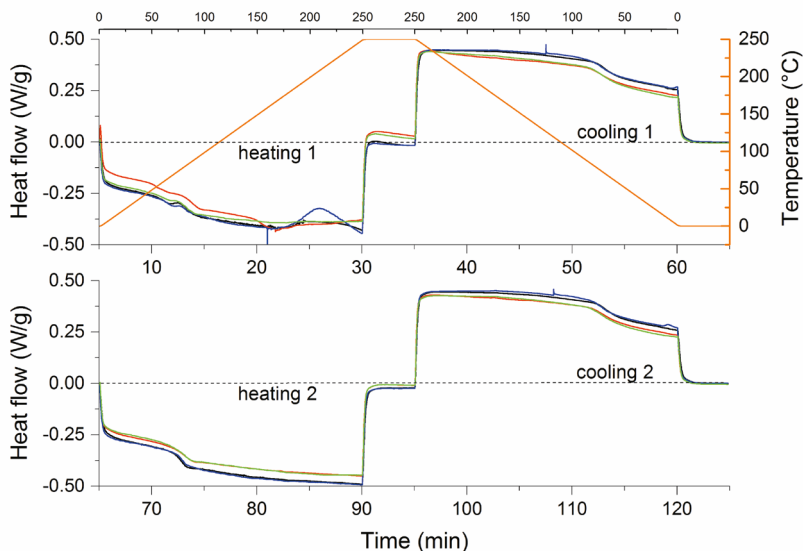
Figure 3.9 DSC thermograms as functions of time for samples 1 (black), 2 (red), 3 (blue), and 4 (green) after the rheology experiment. Temperature profile depicted in orange and as top X-axis to help the reader. The exotherm is directed upwards.

250 °C. This indicated that for both polyamides, the reaction with TGIC proceeded more readily than with Primid.

During the cooling run, none of the samples showed crystallization, indicating that the networks were amorphous. A neat glass transition was observed. The second heating run showed only one T_g value of 78 - 81 °C for all samples, indicating that the distinction between the domains in the samples had disappeared. This verifies that the T_g value at 49 - 61 °C was caused by unreacted species. Furthermore, no curing is observed in this heating run. The second cooling run is a copy of the first cooling run.

The DSC thermograms of the rheology samples indicated that none of the formulations were fully cured after the rheology measurements. As mentioned before, amine end groups present in the resin can react twice with one epoxy of TGIC while the carboxylic acid can react only once with both the epoxy as well with the hydroxyl of Primid. Therefore, the high amine value of **B1** was expected to yield the highest network density when cured with TGIC. However, all samples had very similar T_g values after curing and all the formed networks appeared to be amorphous.

3.4.3   Coating properties

The resins described in this chapter have been tested on standard chromated aluminium Q-panels for their coating performance upon curing. It was decided not to add other additives like flow agents, degassing agents, and pigments to make a fair comparison between the resins prepared. The resins were cured with TGIC and Primid, both with 5 mol% excess relative to the amount of reactive resin end-groups. To properly assess a powder coating, at least 100 gram of the formulation should be prepared, of which about 50 wt% consists of the resin. Unfortunately, this amount of resin could not be prepared due to limited availability of monomer and, consequently the resins were cured from solution in smaller scale experiments. The use of *N*-methylpyrrolidone as solvent led to strong discoloration and therefore *N,N*-dimethylacetamide (DMAc) was selected as the most suitable solvent in terms of dissolving power and final coating appearance. It was observed that, at room temperature, a solution of polyamide resin (C_{solids} = 17 wt%) in DMAc formed a physical gel. To prevent this gelation, the coatings were applied onto a heated Q-panel. Based on test panels and the results of the rheology experiments, the wet paints were cured at 180 °C for one hour in an inert atmosphere.

Comparing the resulting coatings, almost all panels showed dewetting despite the fact that the surface energy of the aluminum surface was increased by roughening with scotch brite (see Figure 3.10). Especially for resin **B2**, a very irregular coating was obtained. For **A**, many craters were observed with both curing agents. **B1** produced the best results: with TGIC a fairly smooth surface with some craters formed. This indicated that the surface tension of the resin solution is rather high. The surface tension is a measure for the force that tries to decrease the surface area. A surface with a low surface energy will not wet properly, and contamination with hydrophobe particles (*e.g.* dust particles) can cause cratering. With Primid the coating was smooth but a large amount of material flowed to the edges. The large difference between **B1** and **B2** is due to removal of low molecular weight chains in the precipitation. These have a higher mobility than higher molecular weight polymers.

The thickness of the coatings was measured around 10 μm which was roughly half of the calculated value. This can partly be explained by the application of the paint

TGIC

Primid
XL-552

A   **B1**   **B2**
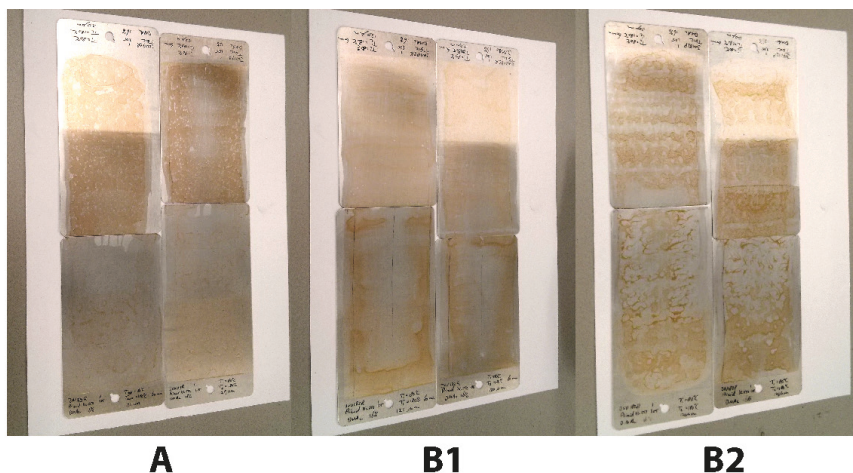
Figure 3.10 Q-panels coated with cured polyamide resins (1:1.05 resin/curing agent) from solution, C_{solids} = 17 wt%, t_{cure} = 60 minutes at 180 °C under argon atmosphere. The larger 15 cm panels have been partially roughened with scotch brite.

at 80 °C. This decreased the viscosity and it was observed that all solutions flowed between the edge of the doctor blade and the panels. This produced a wider coating than intended, reducing its thickness. The color of the coatings is subject to thickness and substrate, but the color is reasonably light.

Several tests have been performed on the coated panels. The results are collected in Table 3.5. As mentioned, the thicknesses of the coatings were low. Despite that, all the coatings passed the solvent resistance double rub test with acetone without showing damage. To further examine the solvent resistance of these films, ethanol was applied during the double rub test. Ethanol is a better solvent for amorphous polyamides. Repeating the test with ethanol revealed large differences between the coatings. Except for **B1** cured with TGIC, all coatings failed well before reaching 100 double rubs. **B1** cured with TGIC did lose its gloss during the rubbing, probably due to swelling of the coating, but it remained undamaged and regained gloss upon evaporation of the ethanol. The failure of the other formulations indicates that network formation was insufficient in most cases. Especially formulations cured with Primid were easily damaged. For the combinations of **B1** and **B2** cured with Primid this was expected as the curing chemistry should yield unreacted chains in the final coatings. These results are in agreement with the observations from the rheological and DSC experiments described in the previous two sections. Also these experiments

Table 3.5   Ratio between reactive groups, gel point, and test results of the coatings from A, B1, and B2.

Polymer	Curing agent	r	p_c	D	Pencil hardness	Reverse impact	Double rub	
				µm			acetone	ethanol
A	TGIC	0.94	0.73	9-15	2H	No fractures	100+	45
A	Primid XL-552	0.95	0.59	8-15	2H	No fractures	100+	10
B1	TGIC	0.95	0.44	11-16	4H	No fractures	100+	100+
B1	Primid XL-552	0.89	0.61	4-12	F	No fractures	100+	10
B2	TGIC	0.94	0.44	3-13	n.d.	No fractures	100+	24
B2	Primid XL-552	0.96	0.59	0-60	n.d.	No fractures	100+	8

showed insufficient cross-linking of the resins, especially when Primid was used as the curing agent.

Pencil hardness values of the coatings were between F and 4H. This is similar to literature, and for **B1** with TGIC it is even higher than common values.[1] The pencil hardness test could not be performed on the coatings made from **B2** as the highly irregular surface is unsuitable. The reverse impact test, in which a 1 kg weight is dropped from 1.00 m on the back of the panels, was passed by all compositions. The thin coating may have helped to prevent cracks. Although even the thicker areas, especially in **B2**-Primid, were free of fractures.

In summary, it was possible to produce a coating with the described polyamide resins. Network formation was inadequate for most compositions. For all experiments, TGIC performed better than Primid. During the coating tests on aluminum panels, only polyamide **B1** could be sufficiently cross-linked using the epoxy-based TGIC. The introduction of a small amount of branching points in the polymers can increase the network density, and hence is a necessity to obtain better solvent resistance and overall coating performance. After this modification it would be interesting to produce small scale powder paints for testing. Working without solvent may also solve the problems with dewetting of the substrate. Alternatively, the wetting could also be improved by partly replacing the **BDA** with bio-based neopentylglycol analogues.

3

3.5 Conclusions

In this chapter, the synthesis, characterization, and testing of polyamides based on pimelic acid, butane-1,4-diamine, and isoidide diamine have been described. These have been developed for powder coating applications The M_n values of these polyamides were between 3,000 and 4,000 g mol^{-1} and they had suitable values for functionality, with both amine as carboxylic acid end groups. The T_g values exceeded 60 °C and the crystallinity was low with $\Delta H_m \leq 20$ J g^{-1} in the first heating run. Controlled heating and curing during the DSC experiment produced amorphous polyamides.

The curing of the polyamide resins with TGIC or Primid XL-552 (see Figure 3.1) was investigated using a rheometer and subsequent DSC analysis. The data indicated that a curing temperature of 150 °C is insufficient to produce a fully cross-linked product. Furthermore, TGIC performs significantly better than Primid for both carboxylic acid and amine-terminated resins. After the experiment, the gel content of systems with Primid was less than 25%. However, for TGIC it was over 66% (up to 97%). The results of DSC analysis of the cured discs demonstrated that additional curing occurred at higher temperatures. Therefore, a higher temperature than 150 °C is necessary for curing the resins. Furthermore, all the cured samples were amorphous.

Standard aluminum Q-panels were coated with a solution of resin and curing agent in DMAc. Curing was done at 180 °C in an inert atmosphere during 1 hour based on the rheology results. Dewetting of the coatings on the aluminum panels was observed. Especially resin **B2** formed a very irregular coating. The other two resins, *i.e.* **A** and **B1**, resulted in coatings showing cratering of which **B1** formed the smoothest coatings. Network formation was shown to be inadequate as ethanol double rubs damaged most of the coatings. Pencil hardness values were between F and 4H which is similar to literature. The reverse impact tests showed the coatings to be flexible as no fractures were observed. A remark has to be made that the coatings were rather thin with thicknesses around 10 μm.

In conclusion, the developed resins can be used with standard cross-linkers of which the epoxy-based cross-linker showed better results than the *β*-hydroxyalkylamide-based curing agent. To obtain well-performing coatings, a higher cross-link density

of the network is necessary and therefore the functionality of the resins needs to be increased. Furthermore, the wetting of the substrates is poor. Therefore, either the resins have to be modified to reduce their surface energy, or additives have to be added to reduce the surface tension of the paint.

3.6 References

(1)   Misev, T. .; van der Linde, R. Prog. Org. Coatings 1997, 34 (1-4), 160–168.

(2)   Minesso, A.; Moens, L.; Amor, A. H. Powder compositions. WO2009106454 A1, 2008.

(3)   Wicks, Z. W. J.; Jones, F. N.; Pappas, S. P. J. Coat. Technol. 1999, 71 (895), 67–73.

(4)   Wicks, Z. W. J.; Jones, F. N.; Pappas, S. P. J. Coat. Technol. 1999, 71 (892), 41–46.

(5)   Weiss, K. D. Prog. Polym. Sci. 1997, 22 (2), 203–245.

(6)   Wicks, Z. W. J.; Jones, F. N.; Pappas, S. P. J. Coat. Technol. 1999, 71 (893), 47–51.

(7)   Loutz, J. M.; Demarteau, W.; Vandervorst, D. Characterization and Control of Odours and VOC in the Process Industries, Studies in Environmental Science; Elsevier, 1994; Vol. 61.

(8)   O'Keeffe, L. J.; Nixon, S. A.; Cameron, C.; Penman, A. K. Coating compositions. WO1991014745, 1991.

(9)   Belder, E. G.; Linde, R. van der; Schippers, J. Polyester and its use in powder coating. US4528341, 1985.

(10)   Misev, T. A. Powder Coatings: Chemistry and Technology, 1st ed.; Wiley: Chichester, 1991.

(11)   Awasthi, S.; Agarwal, D. J. Coatings Technol. Res. 2007, 4 (1), 67–73.

(12)   Noordover, B. A. J. Biobased step-growth polymers chemistry, functionality and applicability, Eindhoven, University of Technology, 2007.

(13)   Haveren, J.; Oostveen, E. A.; Miccichè, F.; Noordover, B. A. J.; Koning, C. E.; Benthem, R. A. T. M.; Frissen, A. E.; Weijnen, J. G. J. J. Coatings Technol. Res. 2007, 4 (2), 177–186.

(14)   Raquez, J.-M.; Deléglise, M.; Lacrampe, M.-F.; Krawczak, P. Prog. Polym. Sci. 2010, 35 (4), 487–509.

(15)   Gioia, C.; Vannini, M.; Marchese, P.; Minesso, A.; Cavalieri, R.; Colonna, M.; Celli, A. Green Chem. 2014, 16 (4), 1807–1815.

(16)   Gubbels, E.; Drijfhout, J. P.; Posthuma-van Tent, C.; Jasinska-Walc, L.; Noordover, B. A. J.; Koning, C. E. Prog. Org. Coatings 2014, 77 (1), 277–284.

(17)   Resins and Curatives: The Binder System for Thermosetting Powder Coatings, Paint & Coatings Industry 2000.

(18)   Van Benthem, R. A. T. M. Prog. Org. Coatings 2000, 40 (1), 203–214.

(19)   Belder, E. G.; Rutten, H. J. J.; Perera, D. Y. Prog. Org. Coatings 2001, 42 (3-4), 142–149.

(20)   Salla, J. M.; Ramis, X.; Morancho, J. M.; Cadenato, A. Thermochim. Acta 2002, 388 (1-2), 355–370.

(21)   Ramis, X.; Cadenato, A.; Morancho, J. .; Salla, J. . Polymer 2003, 44 (7), 2067–2079.

(22)   Kronberger, K.; Hammerton, D. A.; Wood, K. A.; Stödeman, M. . JOCCA-Surface Coatings Int. 1991, 74 (11), 405–410.

(23)   Franiau, R. P. Eur. Coatings J. 2002, 10, 24.

3

(24) Mitchell, M. A.; Eckert, D.; Tomlin, A. S. Crosslinking; surface treatment. US6376618, 2002.

(25) Durand, D.; Bruneau, C.-M. Polymer 1982, 23, 69–72.

(26) Durand, D.; Bruneau, C.-M. Br. Polym. J. 1981, 13 (1), 33–40.

(27) Roller, M. Polym. Eng. Sci. 1986, 26 (6), 432–440.

(28) Winter, H. H. J. Rheol. 1986, 30 (2), 367.

(29) Osterhold, M. Prog. Org. Coatings 2000, 40, 131–137.

(30) Osterhold, M.; Niggemann, F. Prog. Org. Coatings 1998, 33 (1), 55–60.

(31) Vorster, O. C.; Halasz, L. Suid-Afrikaanse Tydskr. vir Natuurwetenskap en Tegnol. 2004, 23 (1/2), 13–21.

(32) Thiyagarajan, S.; Gootjes, L.; Vogelzang, W.; Wu, J.; van Haveren, J.; van Es, D. S. Tetrahedron 2011, 67 (2), 383–389.

(33) Thiyagarajan, S.; Gootjes, L.; Vogelzang, W.; van Haveren, J.; Lutz, M.; van Es, D. S. ChemSusChem 2011, 4 (12), 1823–1829.

(34) Lee, S. S.; Han, H. Z. Y.; Hilborn, J. G.; Månson, J. A. E. Prog. Org. Coatings 1999, 36, 79–88.

(35) Mezger, T. G. The Rheology Handbook: For Users of Rotational and Oscillatory Rheometers; Vincentz Network GmbH & Co KG, 2006.

3

Chapter 4

Poly(hydroxy urethane)s based on diglycerol dicarbonate

A series of amorphous non-isocyanate poly(hydroxy urethane)s (PHU) was synthesized from diglycerol dicarbonate in bulk conditions at mild temperatures, without using a catalyst. Diglycerol dicarbonate has been synthesized from diglycerol and dimethyl carbonate and was subsequently reacted with various diamines to form PHUs. These fully bio-based PHUs were amorphous and displayed a broad range of T_g values i.e. from -7 to 66 °C. 1D and 2D NMR techniques were used to determine the ratio between primary and secondary hydroxyl groups formed along the PHU backbone, which was found to be 3:7 for all compositions. The number-average molecular weights were calculated from NMR data and range from 4,100 to 9,400 g mol^{-1}. In FTIR spectra, residual cyclic carbonate groups were observed, which is in agreement with the loss of diamine as detected by NMR. TGA analysis indicated that the polymers are stable up to 200 °C. The polymers synthesized are expected to perform well in e.g. coating applications, given their molecular and thermal properties as well as the abundance of reactive hydroxyl functionalities present along the PHU backbone, which can be used for curing purposes and/or further functionalization.

4.1 Introduction

Polyurethanes are widely used, versatile materials having properties which can be tuned to match the application requirements. As a result, polyurethanes are found in applications such as foams, adhesives, coatings, and elastomers. However, the production of polyurethanes has remained a major concern as it involves the synthesis and use of toxic diisocyanates.[1] Several chemical routes have been developed throughout the years to avoid these issues, yet none of these pathways is currently used for the large scale production of non-isocyanate polyurethanes (NIPU).[2-8] Still, the addition reaction between cyclic carbonates and amines to form poly(hydroxy urethane)s (PHU) has recently been highlighted in an increasing number of publications.[9-14] The reaction between five-, six-, or seven-membered cyclic carbonates and an amine results in an additional hydroxyl group adjacent to the urethane linkage formed, which may be a primary or a secondary hydroxyl group.[15-21] The presence of these hydroxyl groups is claimed to enhance the chemical and hydrolytic stability of these materials compared to isocyanate-based polyurethanes.[22,23] The hydroxyl groups lead to an increased polarity of the polymer chain, which may increase the solubility in more polar solvents.

In this chapter, the synthesis and use of diglycerol dicarbonate (**DGC**) in combination with various (potentially) renewable aliphatic diamines for the preparation and characterization of the corresponding PHUs is reported (Figure 4.1). To investigate the influence of the monomer size on the properties, butane-1,4-diamine (**BDA**), pentane-1,5-diamine (**PDA**), nonane-1,9-diamine (**NDA**), and dimerized fatty acid diamine (**FDA**) have been selected. Isoidide diamine (**IIDA**) is used to determine the effect of sterically less accessible amine groups and the effect of the rigidity, caused by its cyclic structure, on the resulting polymer characteristics. Recently, the synthesis of **FDA**-based PHUs has been reported by Carré *et al.* for a similar dicarbonate.[13] To the best of our knowledge, the use of **IIDA** has not yet been described using this chemistry. Glycerol is an abundant bio-based monomer which is produced as a major side product (>10 wt%) of the biodiesel industry.[24-26] Glycerol can be dimerized to form the tetrafunctional polyol diglycerol and subsequently
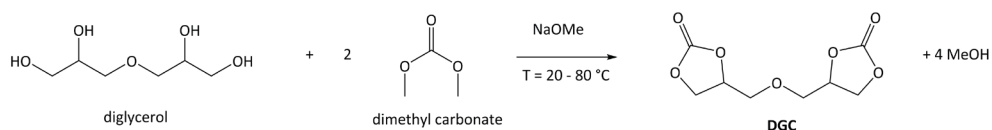
Scheme 4.1 **Synthesis of diglycerol dicarbonate from diglycerol and dimethyl carbonate.**

used in polymerization reactions.[27–29] Furthermore, diglycerol can be converted into diglycerol dicarbonate by a reaction with a dialkyl carbonate. Five-membered cyclic carbonate groups are formed as shown in Scheme 4.1.[30,31] Recently, this reaction has regained attention by the work of Stewart *et al.* with the development of reusable Mg-Al hydrotalcite catalysts.[32] Previously, Whelan, Hill and Cotter reported the use of **DGC** for the synthesis of PHUs through its polymerization with ethylene-1,2-diamine and a trifunctional cross-linker. Detailed characterization of the obtained polymer was not reported.[30]

Here, the syntheses and characterization are described of PHUs based on **DGC** using benign chemistry and reduced reaction times to obtain polymers which have the potential to become fully renewable. In addition, the application of melt polymerization as a synthetic method increases the industrial relevance of these PHUs in contrast with the often reported production of non-isocyanate polyurethanes (NIPU) in high-
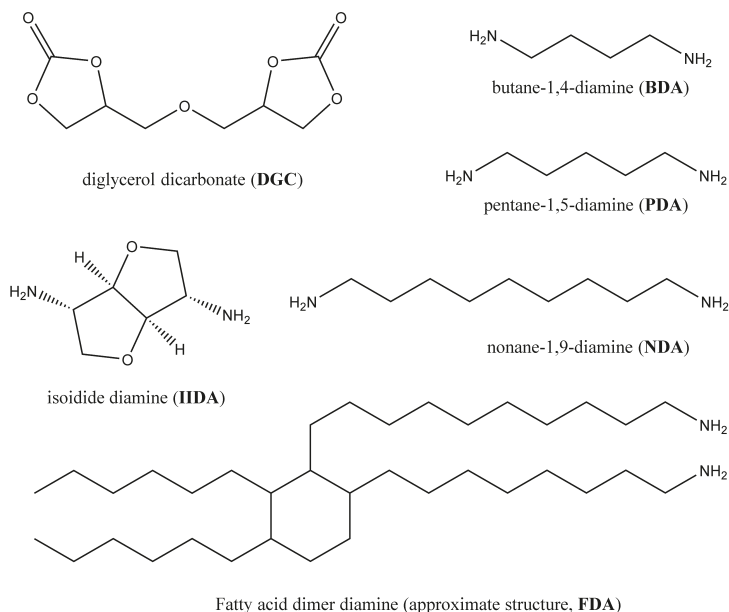

Figure 4.1 **Structural formulas of the monomers used for PHU synthesis**

boiling, polar solvents such as DMF and DMSO.

4.2 Materials and methods

4.2.1 Materials

Diglycerol (≥75% α,α, impurities consist of mono-, α,β-di-, β,β-di-, and triglycerol) was obtained from Solvay. Dimethyl carbonate (99%) and sodium methoxide were purchased from Acros. The reactants butane-1,4-diamine (**BDA**, 99%) and pentane-1,5-diamine (**PDA**, ≥ 97%) were purchased from Sigma-Aldrich. 1,9-Nonanediamine (**NDA**, 99%) was ordered at Alfa Aesar. Deuterated DMSO was purchased from Cambridge Isotope Laboratories, Inc. Methanol p.a. was obtained from Merck. Isoidide diamine (**IIDA**, ≥ 95%) was kindly provided by Wageningen UR Food and Biobased Research.[33,34] Priamine™ 1075 (**FDA**, 98.7 wt% diamine, 1 wt% triamine) was kindly provided by Croda. All chemicals were used as received without further purification.

4.2.2 Methods

NMR spectroscopy

^{1}H-NMR (delay time 5 s, 32 scans, 90°), ^{13}C-NMR (delay time 1 s, 2000 scans), as well as 2D gradient correlation spectroscopy (gCOSY), gradient heteronuclear single-quantum coherence spectroscopy (gHSQC), and gradient heteronuclear multiple-bond correlation spectroscopy (gHMBC) NMR measurements were performed on an Agilent 400-MR NMR system in DMSO-d_6 or in a mixture of DMSO-d_6 and CDCl$_3$ (1:1 v/v). Data was acquired using VnmrJ3 software. Chemical shifts are reported in ppm relative to tetramethylsilane (TMS). Number average molecular masses (M_n) were calculated using Eq-2.1. Carbonate, amine, and hydroxyl values were calculated by equations Eq-4.1, Eq-3.4, Eq-4.2, and Eq-4.3 which were adapted from Eq-3.2 for use with ^{1}H-NMR data:

$$CV = \frac{\overline{F}}{M_n} \cdot \sum_{i=0}^{n} \left[\frac{\left(\dfrac{I_{\text{carbonate},i}}{H_i} \right)}{\sum_{j=0}^{n} \dfrac{I_{\text{end},j}}{H_j}} \right] \qquad \text{Eq-4.1}$$

The hydroxyl value for primary hydroxyls is calculated using:

$$pOHV = \frac{\overline{F}}{M_n} \cdot \sum_{i=0}^{n} \left[\frac{\left(\dfrac{I_{\beta,i}}{H_i} \right)}{\sum_{j=0}^{n} \dfrac{I_{end,j}}{H_j}} \right] \qquad \text{Eq-4.2}$$

The hydroxyl value for secondary hydroxyls is calculated using:

$$sOHV = \frac{\overline{F}}{M_n} \cdot \sum_{i=0}^{n} \left[\frac{\left(\dfrac{I_{\alpha,i}}{H_i} \right)}{\sum_{j=0}^{n} \dfrac{I_{end,j}}{H_j}} \right] \qquad \text{Eq-4.3}$$

in which F is the average functionality (no branching: $F = 2$) and M_n the number average molecular mass of the resin, $I_{carbonate}$ the intensity of the next to the free carbonate end groups, I_α and I_β are the intensities of the protons belonging to the α- and β-constitutional isomers respectively, I_{amine} the intensity of the protons (H_{BDA} = 2, H_{FDA} = 2) next to the free amine end groups, and I_{end} is the sum of I_{amine} and the intensity for unreacted cyclic carbonate.

TGA

Thermogravimetric analysis (TGA) was performed on a TA Q500 instrument (TA Instruments). Samples with a typical weight of 2 to 10 mg were heated at a rate of 10 °C min^{-1} to 600 °C in an N$_2$ atmosphere.

DSC

Differential Scanning Calorimetry (DSC) was performed on a TA Q100 DSC (TA Instruments). Approximately 5 mg of dried polymer was accurately weighed and sealed into an hermetically closed aluminum pan. Temperature profiles were measured from -80 °C to 150 °C and consisted of two heating runs and one cooling run, at a heating/cooling rate of 10 °C min^{-1}. TA Universal Analysis software was used for data acquisition and analysis. The value for the T_g was determined from the inflection point of the curve during the second heating run.

FTIR

IR measurements were performed on a Varian Excalibur 3100 FT-IR Spectrometer, equipped with a diamond Specac Golden Gate attenuated total reflection (ATR) setup

4

over a spectral range of 4000 to 650 cm^{-1} with a resolution of 4 cm^{-1}. 100 scans were signal-averaged and the resulting spectra were analyzed using Varian Resolutions Pro software.

SEC

Size exclusion chromatography (SEC) was performed on a Waters Alliance system equipped with a Waters 2695 separation module, a Waters dual λ absorbance detector, a Viscotek 270 dual detector, a Viscotek 250 dual detector, and a PSS GRAM guard column followed by PSS GRAM columns in series with a pore size 100 Å (10 μm particles) and 3000 Å (10 μm particles) respectively at 60 °C. *N*, *N*-dimethylacetamide (DMAc, Biosolve AR) with lithium chloride (50 mmol L^{-1}) was used as an eluent at a flow rate of 1 mL min^{-1}. The molecular weights were calculated against polystyrene standards (Polymer Laboratories, M_p = 580 g mol^{-1} up to M_p = 7.5·10^6 g mol^{-1}). Before SEC analysis was performed, the samples were filtered through a 0.2 μm PTFE filter. Samples were prepared in eluent at a concentration of 2-3 mg mL^{-1}.

4.2.3   Synthetic procedures

Polymerization of DGC with BDA (DGC-BDA)

DGC (1.007 g, 4.62 mmol) and **BDA** (0.422 g, 4.79 mmol) were charged into a glass reactor equipped with a double helical ribbon impeller (see Figure 4.2). Under an inert argon atmosphere, the reactants were stirred at room temperature for 7 minutes after which the reactor was heated to 80 °C using a silicon oil heating bath. After 2 hours, the temperature was increased to 100 °C. After 5 hours, the polymer was obtained as a white brittle solid. Upon heating and subsequent cooling, a transparent, colorless, solid remained.

Polymerization of DGC with PDA (DGC-PDA)

DGC (1.012 g, 4.64 mmol) and **PDA** (0.481 g, 4.71 mmol) were charged into a glass reactor equipped with a double helical ribbon impeller (see Figure 4.2). Under an inert argon atmosphere, the reactants were stirred at room temperature for 10 minutes after which the reactor was heated to 80 °C using a silicon oil heating bath. After 2 hours,

Figure 4.2 **Reactor setup used for the synthesis of poly(hydroxy urethane) resins. A magnetically coupled stirring setup is fitted to ensure a closed system. Properties of the double helical ribbon impeller: diameter 13 mm, ribbon width 2 mm, shaft diameter 3 mm, length 30 mm, pitch 1 rotation/10 mm, stainless steel.**

the temperature was increased to 100 °C. After a total reaction time of 5 hours, the polymer was obtained as a yellow brittle solid. Upon heating and subsequent cooling, a transparent colorless, solid was formed.

Polymerization of DGC with NDA (DGC-NDA)

DGC (0.504 g, 2.31 mmol) and **NDA** (0.373 g, 2.36 mmol) were charged into a glass reactor equipped with a double helical ribbon impeller (see Figure 4.2). Under an inert argon atmosphere, the reactants were stirred at room temperature for 1 minute after which the reactor was heated to 80 °C using a silicon oil heating bath. After 5 hours, the polymer was obtained as a transparent, colorless, glassy solid.

Polymerization of DGC with FDA (DGC-FDA)

DGC (0.497 g, 2.28 mmol) and **FDA** (1.218 g, 2.28 mmol) were charged into a glass reactor equipped with a double helical ribbon impeller (see Figure 4.2). Under an inert argon atmosphere, the reactants were stirred at room temperature for 5 minutes after

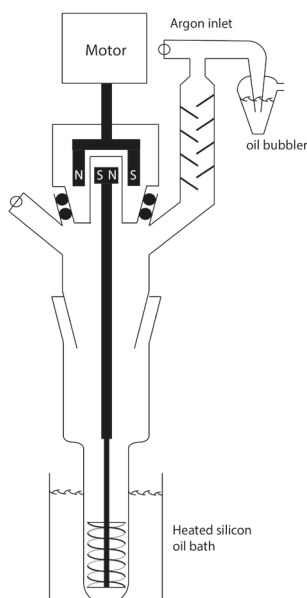which the reactor was heated to 80 °C using a silicon oil heating bath. After 2 hours, the temperature was increased to 100 °C. After a total reaction time of 5 hours, the polymer was obtained as a yellow rubbery material.

Polymerization of DGC with IIDA (DGC-IIDA)

DGC (0.500 g, 2.29 mmol) and **IIDA** (0.352 g, 2.44 mmol) were charged into a glass reactor equipped with a double helical ribbon impeller (see Figure 4.2). Under an inert argon atmosphere, the reactants were heated to 120 °C using a silicon oil heating bath. 30 minutes after a homogeneous, stirred melt was obtained, the temperature was increased to 140 °C. After 68 hours, the polymer was obtained as a brittle beige solid.

General data:

^{1}H-NMR (400 MHz, DMSO-d_6) δ_H (ppm) 7.10 NH (s, 0.9H), 6.74 NH (s, 0.1H), 4.91 sec. OH (s, 0.7H), 4.75 prim. OH (s, 0.3H), 4.67 β2 (m, 0.3H), 3.91 α3 (m, 0.7H), 3.85 α3 (m, 0.7H), 3.74 α2 (b, 0.7H), 3.50 β1 (m, 0.6H), 3.46 β3 (m, 0.6H), 3.36 α1 (m, 1.4H), 2.94 Am1 (q, 2H), 1.36 Am2 (m, 2H). ^{13}C-NMR (100 MHz, DMSO-d_6) δ_C (ppm) 156.26, 155.91, 73.85, 73.05, 72.65, 72.54, 70.49, 69.91, 69.81, 67.80, 65.42, 60.09, 30.51, 26.96, 26.77.

4.3 Synthesis of poly(hydroxy urethane) resins

4.3.1   Synthesis of PHUs

Poly(hydroxy urethane)s based on the bio-based monomer diglycerol dicarbonate and different aliphatic diamines have been synthesized in the melt as shown in Scheme 4.2. Without a catalyst, the reaction proceeds readily and the polymers are obtained at mild temperatures within 5 hours. **DGC-IIDA** required a longer reaction
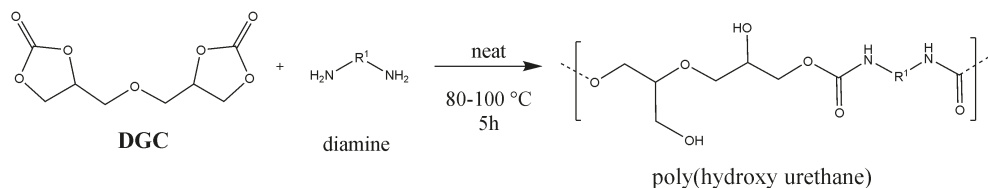
Scheme 4.2   **Synthesis of DGC-based poly(hydroxy urethane)s.**

time as the reaction temperature was below the melting temperature of the **IIDA** monomer. Therefore, the reaction rate was limited by the slow dissolution of **IIDA** into the melt. Almost all research groups describing cyclic carbonate-amine reactions report reaction times of 24 h at similar temperatures in solution. However, also several examples prepared in bulk have been reported.[9,10,13,35] In the polymerization described here, the melting point of **DGC** (T_m = 65 °C) allows for bulk reaction conditions at mild temperatures. Therefore, the synthesis requires relatively short reaction times to obtain high conversions because of the high functional group concentration and, as a consequence, side reactions are largely prevented. Furthermore, no high boiling solvent has to be removed from the product once the reaction is completed.

DGC-FDA is a transparent rubbery material. The other polymers are obtained as opaque solids but become transparent when they are thermally treated by heating above the melting temperature followed by slow cooling. This indicates the initial presence of a poorly defined crystalline phase which doesn't recrystallize upon controlled cooling. **DGC-IIDA** has an ochre appearance which developed during the synthesis and is thought to originate from some discoloration of the sugar-based **IIDA**. Upon prolonged exposure to air, the polymers absorb moisture to become sticky.

The molecular weight distributions of the poly(hydroxy urethane)s were analyzed using a SEC system with DMAc as the eluent and are reported in Table 4.1. Number-average molecular weight (M_n) values compared to PS standards were found to range
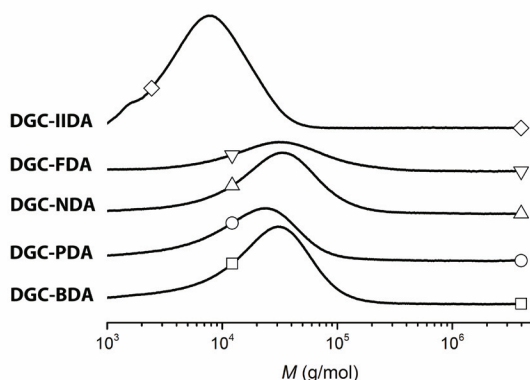
4

Figure 4.3   SEC traces of DGC-BDA (□), DGC-PDA (○), DGC-NDA (△), DGC-FDA (▽), and DGC-IIDA (◇).

Table 2.3   Molecular weights and compositions of **PA**-based polyamides determined by SEC and ^{1}H-NMR.

Polymer	SEC[a]		^{1}H-NMR[b]					
	M_n g mol^{-1}	$Đ$	X_{feed}[c]	$X_{copolymer}$[c]	$X_{end-groups}$[d]	M_n g mol^{-1}	DP_n	% α[e]
DGC-BDA	11,000	2.8	100 / 103.7	100 / 102.6	29 / 71	7,300	47.6	69
DGC-PDA	9,200	2.8	100 / 101.5	100 / 95.9	98 / 2	7,500	46.5	70
DGC-NDA	13,100	2.8	100 / 102.2	100 / 94.8	90 / 10	7,200	38.2	69
DGC-FDA	13,500	3.2	100 / 100.0	100 / 92.0	100 / 0	9,400	25.4	68
DGC-IIDA	4,900	1.8	100 / 106.6	100 / 89.4	100 / 0	4,100	22.3	69

[a] Number-average molecular weight and Đ measured by SEC in DMAc against PS standards; [b] Number-average molecular weight, number-average degree of polymerization, and composition determined by ^{1}H-NMR in DMSO-d$_6$; [c] Molar ratio of DGC / diamine; [d] Carbonate / amine end-groups; [e] Percentage of secondary hydroxyl groups formed during the reaction.

Table 4.2   End-group values for poly(hydroxy urethane)s based on ^{1}H-NMR.

Polymer	CV mmol g^{-1}	AmV mmol g^{-1}	pOHV mmol g^{-1}	sOHV mmol g^{-1}
DGC-BDA	0.08	0.19	1.97	4.43
DGC-PDA	0.21	0.06	1.90	4.16
DGC-NDA	0.25	0.03	1.59	3.59
DGC-FDA	0.21	0	0.83	1.77
DGC-IIDA	0.67	0	1.90	3.93

between 4,900 and 13,500 g mol^{-1} with $Đ$ values ranging from 1.8 to 3.2. The $Đ$ values are relatively high due to a clear presence of residual monomers and low molecular weight species. Solution-based polymerization is commonly followed by a precipitation step to separate the polymer from the solvent. By precipitation, the lower molecular weight species are largely removed from the product as they remain in the solvent. In the melt polymerization method applied here, the sample is not submitted to such a purification procedure to allow for analysis of the true reaction product. The SEC traces in Figure 4.3 clearly show the presence of low molecular weight oligomers ($M < 10^4$ g mol^{-1}) in all samples, in particular for **DGC-IIDA**. Probably, this is the result of the rather low reactivity of the amine groups of **IIDA** as they are more sterically hindered.

The poly(hydroxy urethane)s were analyzed with ^{1}H-NMR (see Figure 4.4 and
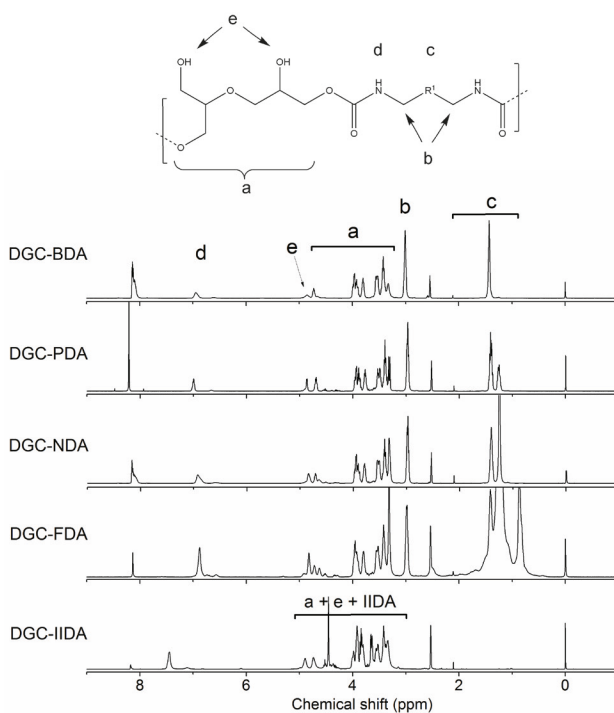
Figure 4.4 ^{1}H-NMR spectra of the synthesized poly(hydroxy urethane)s in DMSO-d_6:CDCl$_3$ (1:1 *v/v*). The signal at 8.1 ppm originates from CHCl$_3$. R^1 consists of alkyl residues depending on the diamine used. The spectrum of **DGC-IIDA** has been assigned separately because of large structural differences compared to the other polymers in the series.

Table 4.1), ^{13}C-NMR, and the 2D NMR techniques gCOSY, gHSQC, and gHMBC. Two different solvents were used: DMSO-d_6 to visualize the hydroxyl and urethane bonds, and DMSO-d_6:CDCl$_3$ (1:1 *v/v*) as **DGC-FDA** is not soluble in DMSO. Furthermore, this mixture separates the signal for the free amine end-groups from the residual DMSO resonance. Table 4.2 reports the end group values of the polymers, which indicate that functionality remained after synthesis. The carbonate (*CV*) and amine (*AmV*) values decrease with increasing degree of polymerization, which the concentration of primary (*pOHV*) and secondary (*sOHV*) hydroxyls increases as these are produced during reaction. All polymers show signals of the original cyclic carbonate at δ = 4.9, 4.5, and 4.3 ppm, indicating the presence of residual cyclic carbonate end-groups. In addition, **DGC-BDA**, **DGC-PDA**, and **DGC-NDA** also show amine end-groups at δ = 2.5 ppm, indicating incomplete conversion.

4
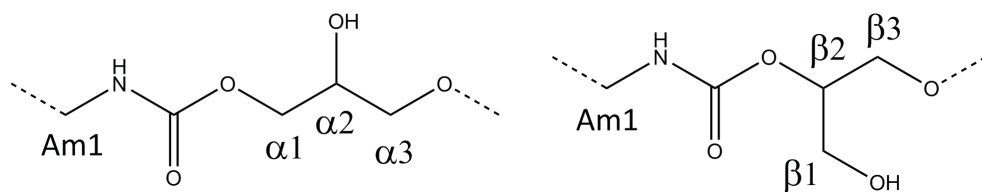
Scheme 4.3   Structures of constitutional isomers named α and β.
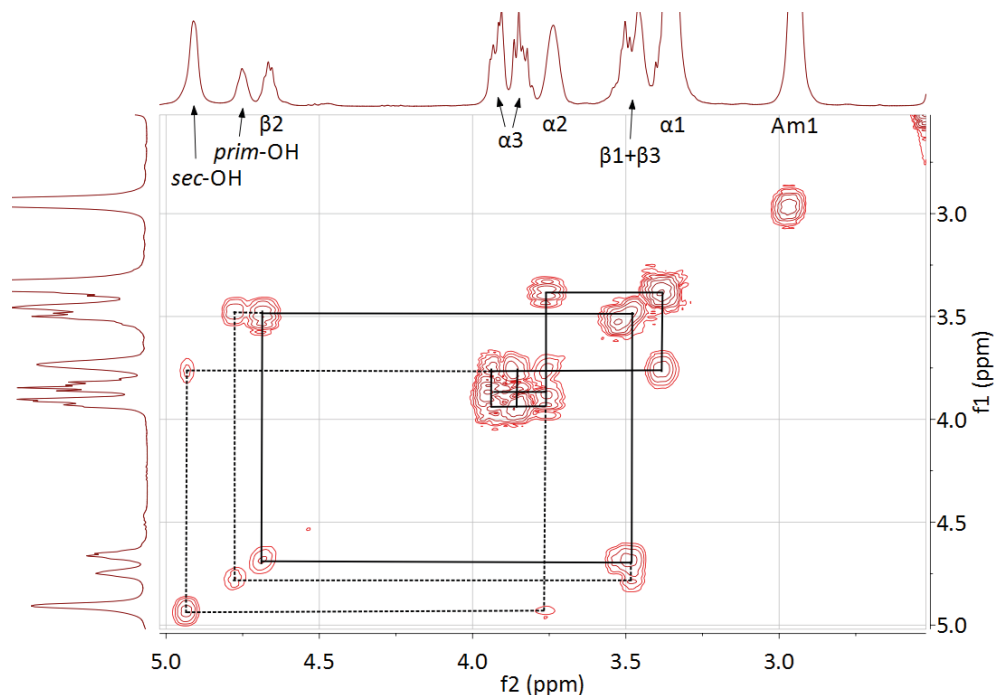
Figure 4.5   gCOSY spectrum of **DGC-BDA** in DMSO-d_6.

Using ^{1}H-NMR, M_n values were calculated, see Table 4.1. Like in SEC, **DGC-IIDA** has the lowest degree of polymerization resulting in the lowest M_n value of 4,100 g mol^{-1}. The considerable loss of diamine from feed to the final polymer confirms that **IIDA** has the least reactive amine functionalities. The long reaction time allows for side reactions to occur, leading to the reported discoloration. The other poly(hydroxy urethane)s have similar number-average molecular weights ranging from 7,200 to 9,400 g mol^{-1}. As expected, the M_n values determined from ^{1}H-NMR are lower than the values determined by SEC. Curiously, although the reactor can be considered to be a closed system, loss of diamine is observed for all syntheses. Especially in the case of the non-volatile **FDA**, this is unexpected. The observed losses may be due
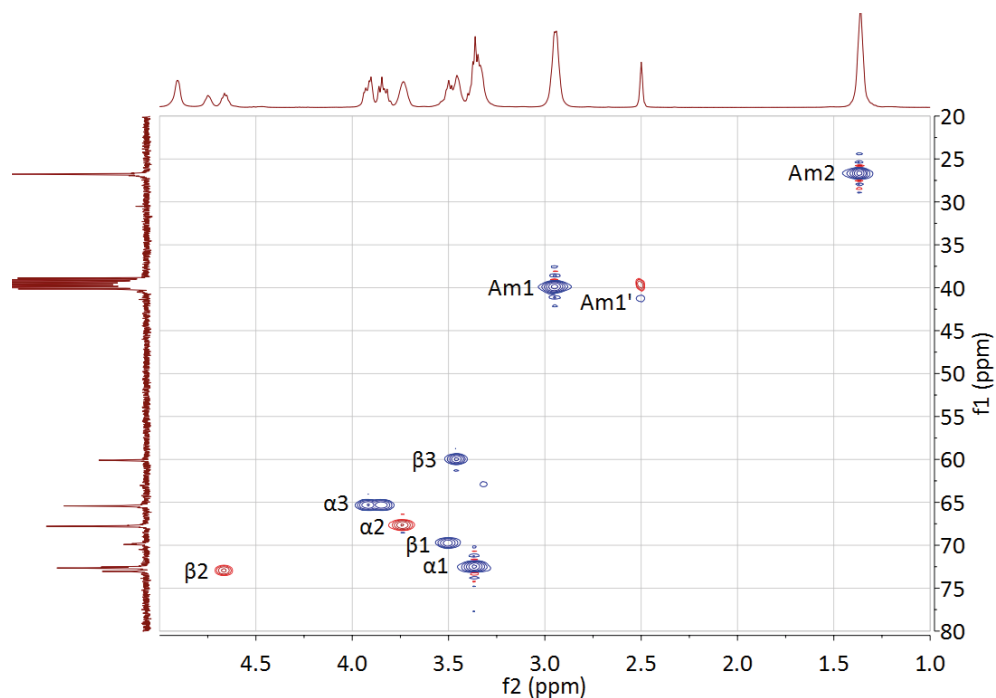
Figure 4.6 gHSQC spectrum and assignment of the α- and β-segments in DGC-BDA in DMSO-d_6. The indication is corresponding to Scheme 4.3.

to the geometry of the reactor, which is narrow (H/D = 8.3) and the impeller has very little clearance at the bottom of the reactor, leading to difficulties with keeping all monomers in the reaction melt. In addition, the difference in polarity between the apolar **FDA** and much more polar **DGC** as well as the corresponding more polar oligomers may have caused phase separation, resulting in an inhomogeneous reaction mixture and/or NMR sample.

The cyclic carbonate is asymmetrical due to the side-group. Therefore, the ring-opening with an amine will lead to the formation of two constitutional isomers. In this paper, the reaction product containing a secondary OH-group will be named α, and the product containing a primary OH-group will be named β (see Scheme 4.3). Their presence has been analyzed by gCOSY, gHSQC, and gHMBC and their relative abundance has been calculated by ^{1}H-NMR.

The gCOSY spectrum in Figure 4.5 shows two spin-correlated motifs in the 3.0 < δ < 5.0 ppm region which is where signals related to the glycerol residue are expected.

One motif, either α or β, is a combination of δ = 4.7 and 3.5 ppm and the other one is formed by δ = 3.9, 3.75, and 3.4 ppm. The signals assigned to the two different types of hydroxyl groups are indicated with the dotted lines. The addition of a drop of D_2O to the sample decreased the intensity of the OH signals due to exchange of the hydroxyl proton for a deuterium atom which has no resonance in this frequency range. The two constitutional isomers are investigated in more detail using gHSQC (Figure 4.5).

Using the difference in phase of the signals for CH_2 and CH, together with the knowledge that the resonance of β2 should be located more downfield than the signal of α2 due to the close presence of the urethane bond, α2 and β2 can be assigned. The signals in ^{1}H-NMR for β1 and β3 are overlapping at δ = 3.5 ppm and this correlation is also proven with gHMBC (Figure 4.12). The observed relative abundances of segments α and β are independent of the structure of the diamine used and were found to be 69% and 31%, respectively, which is similar to values previously reported by Ochiai (between 77:23 and 65:35).[17] Tomita and Steblyanko report slightly higher values of approximately 75-87% for the α motif.[15,16] A clear explanation for the discrepancy between the reported results in the two latter publications can't be provided, as Ochiai as well as Tomita and Steblyanko used identical bisphenol A-based dicarbonates. Possibly, the reaction medium chosen has an influence. In the ^{13}C-NMR spectrum, this ratio can also be observed for the signals of the α1 (δ = 72.5 ppm) and β1 carbons (δ = 69.8 ppm). These split in 2 peaks for α-O-α, α-O-β, and β-O-β segments in the
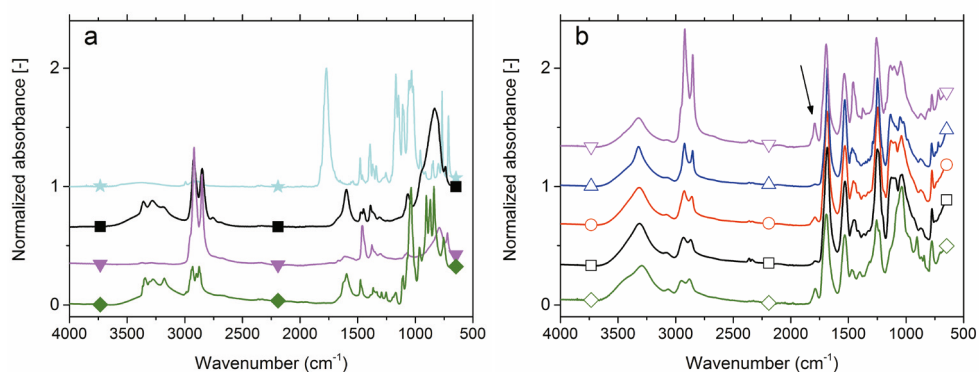

Figure 4.7　　FT-IR-ATR spectra of the starting compounds (a) **DGC** (cyan ★), **BDA** (black ■), **FDA** (magenta ▼), **IIDA** (green ◆), and the polymers (b) **DGC-BDA** (black □), **DGC-PDA** (red ○), **DGC-NDA** (blue △), and **DGC-FDA** (magenta ▽), and **DGC-IIDA** (green ◇). The arrow indicates the presence of residual cyclic carbonate.

chain. Furthermore, the same ratio can be observed for the quaternary carbon atoms of the urethane bond at $\delta = 156$ ppm (Figure 4.13). Note that the intensity of quaternary carbon atoms is less accurate.

FT-IR is a very useful tool to monitor the reaction between the cyclic carbonate and amines. The spectrum of **DGC** in Figure 4.7 has a clear vibration band at 1771 cm^{-1} which corresponds to the carbonyl group of the cyclic carbonate. The peak disappears during the reaction in favor of the amide I and II peaks at 1684 - 1693 cm^{-1} and 1529 - 1536 cm^{-1}. In agreement with the NMR analysis, a residual signal assigned to the cyclic carbonate can be observed for all polymers, meaning that cyclic carbonate end-groups and/or residual monomer are present in the products. The formed hydroxyl groups can be observed at 3320 cm^{-1}.

4.3.1   Thermal properties of PHUs

The thermal stability of the PHUs was assessed using TGA analysis, of which the results are collected in Figure 4.8 and Table 4.3. **DGC-FDA** showed a higher stability than the other polymers, with the onset of the major degradation step occurring at approximately 240 °C. The PHUs based on **BDA**, **PDA**, **NDA**, **IIDA** showed a similar trend: an initial weight loss between 100 °C and 150 °C prior to the major degradation step starting at approximately 200 °C. This behavior was also reported by Carré *et al.*[13] The samples were dried under reduced pressure with P$_2$O$_5$ prior to the measurement,

4
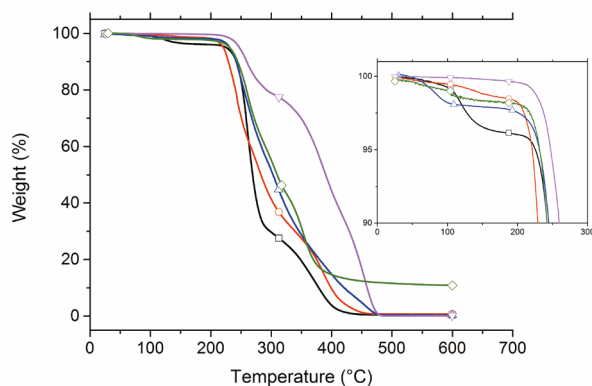
Figure 4.8   TGA traces of **DGC-BDA** (black □), **DGC-PDA** (red ○), **DGC-NDA** (blue △), **DGC-FDA** (magenta ▽), and **DGC-IIDA** (green ◇) under N$_2$ atmosphere recorded at a heating rate of 10 °C min^{-1}. The inset shows an expanded view of the region of onset.
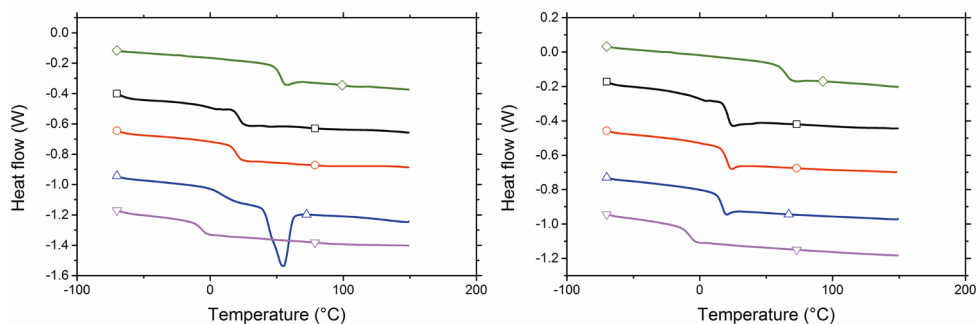
Figure 4.9 DSC traces of the first (*left*) and second (*right*) heating run of **DGC-BDA (black □), DGC-PDA (red ○), DGC-NDA (blue △), DGC-FDA (magenta ▽), and DGC-IIDA (green ◇) recorded at a heating rate of 10 °C min^{-1}. Exo up.**

hence the initial weight loss is most likely originating from the evaporation of residual monomer and/or oligomers and not the evaporation of water. As expected, after the first degradation step in which the urethane bond dissociates, the longer chain diamines showed a higher stability. Furthermore, **DGC-IIDA** showed a significantly higher residual weight (11 wt%) than the other samples. This has been previously observed for similar compounds based on **IIDA**.[36–38]

The phase transition behavior of the polymers has been investigated using DSC. DSC thermograms of the PHUs are shown in Figure 4.9. None of the polymers show melting of a crystalline phase during the second heating, suggesting that all polymers are amorphous. However, directly after synthesis most of the polymer were opaque, white solids, indicating the presence of a crystalline phase. For **DGC-NDA**, melting of a crystalline phase was observed in the first heating cycle of the DSC measurement

Table 4.3 Thermal data of the synthesized poly(hydroxy urethane)s obtained at heating rates of 10 °C min^{-1}.

Polymer	TGA			DSC
	T_{onset}	$T_{d,10\%}$	$T_{d,max}$	T_g
	°C	°C	°C	°C
DGC-BDA	202	242	261	21
DGC-PDA	190	229	243	21
DGC-NDA	196	242	257	17
DGC-FDA	201	259	455	-7
DGC-IIDA	180	245	261	66

with a melting enthalpy of $\Delta H_{m,1} = 30$ J g^{-1}. An explanation for these observations would be that the shear force in the laminar flow field, introduced by the helical ribbon impeller, orients the polymer chains and creates the possibility to form crystalline domains. Under quiescent conditions however, the polymer doesn't crystallize from the melt. This is attributed to the combination of two effects: the relatively short **DGC** residue in combination with the presence of both the α- and β-motifs which forms a poorly defined hard segment. This hinders ordering between polymer chains and largely prevents crystallization. Similar dicarbonate-based polymers are generally reported to be amorphous.[11,13,15]

As expected, the T_g values vary with the length and flexibility of the diamine spacer (see Table 4.3). The T_g values of **DGC-BDA**, **DGC-PDA**, and **DGC-NDA** are rather similar, ranging from 17 to 21 °C, while the flexible fatty acid component of **DGC-FDA** leads to a significantly lower T_g value of -7 °C. The rigid, bicyclic structure of **IIDA** increases the T_g value to 66 °C. To the best of our knowledge, this is the highest value reported for amorphous aliphatic NIPUs, even exceeding the T_g values reported for the isosorbide-IPDA structures described by Besse *et al.*[23] The comparison between **DGC-BDA** and **DGC-IIDA** is interesting as for both diamines the chain length between the urethane linkages is four carbon atoms. The fixed conformation in **IIDA**, which is due to its rigid bicyclic structure, has a large effect on the T_g value but does not introduce crystallinity.

The structure of the PHUs is very similar to the polymers reported by Sheng *et al.*[9] Compared to the NIPUs of this chapter, the extra ethylene glycol spacer in the glycerol-based dicyclic carbonates of Sheng *et al.* decreased the T_g value of their systems by about 15 °C.

The amorphous NIPUs described in this manuscript display properties which make them very interesting materials for coating applications. The high number of hydroxyl groups present along the polymer backbone can be used for cross-linking or post-synthesis modifications. The broad range of T_g values that these polymers display allows fine-tuning of the T_g value for a specific application by mixing the diamines in an appropriate ratio. In a separate article, the use of these polymers in coating applications will be investigated.

4

4.4 Conclusions

The successful use of diglycerol dicarbonate in the synthesis of fully bio-based non-isocyanate polyurethanes is reported in this chapter. A melt-based, non-catalyzed polyaddition reaction yielded poly(hydroxy urethane)s with SEC-based M_n values between 4,900 and 13,500 g mol^{-1}. ^{1}H-NMR calculations gave M_n values between 4,100 and 9,400 g mol^{-1}. Using 2D NMR techniques, the molecular structure could be fully elucidated. Based on these assignments, the ratio between primary and secondary hydroxyls formed in the reaction was determined to be 31:69 for all polymers.

A thermal evaluation of the polymers with DSC indicated that all polymers were amorphous after cooling at 10 °C min^{-1} from the melt, which is attributed to the random distribution of α- and β-motifs along the main chain, hindering the ordering between chains. Shear of the polymers in the laminar flow field in the melt can induce the formation of crystalline domains which will not form under quiescent conditions during cooling from the melt. By varying the diamine used in the synthesis, T_g values were obtained between -7 and +66 °C. This allows for these interesting materials to be applied in, *e.g.* coating systems.

4.5 References

(1)   Bayer, O. Angew. Chemie 1947, 59 (9), 257–272.

(2)   Groszos, S. J.; Drechsel, E. K. Method of preparing a polyurethane. US2802022, 1957.

(3)   Kihara, N.; Endo, T. J. Polym. Sci. Part A Polym. Chem. 1993, 31 (11), 2765–2773.

(4)   Neffgen, S.; Kušan, J.; Fey, T.; Keul, H.; Höcker, H. Macromol. Chem. Phys. 2000, 201 (16), 2108–2114.

(5)   Schmitz, F.; Keul, H.; Höcker, H. Polymer. 1998, 39 (14), 3179–3186.

(6)   Versteegen, R. M.; Sijbesma, R. P.; Meijer, E. W. Angew. Chem. Int. Ed. Engl. 1999, 38 (19), 2917–2919.

(7)   Ihata, O.; Kayaki, Y.; Ikariya, T. Angew. Chem. Int. Ed. Engl. 2004, 43 (6), 717–719.

(8)   Calle, M.; Lligadas, G.; Ronda, J. C.; Galià, M.; Cádiz, V. J. Polym. Sci. Part A Polym. Chem. 2014, 52 (21), 3017–3025.

(9)   Sheng, X.; Ren, G.; Qin, Y.; Chen, X.; Wang, X.; Wang, F. Green Chem. 2015, 17 (1), 373–379.

(10)   Maisonneuve, L.; More, A. S.; Foltran, S.; Alfos, C.; Robert, F.; Landais, Y.; Tassaing, T.; Grau, E.; Cramail, H. RSC Adv. 2014, 4 (49), 25795–25803.

(11)   Benyahya, S.; Boutevin, B.; Caillol, S.; Lapinte, V.; Habas, J.-P. Polym. Int. 2012, 61 (6), 918–925.

(12)   Bähr, M.; Bitto, A.; Mülhaupt, R. Green Chem, 2012, 14, 1447–1454.

(13)   Carré, C.; Bonnet, L.; Avérous, L. RSC Adv. 2014, 4, 54018–54025.

(14)   Annunziata, L.; Diallo, A. K.; Fouquay, S.; Michaud, G.; Simon, F.; Brusson, J.-M.; Carpentier, J.-F.; Guillaume, S. M. Green Chem. 2014, 16 (4), 1947–1956.

(15)   Steblyanko, A.; Choi, W.; Sanda, F.; Endo, T. J. Polym. Sci. Part A Polym. Chem. 2000, 38 (13), 2375–2380.

(16)   Tomita, H.; Sanda, F.; Endo, T. J. Polym. Sci. Part A Polym. Chem. 2001, 39 (6), 851–859.

(17)   Ochiai, B.; Satoh, Y.; Endo, T. Green Chem. 2005, 7 (11), 765–767.

(18)   Tomita, H.; Sanda, F.; Endo, T. J. Polym. Sci. Part A Polym. Chem. 2001, 39 (23), 4091–4100.

(19)   Tomita, H.; Sanda, F.; Endo, T. J. Polym. Sci. Part A Polym. Chem. 2001, 39 (6), 860–867.

(20)   Helou, M.; Carpentier, J.-F.; Guillaume, S. M. Green Chem. 2011, 13 (2), 266–271.

(21)   Anders, T.; Keul, H.; Möller, M. Des. Monomers Polym. 2011, 14 (6), 593–608.

(22)   Benyahya, S.; Desroches, M.; Auvergne, R.; Carlotti, S.; Caillol, S.; Boutevin, B. Polym. Chem. 2011, 2 (11), 2661–2667.

(23)   Besse, V.; Auvergne, R.; Carlotti, S.; Boutevin, G.; Otazaghine, B.; Caillol, S.; Pascault, J.-P.; Boutevin, B. React. Funct. Polym. 2013, 73 (3), 588–594.

(24)   Zhou, C.-H.; Beltramini, J. N.; Fan, Y.-X.; Lu, G. Q. Chem. Soc. Rev. 2008, 37 (3), 527–549.

(25)   Corma, A.; Iborra, S.; Velty, A. Chem. Rev. 2007, 107 (6), 2411–2502.

(26)   Chiu, C.-W.; Dasari, M. A.; Suppes, G. J.; Sutterlin, W. R. AIChE J. 2006, 52 (10), 3543–3548.

(27)   Medeiros, M. A.; Araujo, M. H.; Augusti, R.; de Oliveira, L. C. A.; Lago, R. M. J. Braz. Chem. Soc. 2009, 20 (9), 1667–1673.

(28)   Dakshinamoorthy, D.; Weinstock, A. K.; Damodaran, K.; Iwig, D. F.; Mathers, R. T. ChemSusChem 2014, 7 (10), 2923–2929.

(29)   Zhang, H.; Grinstaff, M. W. Macromol. Rapid Commun. 2014, 35, 1906–1924.

(30)   Whelan Jr., J. M.; Hill, M.; Cotter, R. J. Multiple cyclic carbonate polymers. US3072613, 1963.

(31)   Jerome, F.; de Sousa, R.; Barrault, J.; Pouilloux, Y. Method for preparing dithiocarbamates in particular from polyols of the glycerol type. US20120264941, 2012.

(32)   Stewart, J. A.; Weckhuysen, B. M.; Bruijnincx, P. C. A. Catal. Today 2015. *in press*, DOI 10.1016/j.cattod.2014.06.035

(33)   Thiyagarajan, S.; Gootjes, L.; Vogelzang, W.; van Haveren, J.; Lutz, M.; van Es, D. S. ChemSusChem 2011, 4 (12), 1823–1829.

(34)   Thiyagarajan, S.; Gootjes, L.; Vogelzang, W.; Wu, J.; van Haveren, J.; van Es, D. S. Tetrahedron 2011, 67 (2), 383–389.

(35)   Bähr, M.; Mülhaupt, R. Green Chem. 2012, 14 (2), 483–489.

(36)   Wu, J. Carbohydrate-based building blocks and step-growth polymers, Eindhoven, University of Technology, 2012.

(37)   Li, Y.; Noordover, B. A. J.; van Benthem, R. A. T. M.; Koning, C. E. Eur. Polym. J. 2014, 52, 12–22.

(38)   Li, Y.; Noordover, B. A. J.; van Benthem, R. A. T. M.; Koning, C. E. Eur. Polym. J. 2014, 59, 8–18.

4

4.6 Additional figures
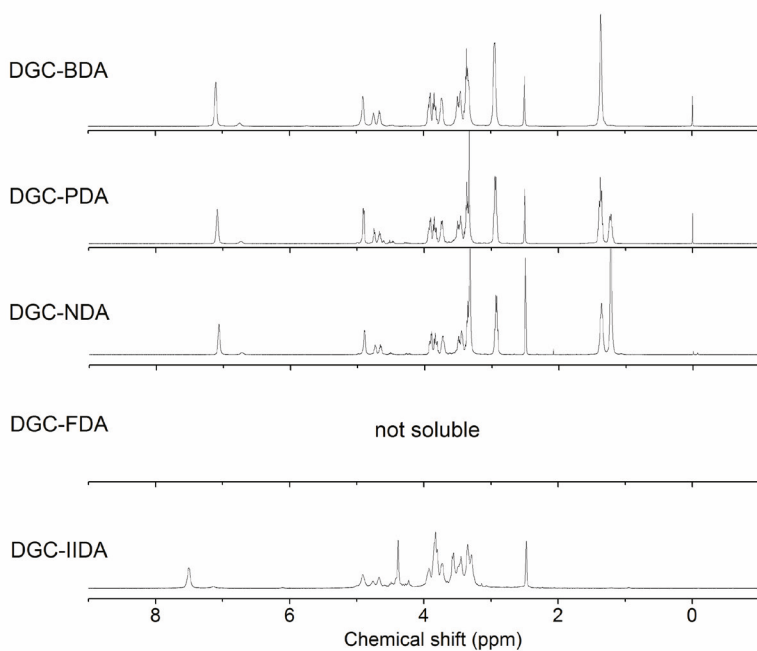
Figure 4.10 ¹H-NMR spectra of the synthesized NIPUs in DMSO-d_6.
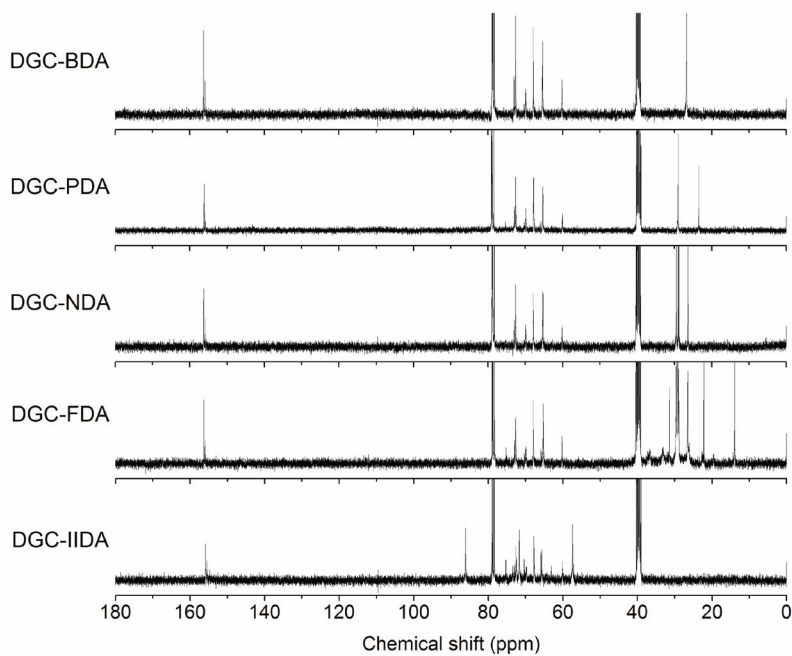
Figure 4.11 ¹³C-NMR spectra of the synthesized NIPUs in DMSO-d_6:CDCl$_3$ (1:1 *v/v*).
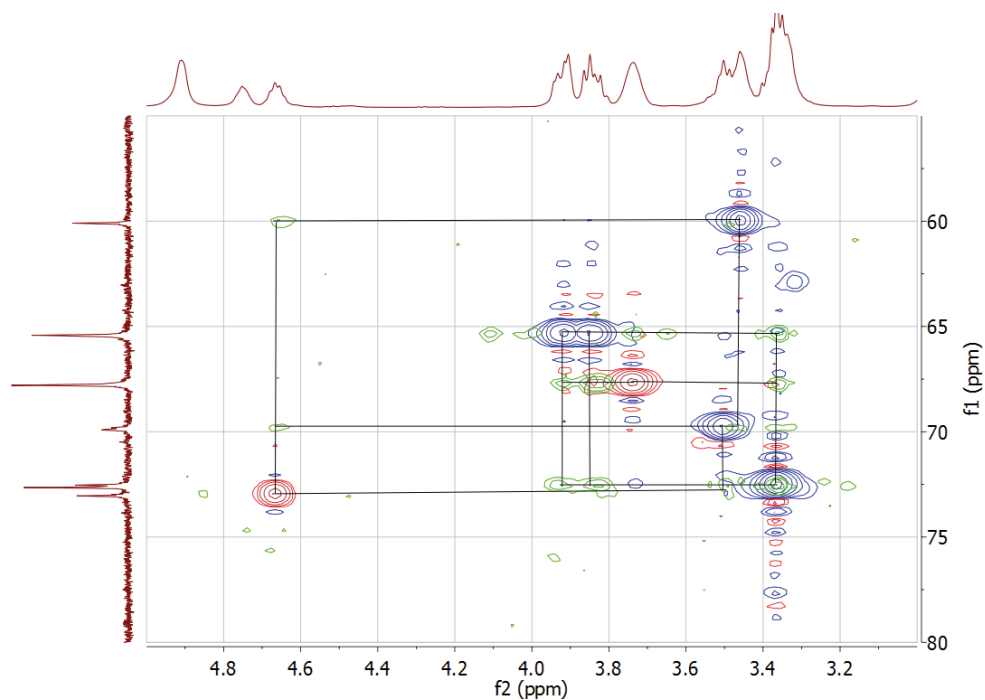
Figure 4.12   gHSQC (red-blue) and gHMBC (green) overlay of **DGC-BDA** in DMSO-d_6.
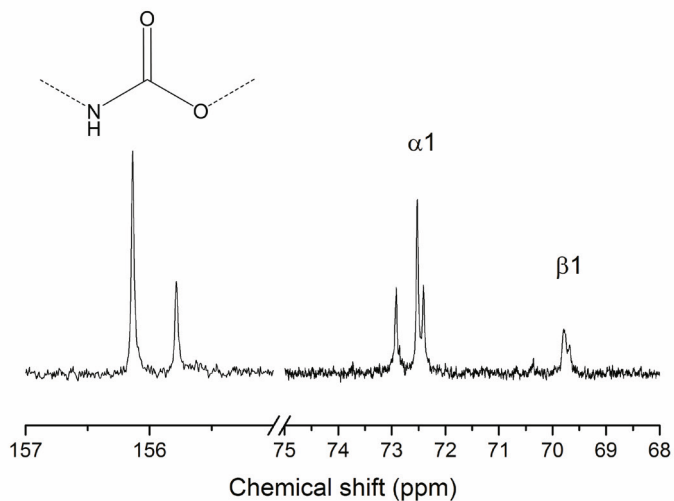
Figure 4.13   Zoom of the ^{13}C-NMR spectrum of **DGC-BDA** in DMSO-d_6.

Chapter 5

Water-borne dispersions from bio-based poly(hydroxy urethane)s

*Water-borne dispersions have been prepared starting from poly(hydroxy urethane)s, building on the results presented in Chapter 4 of this thesis. The fully bio-based polymers were synthesized from diglycerol dicarbonate (**DGC**), butane-1,4-diamine (**BDA**), and fatty acid dimer diamine (**FDA**). A carboxylic acid functionality was introduced by reaction of the formed pendent hydroxyl functionalities with the renewable compounds succinic or citric anhydride. DSC analysis of the polymers showed two T_g values which indicated phase separation of BDA- and FDA-rich phases. The prepared polymers were dispersed in water using three types of dispersers: a rotor-stator system which collected a significant amount of polymer in its internal parts, a helical ribbon impeller which is also used for the polymer synthesis, and a blade disperser which, because of its dimensions, required a larger volume of material. All dispersions had average particle sizes larger than 220 nm, independent of the used dispersion technique or stabilization mode. The ζ-potential values were most often between -30 and -40 mV. Microscopy techniques were employed to analyze the particles. Optical microscopy and cryo-TEM revealed bilayer structures in dispersions produced with a blade disperser. Cryo-TEM and cryo-SEM images indicated that a part of the polymeric material had dissolved in the water phase. These observations were attributed to formation of blocks of **BDA** and **FDA** during synthesis: the polar **BDA**-rich polymers may be able to dissolve in water, the **FDA**-rich polymers formed the particles, and polymers bearing both blocks could form bilayers.*

5.1 Introduction

Polyurethane dispersions (PUD) are a type of industrial coatings that continues to grow its market share at the expense of traditional solvent-borne systems. Their main advantages are the low VOC emissions due to the use of water as a continuous phase, the fact that they are nontoxic, and that these systems possess a great flexibility in the type of monomeric structures which can be incorporated.[1,2] Commonly, prepolymer polyurethanes are synthesized with isocyanate end-groups and an ionic moiety incorporated along the main chain. In the prepolymer mixing process, the prepolymers are dispersed from a low-boiling solvent into water where they are chain extended with diamines to produce the final high molecular weight PUD (Figure 5.1). An alternative route is the acetone process in which the prepolymers are first chain extended in acetone and subsequently dispersed into the water phase.[3] Typically, water is added to the polymer solution but it is possible to reverse this order. The concentration of the polymer in a solvent should be as high as possible as the presence of solvent in the final dispersion is undesirable. The solvent can be removed after dispersing when acetone or MEK are used, but for systems using solvents like NMP
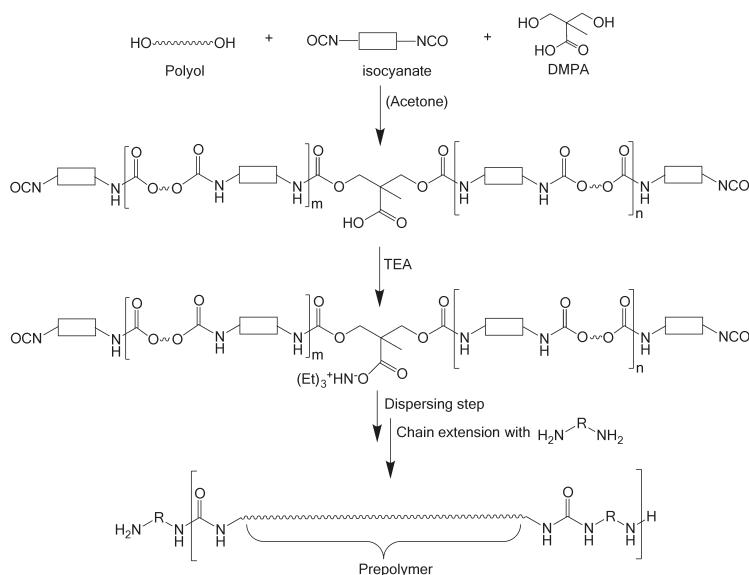
Figure 5.1   **Synthesis of polyurethane dispersions based on a prepolymer mixing process.[4]**

this not possible.

The most commonly used ionic moiety to stabilize PUDs is 2,2-dimethylolpropionic acid (DMPA).[4–7] Its two hydroxyl groups can react with the diisocyanates and therefore the moiety is incorporated in the main chain. The tertiary carboxylic acid group, which is unreactive during the prepolymer synthesis, can subsequently be neutralized using a base to create an ion pair. Often, an organic base such as triethylamine (TEA) is used as it evaporates during film formation. Inorganic bases will remain in the coating and increase the water uptake in the dried films.[7] The ion-pair creates a surface charge resulting in an electrostatic barrier that provides for colloidal stability. A measure of electrostatic repulsion is the ζ-potential. As a rule-of-thumb, an absolute ζ-potential value of 30 mV or larger is necessary to maintain a dispersion stable against Brownian motion.[8,9]

Well-stabilized polyurethanes are dispersed easily. To homogenize the particle sizes, different systems can be used.[10] Figure 5.2 shows a toothed rotor-stator system and a dispersing blade system. Both systems provide for sufficient shear forces to break up large particles into smaller ones. In both systems it is required that the viscosity of the dispersed phase (polymer) is much larger than that of the dispersing
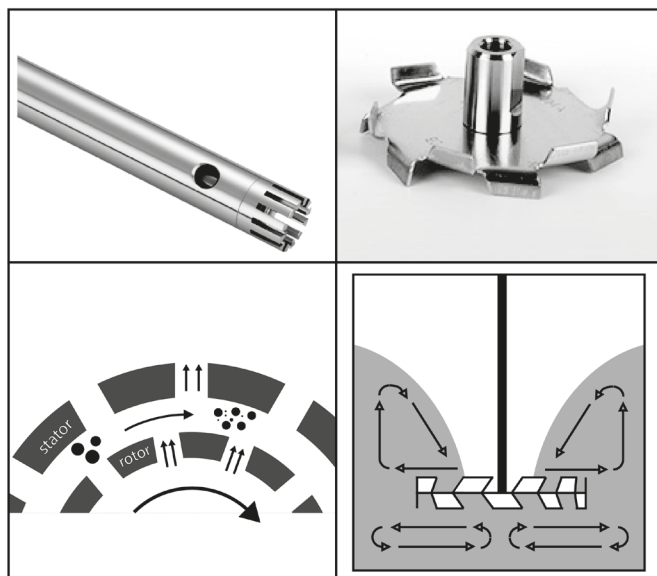
Figure 5.2   **Common rotor systems used for dispersing particles.** *Left*: **a toothed rotor-stator;** *right*: **a dissolver blade.[10,11]**

5

medium (water).

In recent years there have been numerous investigations into the production of (partially) bio-based PUDs.[12] This effort has focused on the three main ingredients of the polyurethanes: the polyol, the diisocyanate, and the intramolecular emulsifier. The polyol has received most of the attention as this part constitutes the largest portion by weight of the polymer. Especially rapeseed oil and soybean oil derivatives have often been used as polyols.[13–16] Fatty acid derivatives have also been described to act as polyols.[17,18] Other examples are hydroxyl telechelic natural rubber, and tannic acid derivatives.[19,20] In these examples, the polyester polyol was replaced by bio-based alternatives. However, petroleum-based isophorone and hexamethylene diisocyanate (IPDI and HDI) were still used as diisocyanates. Li *et al.* described the use of bio-based diisocyanates prepared from dimerized fatty acid (DDI) and lysine (EELDI) combined with isosorbide and DMPA to achieve near-fully bio-based PUDs.[21,22] Chen *et al.* reported the conversion of epoxidized linseed oil to a family of multihydroxy fatty acids to serve as a bio-based alternative to DMPA.[23] All these efforts could in principle be combined to design fully bio-based alternatives to traditional PUDs.

One has to consider that the synthesis of these monomers from the naturally occurring compounds commonly uses non-renewable chemicals, which in case of isocyanate production are toxic themselves. Few reports describe PUDs synthesized from non-isocyanate polyurethanes (NIPU) which circumvents the use of isocyanates altogether. Tramontano and Blank reported the use of dispersed NIPU prepolymers for cured coatings using melamine or polyisocyanates for cross-linking.[24–27] Their NIPUs were synthesized sequentially. The monomers are not explicitly reported but most likely hexane-1,6-diamine is reacted with propyl-1,2-carbonate to form a dicarbamate. This monomer is transurethanized with a polyol and a triol. Residual hydroxyl groups are reacted with an anhydride to provide carboxylic acid functionality. Their work shows the feasibility of NIPUs in the production of polyurethane dispersions, although not all systems are completely isocyanate-free.

NIPUs synthesized from cyclic carbonates and diamines have not been reported for PUD applications to the best of the authors knowledge. These poly(hydroxy urethane)s (PHU) bear a significantly higher hydroxyl functionality compared to conventional

polyurethanes, making them more hydrophilic. This chapter describes the synthesis of PHU and their use in water-borne dispersions. As non-commercial monomers were used, the supply of these starting materials was limited, which resulted in a reduced number of experiments which could be carried out. Therefore, the research described in this chapter is of an exploratory nature.

5.2 Materials and methods

5.2.1 Materials

The reactants butane-1,4-diamine (**BDA**, 99%), succinic anhydride (**SA**, 99+%), citric acid (99.5+%), acetic anhydride (98+%), and triethylamine (TEA, 99.5%) were purchased from Sigma-Aldrich. Priamine™ 1075 (**FDA**, AmV = 210 mg KOH g^{-1}) was kindly supplied by Croda. Diglycerol dicarbonate (**DGC**) was synthesized by Wageningen UR Food and Biobased Research. Solvents were obtained from Biosolve in AR grade. Deuterated solvents for NMR spectroscopy were purchased from Cambridge Isotope Laboratories, Inc. All chemicals were used as received without further purification. Citric anhydride (**CA**) was prepared from citric acid and acetic anhydride according to the procedure reported by Repta and Higuchi.[28,29]

5.2.2 Methods

NMR spectroscopy

^{1}H-NMR (delay time 5s, 32 scans, 90°) and ^{13}C-NMR (delay time 1s, 2000+ scans) spectroscopy measurements were performed on a Agilent 400-MR NMR system in DMSO-d_6 and DMF-d_7. Data was acquired using VnmrJ3 software. Chemical shifts are reported in ppm relative to tetramethylsilane (TMS). Number average molecular masses (M_n) were calculated using Eq-2.1.

TGA

Thermogravimetric analysis (TGA) was performed on a TA Q500 instrument (TA Instruments). Dispersions with a typical mass of 40 mg were heated at a rate of 10 °C min^{-1} from 30 to 120 °C in an N$_2$ atmosphere, the temperature was kept isothermal for 60 minutes after which heating continued at a rate of 10 °C min^{-1} to 600 °C.

5

DSC

Differential Scanning Calorimetry (DSC) was performed on a TA Q100 DSC. Approximately 5 mg of dried polymer (60 °C overnight at reduced pressure) was accurately weighed and sealed into an hermetically closed aluminum pan. Temperature profiles were measured from at least -60 °C to 150 °C and consisted of two heating runs and one cooling run, at a heating/cooling rate of 10 °C min^{-1}. TA Universal Analysis software was used for data acquisition and analysis. The value for the T_g was determined from the inflection point in the thermogram during the second heating run.

SEC

Size exclusion chromatography (SEC) was performed at 60 °C on a Waters Alliance system equipped with a Waters 2695 separation module, a Waters dual λ absorbance detector, a Viscotek 270 dual detector, a Viscotek 250 dual detector, and a PSS GRAM guard column followed by PSS GRAM columns in series with a pore size of 100 Å (10 μm particles) and 3000 Å (10 μm particles) respectively. *N,N*-dimethylacetamide (DMAc, Biosolve AR) with lithium chloride (50 mmol L^{-1}) was used as an eluent at a flow rate of 1 mL min^{-1}. The molecular weights were calculated against polystyrene standards (Polymer Laboratories, M_p = 580 g mol^{-1} up to M_p = 7.5·10^6 g mol^{-1}). Before SEC analysis was performed, the samples were filtered through a 0.2 μm PTFE filter. Samples were prepared in eluent at a concentration of 2-3 mg mL^{-1}.

Dispersing

Dispersions were prepared using either an Ultra-Turrax T25 with a S25N-18G dispersing element (rotor-stator) rotating between 7,500 and 15,000 rpm, or with an Ultra-Turrax T50 with a R1303 dissolver (see Figure 5.2) rotating at 4,000 rpm.

pH

pH measurements were performed using a Metrohm 691 pH meter, calibrated with CertiPUR buffer solutions of *pH* 4.01 and *pH* 10.00 before use.

DLS

Dynamic light scattering experiments were performed on a Malvern Zetasizer Nano ZS at 25 °C. Sample parameters were chosen for a dispersed phase (refractive index = 1.59, absorption = 0.1) in a water phase. The *z*-average diameter was

determined using 10 times 10 runs (averaged over 10 measurements). The ζ-potential was determined using 10 runs, averaged over 10 measurements. For **SDD1** this was 50 runs averaged over 20 measurements.

Optical microscopy

Optical microscopy was performed on a Leica Axioplan 2 equipped with a Leica Axiocam and a Hal100 light source. The lenses used were: Plan-NEOFLUAR in magnification 10x, 20x, and 40x for bright- and dark-field, and LD A-Plan (20x) and LD ACHROPlan (32x) for contrast images. Data was recorded using Leica axiovision software.

Cryo-TEM

Cryogenic transmission electron microscopy (cryo-TEM) measurements were performed on an FEI Tecnai 20, type Sphera TEM instrument equipped with a LaB6 filament operating at 200 kV. The sample vitrification procedure was carried out using an automated vitrification robot (FEI Vitrobot Mark III). The sample was diluted 10 times and 3 μl of the diluted sample was applied onto a Quantifoil grid (R 2/2, Quantifoil) excess liquid was blotted away (3 s), and the formed thin film was shot into melting ethane.

Cryo-SEM

Cryogenic scanning electron microscopy (Cryo-SEM) measurements were performed on a FEI Magellan 400 instrument equipped with a Leica cold stage. The system was operated at 2.0 kV. Samples were frozen in liquid nitrogen and subsequently prepared on Leica MED 020/VCT 100. The frozen samples were fractured, the water was partially removed by sublimation for 3 to 15 minutes at -90 °C. After this the samples were coated with tungsten (12 nm).

Viscosity

Viscosity measurements were performed on a Anton-Paar Physica MCR 301 using a concentric cylinder setup (CC27-SN12791). Data was recorded with Rheoplus/32 V3.62 software. The viscosity was recorded (10 data points averaged during 10 seconds) at shear rates ranging from 10^{-3} to 100 s^{-1} at 20 °C.

5
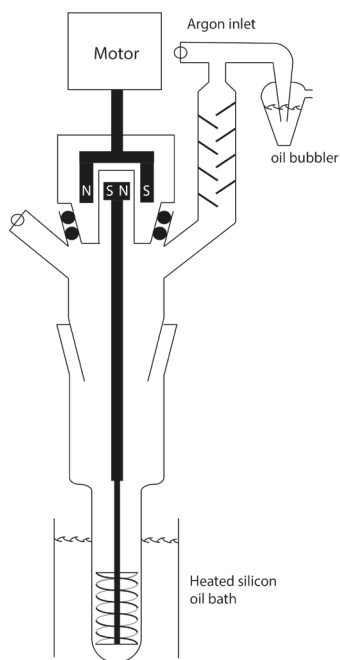
Figure 5.3 *left*: **Reactor setup used for the synthesis of poly(hydroxy urethane) resins and for producing dispersions. A magnetically coupled stirring setup is fitted to ensure a closed system. Properties of the double helical ribbon impeller: diameter 13 mm, ribbon width 2 mm, shaft diameter 3 mm, length 30 mm, pitch 1 rotation/10 mm, stainless steel.** *right*: **SAH1 during dispersing.**

5.2.3   Synthetic and dispersing procedures

Synthesis of PHU1

DGC (5.010 g, 22.96 mmol), **BDA** (1.422 g, 16.13 mmol) and **FDA** (3.671 g, 6.86 mmol) were charged into a glass reactor equipped with a double helical ribbon impeller (see Figure 5.3). Under an inert argon atmosphere, the reactants were stirred at room temperature for 9 minutes, after which the reactor was heated to 80 °C using a silicon oil heating bath. After 2 hours, the temperature was increased to 100 °C. After 5.25 hours, a solution of **SA** (0.805 g, 8.02 mmol) in 4.5 mL 2-butanone was added to the melt. The solvent was allowed to evaporate in roughly 30 minutes. The reaction was terminated after 7.25 h and the polymer was discharged. The polymer was dried overnight under reduced pressure at 60 °C and obtained as a yellow transparent material with a yield of 9.48 g (87 wt% of maximum achievable weight).

Synthesis of PHU2

DGC (3.996 g, 18.01 mmol), **BDA** (0.862 g, 9.78 mmol) and **FDA** (4.901 g, 9.16 mol) were charged into a glass reactor equipped with a double helical ribbon impeller (see Figure 5.3). Under an inert argon atmosphere, the reactants were stirred at room temperature for 8 minutes after which the reactor was heated to 80 °C using a silicon oil heating bath. After 2 hours, the temperature was increased to 100 °C. After 22 hours, the reaction was terminated by dissolving the polymer in toluene. The polymer was dried overnight under reduced pressure at 100 °C and obtained as a yellow transparent material.

Typical procedure for preparing a poly(hydroxy urethane) dispersion using a helical ribbon stirrer setup

DGC (0.501 g, 2.30 mmol), **BDA** (0.145 g, 1.64 mmol), and **FDA** (0.370, 0.69 mmol) were charged into a glass reactor equipped with a double helical ribbon impeller (see Figure 5.3). Under an inert argon atmosphere, the reactants were stirred at room temperature for 10 minutes after which the reactor was heated to 80 °C using a silicon oil heating bath. **SA** (79 mg, 0.79 mmol) is dissolved in 1 mL NMP or 2 mL acetone. After 3 hours of reaction, the **SA** solution is added and solvent is allowed to evaporate if possible. After 5 to 6 hours of reaction, TEA (75 μL, 0.54 mmol in 1 mL NMP, or 110 μL, 0.79 mmol in 2 mL acetone) is added for neutralization of the formed pendent acid groups. From this moment on, the time of events differs between the two solvents.

NMP procedure: After 1 hour the reaction mixture is cooled to 40 °C and 18 mL of demineralized water is added drop wise to the reaction mixture whilst stirring. The mixture forms a white dispersion and is stirred overnight. After 18 hours of dispersing, the dispersion is transferred into a storage container.

Acetone procedure: After 20 minutes, 5 mL of demineralized water at 80 °C is added drop wise to the reaction mixture whilst stirring. The mixture forms a white dispersion and after 15 minutes the mixture is cooled to 40 °C to continue stirring overnight. After 18 hours of dispersing, the dispersion is transferred into a storage container.

5

Typical procedure for preparing a poly(hydroxy urethane) dispersion using a rotor-stator setup

The poly(hydroxy urethanes) were dissolved in NMP (34 wt%, 2 mL) after synthesis and neutralized using a solution of triethylamine (TEA) in the same solvent. The polymer solution was heated to a temperature between 40 and 80 °C. The rotor-stator was fitted and 16 mL of demineralized water was added. The dispersions were prepared by applying high shear (7,500-15,000 rpm) for 15-60 minutes.

Procedure for preparing a poly(hydroxy urethane) dispersion using a dissolver disc setup

A jacketed reactor was filled with 50 mL demineralized water and heated to 50 °C. A neutralized solution of **PHU1** in DMF (51 wt%, 8.5 mL) was added dropwise to the reactor while stirring at 4,000 rpm, which was continued for 15 minutes.

5.3 Poly(hydroxy urethane) resins

In Chapter 4, the synthesis and physical properties of poly(hydroxy urethane)s are reported. Building on those results, these polymers have been tested as resins for water-borne applications. The as-synthesized PHUs have been dispersed from a NMP solution using a rotor-stator setup. Analysis of the dispersions (C_{solids} = 2 wt%) indicated that the poly(hydroxy urethane)s cannot form a colloidally stable dispersion in water without additional stabilization. The ratio between the hydrophilic diglycerol unit and the tunable diamine unit could not be optimized sufficiently to afford colloidally stable systems. The dispersions contained large particles which were visible to the naked eye, while the particle size should be lower than 1 μm. These large particles sedimented within minutes after production of the dispersion. Therefore, the use of the described poly(hydroxy urethane)s as resins in water-borne systems requires an additional stabilizing method to form a stable dispersion. A good approach would be to incorporate ionic groups along the polymer backbone to provide for electrostatic stabilization.
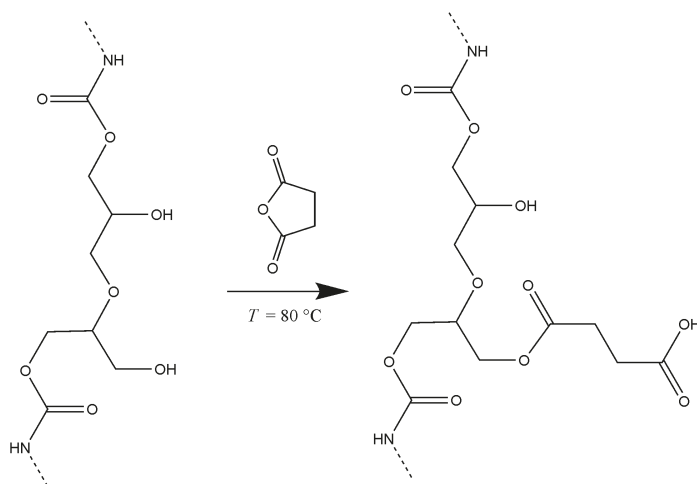
Figure 5.4 **Modification of PHU with succinic anhydride after the polymer synthesis.**

5.3.1 *Carboxylic acid introduction for ionic stabilization*

Ionic stabilization in conventional polyurethanes is often achieved by adding 2-5 weight percent of dimethylolpropionic acid (DMPA) to the reaction mixture during the prepolymer synthesis.[5–7,13] However, the hydroxyl functionality of this monomer is unsuitable for reaction with cyclic carbonates due to its moderate reactivity. Therefore, an alternative compound is necessary. For incorporation into the backbone of the polymer, diamines with a pendent carboxylic acid would be a suitable choice. The incorporation of *L*-Lysine has been attempted, however it was observed that the activity of the *β*-amine was hindered by the presence of the carboxylic acid. Therefore, it acted as a chain stopper during the PHU synthesis and an insufficient amount was incorporated.

The hydroxyl values of the PHU are very high with values for primary hydroxyl groups around 1.8 mmol and for secondary hydroxyl groups around 4.1 mmol per gram polymer. This functionality can be exploited for post-polymerization modification of the polymers. A potentially useful route is to use anhydrides to attach pendent carboxylic acid functionality onto the PHU backbone, similar to the approach followed by Blank *et al.*[26] This route also has been reported for solubilizing cellulose and lignin.[30–33] For every anhydride reacting with a hydroxyl group on the polymer chain, a pendent carboxylic acid group is formed (Figure 5.4). These carboxylic acids

5
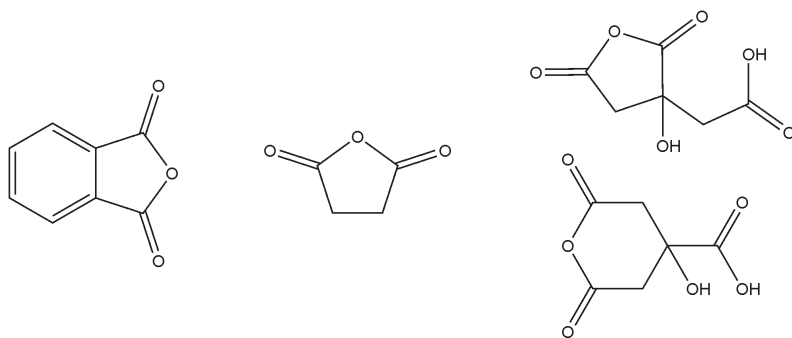
Figure 5.5 **Chemical structures of phthalic anhydride (*left*), succinic anhydride (*middle*), and two isomers of citric anhydride (*right*).**

can subsequently be neutralized by a base. The reaction between an anhydride and a hydroxyl group proceeds at moderate temperatures and without any side products. Most likely, there is a difference in reactivity between primary and secondary hydroxyl groups in this reaction. If unreacted amine groups are still present in the reaction mixture, for example at the chain end of the PHUs, they will readily form amic acid structures through reaction with the anhydrides. Further heating of the reaction mixture could then result in the formation of imide terminated chain ends.

The occurrence of the reaction of the bio-based anhydrides of succinic acid and citric acid (Figure 5.5) with the hydroxyl functionalities along the polymer chain demonstrated to be difficult to confirm analytically. **DGC-BDA** (see Chapter 4) was reacted with phthalic anhydride, after which the residual unreacted anhydrides or diacids formed by ring-opening with water were removed by precipitation in acetone. The solubility of the polymer sample decreased significantly upon addition of the phthalic anhydride because of the introduction of the carboxylic acid groups. Therefore, the samples could not be dissolved in DMSO-d_6, which is normally used as an NMR solvent for these PHUs. HFIP-d_2 did dissolve the polymers. However, the residual solvent signals interfered with the signals of interest to an extent that the results were inconclusive. The reactants and the product could be dissolved in DMF-d_7 which allowed for the analysis of the reaction.

The resulting ^{1}H-NMR and ^{13}C-NMR spectra are shown in Figure 5.6. Two regions indicated that the reaction occurred. The region of δ = 7.5 to 8.5 ppm contained the signals of the aromatic protons of phthalic anhydride. Additional resonances were
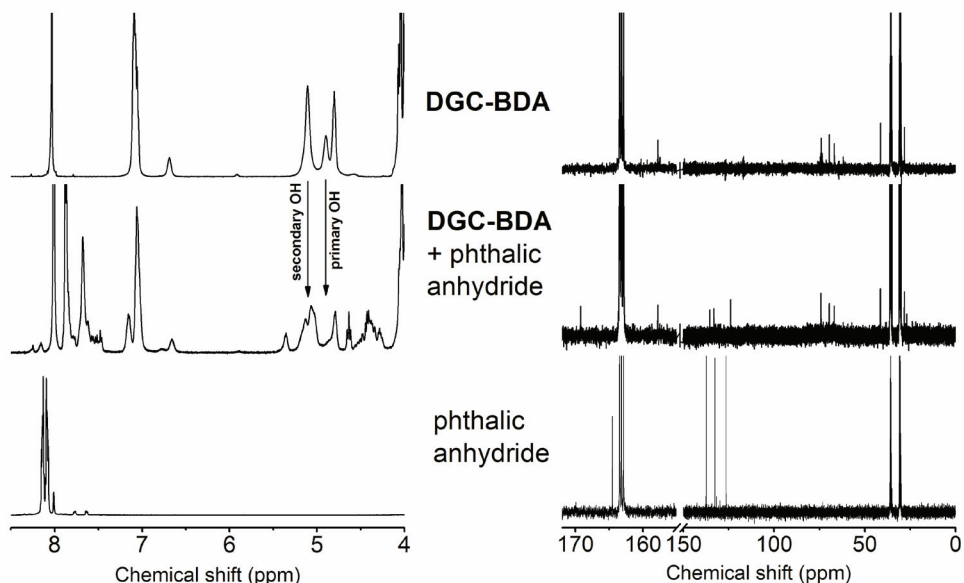
Figure 5.6 ¹H-NMR (*left*) and ¹³C-NMR (*right*) spectra of **DGC-BDA**, **DGC-BDA** after reaction with phthalic anhydride, and phthalic anhydride in DMF-d_7.

observed in the product indicating that the structure of the anhydride had changed. The second region contained the resonances for the hydroxylic protons at δ = 5.1 ppm (secondary) and at 4.9 ppm (primary). The signal at δ = 4.8 ppm was assigned to β2 (see Chapter 4). The resonance for the primary hydroxyl groups could not be observed any more after the reaction. In the ¹³C-NMR spectra, a two ppm upfield shift could be observed for the aromatic ring carbons from δ = 137-126 ppm to δ = 135-124 ppm. These frequencies were absent in the original polymer. The resonance of the quaternary carbons in the anhydride (δ = 165 ppm) shifted to δ = 169 ppm for both the carboxylic acid and ester. These observations verified that the hydroxyl groups, formed during the synthesis of the poly(hydroxy urethane)s, could react with anhydrides to form an ester bond and a free carboxylic acid group. Therefore, the reaction between an anhydride and the PHU was a suitable pathway to introduce pendent carboxylic acid functionalities for electrostatic stabilization of the dispersion.

In this chapter, the amount of anhydride reacted is expressed as mol anhydride per mol monomer. For every urethane bond that forms during polymerization, one hydroxyl group is formed which can react once with an anhydride. This means that the loading is relative to the unmodified polymer, not the of the final polymer. An

5

anhydride loading of 0.10 to polymers with DP_n = 10 will result in that on average every polymer chain will react with one anhydride molecule.

5.3.2   Resin synthesis

In this chapter, two approaches are described to prepare dispersions. One involves the addition of water at the end of the PHU synthesis. This means that the polymer was not discharged prior to the dispersing step. This reduced losses of material but the geometry of the reactor (see Figure 5.3) prevented sampling of the polymer. In the second approach, the PHU was synthesized and discharged first after which the isolated material was dispersed in a separate step. This method required more material but allowed for different dispersing equipment, *e.g.* rotor-stator systems, to be used.

Although phthalic anhydride can potentially be produced from a bio-based feedstock, aliphatic anhydrides are preferred.[34,35] Here, succinic and citric anhydride have been selected.[28,29,36,37] In the synthetic procedure, these anhydrides were introduced after 3 to 5 hours of polymerization to the reaction mixture to react with the remaining amines and the formed hydroxyl groups.

PHU1 and **PHU2** were synthesized for use in dispersions. **PHU1** was modified

Table 2.3   Molecular weights and compositions of **PA**-based polyamides determined by SEC and ^{1}H-NMR.

Polymer	Anhydride	SEC	
		M_n	Đ
		g mol^{-1}	
PHU1[a]	-	7,600	2.8
PHU1	SA	4,700	2.9
PHU2	-	13,900	2.9
SDD1	SA	7,900	2.5
SNH1	SA	6,500	1.9
SNH2	SA	8,100	1.8
SNH3	SA	7,900	2
SNH4	SA	7,800	1.9
CNH1	CA	5,400	2.4

[a] *Prior to addition of SA to the reaction mixture.*
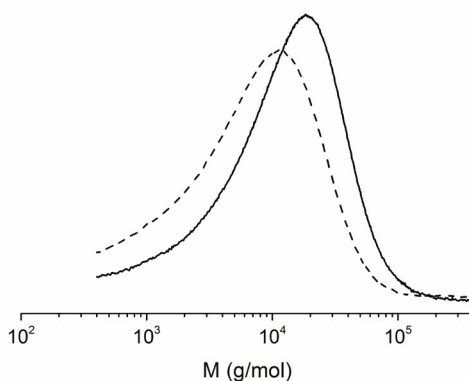
Figure 5.7   SEC trace of **PHU1** before (solid) and after (dashed) reaction of SA with the polymer.

with **SA** while **PHU2** was a polymer without anhydride treatment. Comparing the molecular weight values (Table 5.1), both without modification, it was noted that the excess of diamine used in the synthesis of **PHU2** (5% excess) yielded a significantly higher M_n value than for **PHU1** (stoichiometric ratio between diamine and dicyclic carbonate) due to slight evaporation and deposition of the **BDA** in the bearings of the stirrer setup. The Đ values were similar.

Figure 5.7 shows the SEC traces of **PHU1** with and without the anhydride. For the unmodified polymer, a M_n of 7,600 g mol^{-1} was obtained, and for the modified sample the M_n was 4,700 g mol^{-1}. Most likely, this difference was not originating from a cleavage of the urethane bonds, but from the addition of the carboxylic acid groups which induced a change of the hydrodynamic volume of the polymers. In this case, the polymers with pendent carboxylic acid groups are thought to have a smaller radius of gyration in DMAc and therefore showed increased retention times, compared to the polymers bearing only hydroxyl groups. Unfortunately, the ^{1}H-NMR spectrum was unsuitable to calculate the molecular weight of the modified PHUs, because the resonances were poorly resolved.

DSC analysis of **PHU1** modified with **SA**, showed two T_g values at -3 and 23 °C (see Figure 5.8). **PHU2** without modification also showed two similar T_g values. These T_g values were close to the T_g values of the corresponding homopolymers, *i.e.* **DGC-BDA** and **DGC-FDA**, at -7 and 21 °C, respectively. This indicated that phase separation occurred, leading to a **FDA**-rich phase and a **BDA**-rich phase. The presence of the structural isomers α and β (see Chapter 4) dominated the fine structure in ^{13}C-

Figure 5.8   DSC traces of the first (black) and second (grey) heating run of (*left*) **PHU1** with **SA** and (*right*) **PHU2** without **SA**, recorded at a heating rate of 10 °C min^{-1}.

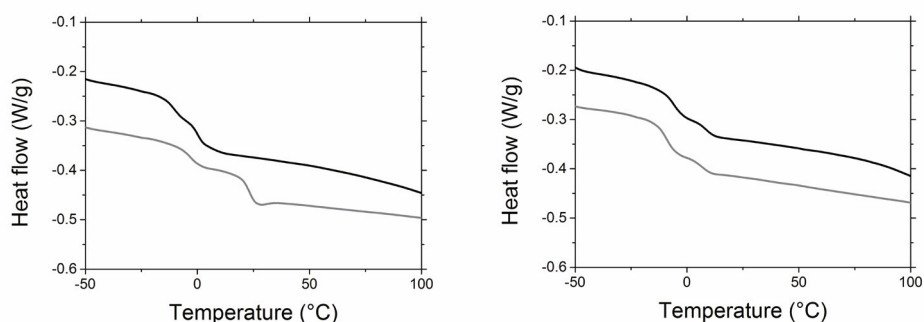NMR to an extent that verification of a blocky polymer structure was impossible. The low molecular weights of the polymers and their low T_g values may necessitate additional chain extension or cross-linking during coating application. To maintain an isocyanate-free system, an option would be to use hexakis(methoxymethyl) melamine as it can cross-link both the carboxylic acids and hydroxyl groups which are both readily available on the polymer backbone.

5.4 Dispersion properties

Three dispersive stirrer set-ups have been selected to prepare the dispersions described in this chapter: a toothed rotor-stator system, a dissolver system (Figure 5.2), and the helix impeller used for the synthesis of the PHUs (Figure 5.3). Furthermore, several solvents have been tested, and both citric anhydride and succinic anhydride have been used to introduce pendent carboxylic acid groups along the PHU backbone. To help the reader distinguish these parameters, a three-letter code has been given:

C/S   Citric anhydride / Succinic anhydride
A/D/N   Acetone / DMF / NMP
D/H/R   Dissolver blade / Helical ribbon impeller / Rotor-stator

The code is ended by a number, *e.g.* **CNR1**. Depending on temperature during dispersing, acetone could evaporate while DMF and NMP remained in the system. NMP and DMF solubilized the polymers completely. Acetone did not dissolve the polymer but functioned as a plasticizer.

5.4.1   Rotor-stator system (XXRX)

The polymer **PHU2** was synthesized in the reactor shown in Figure 5.3. After synthesis, it was transferred to another reactor to allow access for the larger dimensions of the rotor-stator setup. In the second reactor, the modification with the anhydride was performed, followed by neutralization with triethylamine (TEA, $pK_{a,protonated}$ = 10.6), and subsequently the preparation of the dispersions from NMP (Table 5.2). To completely dissolve 1 gram of polymer, roughly 2 mL of NMP was required. The total liquid volume necessary for dispersing in this reactor was 16 mL. Therefore, the

Table 5.2   Dispersions produced from NMP with a rotor-stator system.

Disp.	Stability[a]	Anhydride loading[b]	Neutrali- zation[c]	pH	z-average diameter	PSD[d]	ζ-potential
					nm		mV
CNR1	-	0.04	1.19	8.8			
CNR2	+/-	0.05	0.58	5.7			
CNR3	+	0.05	0.62	5.1	220	0.35	-30
CNR4	-	0.05	0.52	4.9			
CNR5	-	0.05	0.97				
SNR1	-	0.02	0.99	9.2			

[a] + no sedimentation observed, +/- sedimentation with stable top layer, - no dispersed layer; [b] mol anhydride per mol monomer; [c] mol TEA per mol carboxylic acid group; [d] particle size distribution.

predicted solids content when using 1 gram of polymer was 6.4 wt%. However, the actual solids content obtained was considerably lower. Upon opening the rotor-stator system for cleaning, a significant portion of the polymer was found to be located in the internal parts of the stator. Furthermore, severe foaming was observed during the dispersing step. Several dispersions were made in this way and the solid residue and foam were observed in every experiment.

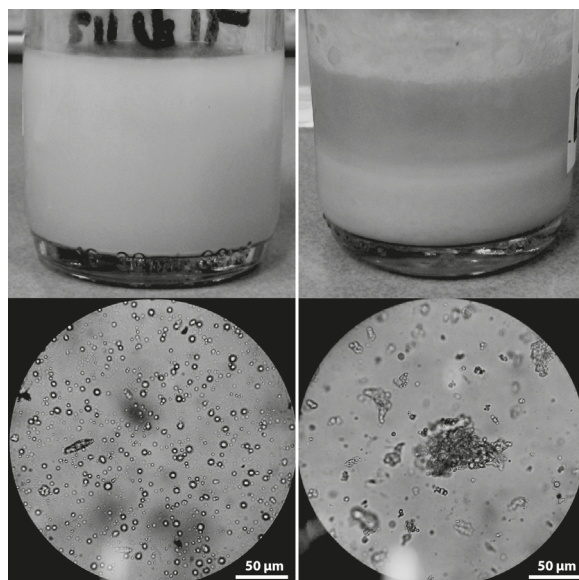Table 5.2 reports the limited amount of data obtained for these unstable

Figure 5.9   Dispersions **CNR3** (*left*) and **CNR4** (*right*) and their corresponding optical microscopy images.

dispersions. These systems were difficult to analyze by light-scattering techniques as particles above 10 μm, which were abundantly present, negatively affected the measurement. One dispersion (**CNR3**) remained stable for a small number of days. This dispersion experienced a higher energy input because the stirrer was active for a longer period of time. The average particle size was in the right range at 220 nm. The ζ-potential was found to be -30 mV, which should be improved. However, the preparation of this dispersion still left a significant amount of residue in the stator. The *pH* values indicated that a higher degree of neutralization was necessary. A *pH* value between 6.5 and 8 would be optimal, as it is above the pK_a of both succinic ($pK_{a,2}$ = 5.6) and citric acid ($pK_{a,3}$ = 5.8) which are therefore mostly deprotonated. And the conditions are not too basic, which would catalyze the hydrolysis of the ester bond with the anhydride moiety.[38–40] For the remainder of the dispersing trials, the use of the rotor-stator system was avoided due to the high losses and poor results.

5.4.2   Helical ribbon impeller (XXHX)

To avoid equipment in which material can be lost and to work on a 1 gram scale, polymers have been dispersed in the reactor in which they were synthesized (see Figure 5.3). At the end of the polymer synthesis, the anhydride was dissolved in acetone and added to the reaction mixture. The carboxylic acid groups that formed were neutralized by TEA in the dispersing solvent (NMP or acetone, respectively). Preheated demineralized water was added to form the dispersion.[41] However, the helical ribbon impeller is not properly designed to apply high shear forces in aqueous systems. Therefore the polymers have to be well-stabilized. Compared to the previous series, the amount of acid groups is increased to a loading of 0.12 (note that the attachment of **CA** onto the PHU backbone results in two pendent carboxylic acid groups per **CA** molecule). Furthermore, the level of neutralization is increased to 1.00 (*i.e.* one molecule of TEA for each carboxylic acid that theoretically has formed). The results are reported in Table 5.3 and Table 5.4.

The dispersions reported in Table 5.3 were produced from a polymer solution in NMP and dispersed using the helical ribbon impeller. These dispersions were visually more stable than those obtained with the rotor-stator system (Table 5.2). Dispersion

Table 5.3 **Dispersions produced from NMP with a helical ribbon impeller system. Values in italic are measured on the stable top layer and do not represent the entire sample.**

Disp.	Stability[a]	Anhydride loading[b]	Neutrali-zation[c]	*pH*	*z*-average diameter	*PSD*	*ζ*-po-tential	Solids content	
					nm		mV	pr. wt%	det.[d] wt%
SNH1	+	0.12	0.99	7.5	210	0.17	-45	5.4	7.2
SNH2	+/-	0.12	1.00	6.8				5.3	4.3
SNH3	+/-	0.12	0.99	6.7	*5440*	*1.00*	*-23*	5.3	3.7
SNH4	+/-	0.12	1.00	7.2	*1920*	*0.99*	*-36*	5.3	4.5
SNH5	+	0.12	1.00	6.6	540	0.52	-35	5.3	5.3
SNH6	+	0.18	1.00	6.7	240	0.19	-38	5.3	5.3
CNH1	+/-	0.06	0.98	7.5				5.3	3.6

[a] + no sedimentation observed, +/- sedimentation with stable top layer, - no dispersed layer; [b] mol anhydride per mol monomer; [c] mol TEA per mol carboxylic acid group; [d] Determined by drying 1 g of dispersion under reduced pressure in presence of P_2O_5.

CNH1 showed phase separation within a few days after dispersing. The clear water layer still contained 3.6 wt% of dissolved solid material. The other dispersions were turbid with various degrees of sedimentation (see Figure 5.10). None of the samples showed the blueish color that is associated with dispersions with average particle sizes below 200 nm. **SNH1**, **SNH5**, and **SNH6** did not show sedimentation after dispersing and the solids contents were similar to the predicted values. **SNH2**, **SNH3**, and **SNH4** did show sedimentation, which led to reduced solids content of the dispersions. As the preparation procedures of **SNH1**, **SNH3**, **SNH4**, and **SNH5** are nearly identical, it is unclear what causes the differences between them.

The *z*-average particle sizes for the stable dispersions were between 210 and 540 nm

5

Figure 5.10 **Dispersions from left to right: SNR1 (42), SNH1 (34), SNH2 (28), CNH1 (23), SNH3 (14), SNH4 (5), SNH5 (2), SNH6 (2). The value between brackets indicates the amount of days since the preparation of the dispersion.**

while the samples with sedimentation had *z*-average particle sizes exceeding 1 μm. All samples showed a broad particle size distribution (*PSD*) with values larger than 0.1 The *PSD* of **SNH3** and **SNH4** were extremely high. **SNH4**, **SNH5**, and **SNH6** had ζ-potentials which were promising (ζ-potential < -30 mV) but further improvement should be made. **SNH1** had a ζ-potential < -40 mV. Increasing the amount of acid groups on the polymer backbone did not lead to a significantly more negative value of the ζ-potential. The increased amount of carboxylic acid groups decreased the average particle size. The *pH* values of these dispersions were in the appropriate range of 6.5 to 8.

The molecular weight distributions of the dispersed polymers have been analyzed. The dispersions were dried to constant weight to obtain the solid material (Table 5.1). The polymers in **SNH1-4** had M_n values of 6,500 to 7,900 g mol^{-1} according to SEC measurements. These were higher than the value of **PHU1**, which was 4,700 g mol^{-1}. The M_n value of **CNH1** was 5,400 g mol^{-1}. This indicated that the polymer synthesis was successful and that the polymers were stable in the dispersions during at least 100 days, the time between dispersing and drying.

The dispersions prepared in this series show improved stabilities compared to those made using the rotor-stator system. Most likely, this is due to a better stabilization of the polymers, as the reduced dispersing power of the helical ribbon impeller is not expected to contribute to more stable dispersions. The increased extent of anhydride modification of the polymers appears to have a beneficial effect on the dispersion stability. However, it remains unclear why similar experiments give a large spread on the results. The poly(hydroxy urethane)s are stable during at least 100 days in water.

As NMP cannot be removed from the dispersion, the use of lower boiling solvents such as acetone and 2-butanone (MEK) is favorable (see Table 5.4). However, instead of dissolving the PHUs, these solvents swell the polymers and act as plasticizers. The amount of residual solvent in the dispersion should be as low as possible. Therefore, the NMP-series was prepared with a large amount of water. Because acetone can be removed, the amount of water in the acetone-series could be reduced. This resulted in dispersions with a higher solids content.

The dispersions prepared from an acetone solution (**SAH1-9**, Figure 5.13) had higher

Table 5.4   **Dispersions produced from acetone with a helical ribbon impeller system. Values in italic are measured on the stable top layer and do not represent the entire sample.**

Disp.	Stabi-lity[a]	BDA: FDA	Anhydride loading[b]	Neutrali-zation[c]	*pH*	*z*-average diameter nm	*PSD*	ζ-po-tential mV	Solids content pr. wt%	det.[d] wt%
SAH1	+	7:3	0.17	1.00	6.8	530	0.37	-34	18.2	17.6
SAH2	+	7:3	0.17	0.97	7.4	420	0.50	-28	18.2	16.8
SAH3	+/--	7:3	0.25	1.01		*3990*	*0.90*	*-36*	18.1	16.7
SAH4	+/--	7:3	0.29	0.98		*620*	*0.70*	*-42*	19.3	11.9
SAH5	+	7:3	0.17	1.50		340	0.48	-38	18.3	17.4
SAH6	+	7:3	0.17	1.79		3300	0.98	-34	17.7	
SAH7	+/-	7:3	0.17	1.00	7.0	*870*	*0.70*	*-51*	29.6	27.3
SAH8	+	6:4	0.16	1.14		700	0.72	-35	19.9	17.7
SAH9	+/-	8:2	0.16	1.14		*550*	*0.83*	*-42*	15.9	12.0

[a] *+ no sedimentation observed, +/- sedimentation with stable top layer, +/-- visible large particles in dispersed layer;*
[b] *mol anhydride per mol monomer;* [c] *mol TEA per mol carboxylic acid group;* [d] *Determined by drying 1 g of dispersion under reduced pressure in presence of* P_2O_5.

solids contents (~18 wt%) than the dispersions prepared using NMP (see Table 5.3 and Table 5.4). **SAH1** and **SAH2** were stable dispersions with an anhydride loading of 0.17. In commercial PUD systems, the amount of DMPA incorporated in polyurethanes for PUDs is around 5 wt% of the polymers.[5–7,13] The number of carboxylic acid groups introduced by an anhydride loading of 0.17 are equal to conventional polyurethanes that bear 10 wt% DMPA. In conclusion, these poly(hydroxy urethane)s required more acid functionality to form a colloidally stable dispersion. Using an anhydride loading of 0.17 and equimolar neutralization with TEA resulted in *pH* values between 6.8 and 7.4. In addition to drying the dispersions to constant weight, the solids content of **SAH1** has been determined using TGA (Figure 5.11). The residual weight ($m_0 = 38$ mg) after 60 minutes at 120 °C was 6.8 mg (18 wt%), which was in agreement with the 17.6 wt% obtained from drying 1 gram of dispersion under reduced pressure and in presence of P_2O_5.

The *z*-average particle sizes of dispersions **SAH1** and **SAH2** were roughly 0.5 μm. The *PSD* values were 0.4 - 0.5. Lower particle size values would result in a better long-term stability. Despite the larger amount of carboxylic acid groups per polymer chain
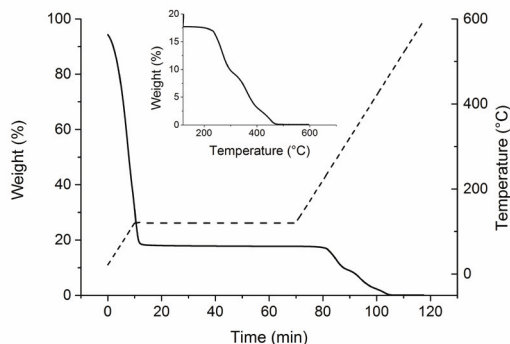
5

Figure 5.11 TGA of **SAH1** (m_0 = 38 mg). After reaching a temperature of 120 °C the temperature was kept constant at this value for 60 minutes to allow for evaporation of water. The heating rate was 10 °C min^{-1}. The inset shows the conventional residual weight *vs.* temperature plot starting at 120 °C (*i.e.* after removal of the continuous water phase).

compared to the previous series, the ζ-potentials were still around -30 mV. This is surprising, as clearly an increased absolute value of the ζ-potential was anticipated. A possible explanation could be that part of the PHU material had dissolved in the water phase, as the polymer has been rendered more polar and is therefore soluble in the continuous phase.

To increase the ζ-potential values, **SAH3** and **SAH4** were produced with increased anhydride loadings (0.25 and 0.29, respectively) while maintaining the same extent of neutralization (see Figure 5.12). Unexpectedly, these dispersions proved to be less stable. Upon discharge these dispersions were homogeneously opaque but they displayed a fast sedimentation of solid material. However, the solids contents of these dispersions indicated that most of the material was dispersed (92 wt% and 62 wt%, respectively). The dispersed layers were analyzed using DLS. The ζ-potentials had indeed improved compared to the values obtained for dispersions that were prepared lower amounts of anhydride, but also the particle size and *PSD* values had increased. Especially the *z*-average particle size of **SAH3** was very large at nearly 4 μm.

SAH5 and **SAH6** were dispersed with an excess of TEA while maintaining the anhydride loading of 0.17 (see Figure 5.12). Both dispersions were stable. **SAH5** had moderate values for the average particle size and the ζ-potential (-38 mV) and an increased value for the *PSD* compared to **SAH1**. **SAH5** had very large values for
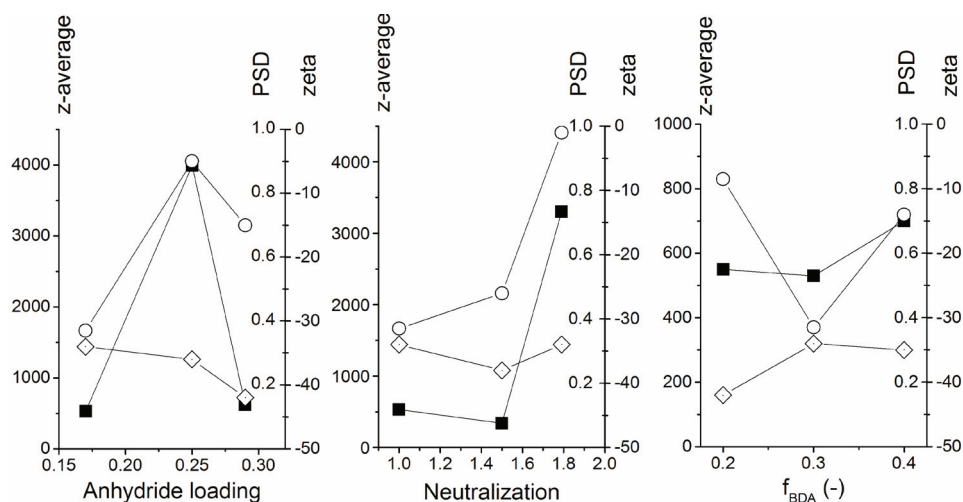
Figure 5.12 *z*-average (■), *PSD* (○), and ζ-potential (◇) as a function of anhydride loading (*left*), neutralization of the acid groups (*center*), or the fraction of **BDA** of the diamines (*right*). Lines have been added to guide the eye. Numerical values are reported in Table 5.4.

the average particle size and the *PSD*, and a moderate ζ-potential of -34 mV. The ζ-potentials thus slightly improved in comparison to **SAH1** and **SAH2**. However, the other properties didn't improve accordingly.

A higher solids content of 30 wt% was targeted with **SAH7**. After dispersing, a two-layer system was observed. The top layer formed a viscous dispersion with a solids content of 27.3 wt%, while the bottom layer was semi-transparent (see Figure 5.13). A dispersion is usually not highly viscous. High viscosity may indicate that polymeric material has dissolved in the continuous phase. Despite that the *z*-average and the *PSD* were rather high, the ζ-potential was -51 mV which was an unexpected improvement. Some polymer remained attached to the stirrer during the dispersion process. This residue was easily rinsed off with fresh demineralized water to form a dispersion. This may indicate that a solids content of 27 wt% is the highest possible solids content at these conditions.

For **SAH8** and **SAH9**, the ratio between **BDA** and **FDA** in the polymer was altered while maintaining the stoichiometric ratio between cyclic carbonates and diamines. As **BDA** is a short aliphatic monomer (4 carbon atoms) and **FDA** is a long aliphatic segment (~20 carbon atoms in the main chain), the overall polarity of the PHU was

5

Figure 5.13 Dispersions from left to right: **SAH1** (16), **SAH2** (9), **SAH7** (9), **SAH8** (2). The value between brackets indicates the amount of days since the preparation of the dispersion.

influenced. For **SAH8** the composition was more apolar. It was observed that the dispersion was stable but roughly 10 wt% of the polymer remained on the stirrer. The particle size and the *PSD* were high and the ζ-potential was -35 mV. **SAH9** contained less **FDA** and was therefore more polar. This dispersion showed sedimentation. The solids content was 75% of the expected value indicating that 25% of the polymer had been lost through sedimentation. Oddly, the value of the ζ-potential was fair at -42 mV, indicating that the dispersion is ionically stable. It is possible that the anhydrides were not mixed homogeneously during the reaction, leading to an inhomogeneous distribution of carboxylic acid groups over the polymer chains.

The use of acetone to disperse the polymers provided stable dispersions from which the solvent can be removed. The particles were generally larger than 0.5 µm with broad particle size distributions. Upon addition of an anhydride loading of 0.25 or higher, negative influences have been observed. This is likely influenced by the observed reduction in *pH*. Increasing the amount of neutralizing agent appeared to provide additional colloidal stability, as expected. However, throughout this series, it was clear that the helical ribbon impeller didn't provide enough shear to decrease the average particle size by breaking up of the initially formed particles. After the initial dispersing step, an additional step would be necessary to break up the particles into multiple particles with a much smaller diameter.
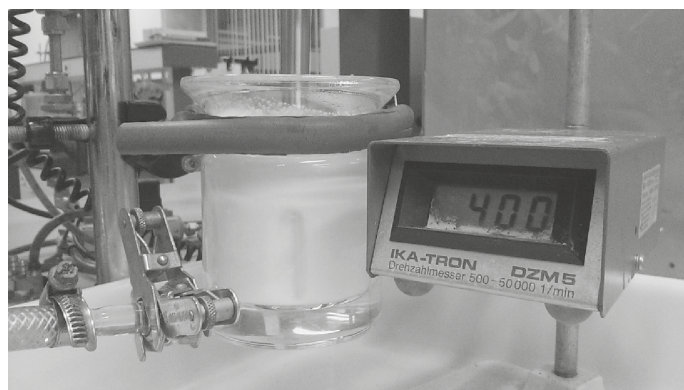
Figure 5.14 Dispersing of **SDD1** using a dissolver blade. The counter displays a RPM value of 4,000 min^{-1}. The temperature of the jacketed reactor was 50 °C.

5.4.3   Dissolver blade (XXDX)

The anhydride-modified PHUs were investigated at a larger volume by the use of a dissolver blade (Figure 5.2). Due to the limited amount of polymer available for dispersing at this scale, only one dispersion could be prepared at a solids content of 14 wt%. DMF was used to dissolve **PHU1** as it proved to be a better solvent than NMP for the PHUs ($C_{max,DMF}$ = 51 wt% *vs.* $C_{max,NMP}$ = 34 wt%). The solution of 10 gram of PHU in 8.5 mL DMF was added dropwise to 50 mL demineralized water whilst stirring.

SDD1 was a homogeneous, yellowish dispersion which did not show sedimentation (Figure 5.15). The solids content was determined using TGA analysis (Figure 5.15) and

Table 5.5 Properties of SDD1 over time.

Time	Stabi-lity[a]	Anhydride loading[b]	Neutrali-zation[c]	pH	z-average diameter nm	PSD	ζ-po-tential mV	Solids content pr. wt%	Solids content det.[d] wt%	η mPa s
0	+	0.18	1.82	7.8	1.200	0.82	-46	14.1	12.6	
19 days	+				1.510	0.95	-37			
95 days	+/-				9.100	0.53	-7			
100+ days	+/-			8.1						5.0

^{a} *+ no sedimentation observed, +/- sedimentation with stable top layer;* ^{b} *mol anhydride per mol monomer;*
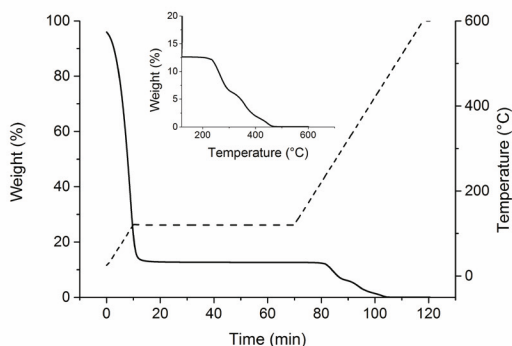^{c} *mol TEA per mol carboxylic acid group;* ^{d} *Determined by TGA analysis.*

5

Figure 5.15 *left*: SDD1 before (a) and after (b) centrifugation at increased gravity ranging from $7 \cdot 10^5$ to $1.7 \cdot 10^6$ m s^{-2}. *right*: TGA of **SDD1** (m_0 = 39 mg). After reaching a temperature of 120 °C the temperature was kept constant at this value for 60 minutes to allow for evaporation of water. The heating rate was 10 °C min^{-1}. The inset shows the conventional residual weight *vs.* temperature plot starting at 120 °C (*i.e.* after removal of the continuous water phase).

was found to amount to 12.6 wt%. Upon further heating, the TGA trace displayed the mass loss of the dried polymer which is similar to the undispersed polymer (results not shown), albeit at temperatures 10 °C lower than unused polymer. The dispersion proved to be very stable as centrifugation at 70,000 to 165,000 times gravity for 8 hours only removed a small fraction of the polymer. Figure 5.15 shows that there was almost no difference between the dispersion before and after centrifugation in terms of the scattering of light which is indicative for the concentration of particles.

The average particle size of **SDD1** was high, and the ζ-potential was well below -30 mV. However, the spread on the ζ-potential was large, indicating that particles with different surface charge density were present (Figure 5.16). After 19 days, the dispersion was measured again and the ζ-potential had homogenized. The average had increased slightly from -46 to -37 mV. Some sedimentation was observed on the bottom of the container on day 95. Over this period, the ζ-potential had increased to -7 mV. Except for some sedimentation, the dispersion was still stable. Most likely, hydrolysis of the ester bonds between the polymer and the succinate had occurred. The succinic acid can then diffuse into the liquid, decreasing the anionic stabilization.

The *z*-average particle sizes were larger than 1 μm and over time increased to 9 μm. The loss of electrostatic stabilization may cause coagulation of the particles
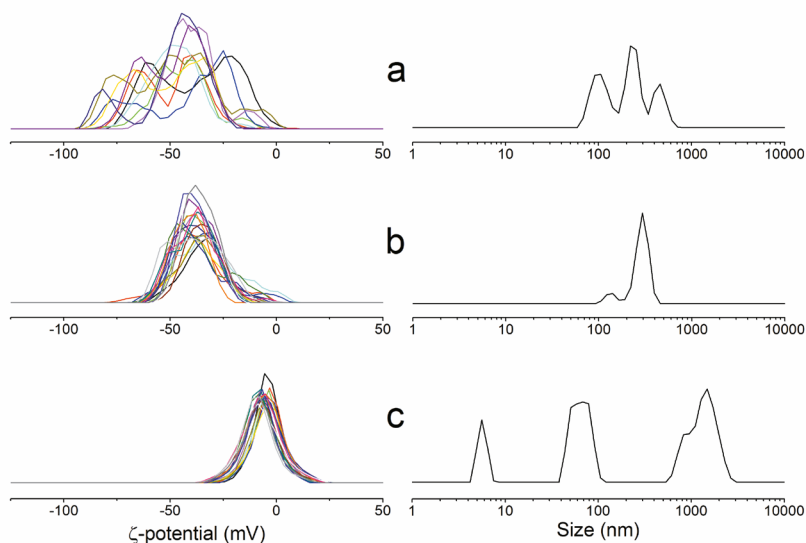
Figure 5.16   **Evolution of the *ζ*-potential (*left*) and number-averaged particle size distribution (*right*) of SDD1 in time: a) after dispersing, b) after 19 days, c) after 95 days.**

causing this large increase in particle size.

After **SDD1** became a neutral dispersion, a sample of the dispersion was dried for molecular weight analysis (see Table 5.1). The M_n value of the polymer after drying was 7,900 g mol^{-1} with a *Đ* value of 2.5, according to SEC with PS standards. This was a very similar value to the polymer prior to modification with succinic anhydride (M_n = 7,600 g mol^{-1}) and considerably higher than the polymer after modification (M_n = 4,700 g mol^{-1}). As the molecular weight difference is attributed to the change in hydrodynamic volume induced by presence of the carboxylic acids, the increase of the M_n value over time is another indication that the ester of the succinic acid was hydrolyzed over time.

The viscosity of the dispersion was measured in a rheometer using a concentric cylinder (Couette) setup with a cone and plate geometry at the bottom. The dispersion showed Newtonian behavior with a viscosity of 5.0 mPa s, which was low compared to other polyurethane dispersions reported.[6,7,13,14,25] The low solids content, large particle size, and broad *PSD* are all factors that can decrease the viscosity.

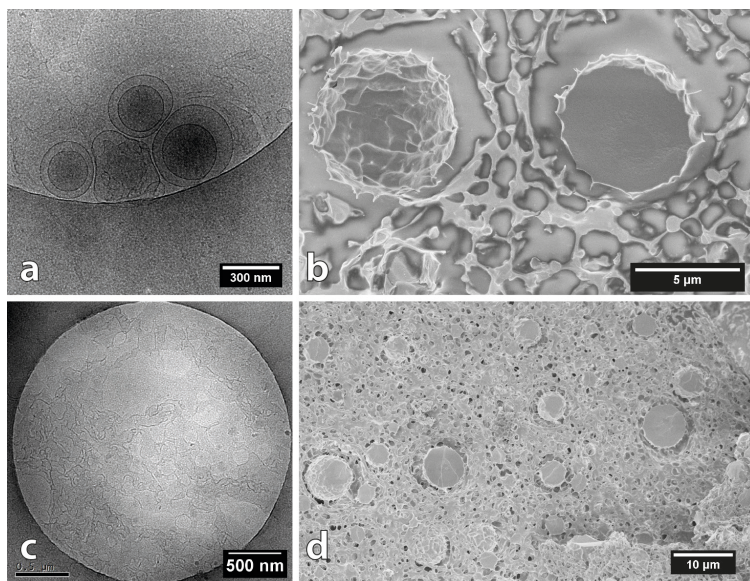Cryogenic scanning and transmission electron microscopy measurements

Figure 5.17   **Microscopy images of SDD1: a, c) Cryo-TEM after 48 days; b, d) Cryo-SEM after 125 days.**

(SEM and TEM, respectively) have been performed on **SDD1** (see Figure 5.17a and c). Cryo-TEM revealed three structures: solid particles, hollow layered particles, and an undefined structure. The solid particles were spherical and had diameters between 200 nm and 2 μm. Solid particles are darkest in the middle with decreasing intensity towards the outside of the particles. The layered particles were clearly observed as circles with diameters between 100 and 900 nm. These structures were so clearly contoured because the vesicle membrane creates the longest path length for the electron beam at the edge of the particles. Many of these particles had a smaller particle inside of them. The formation of layers indicated that the molecules in the membrane were behaving as amphiphiles. It is possible that the polymers in these layers had a blocky composition with both polar (rich in **BDA**) and apolar parts (rich in **FDA**). Phase separation of the polar and apolar phases could have resulted in the formation of polymersomes, which show these structures in TEM. This explanation is also in agreement with the DSC data of these polymers (see Figure 5.8).

An undefined structure was visible in the TEM pictures. In many parts of the sample, dark random lines were observed with darker and lighter spots. Based on the TEM images no clear interpretation could be provided. Therefore, the dispersion

128

was further examined using cryo-SEM (Figure 5.17b and d). The samples were frozen and fractured to reveal the internal composition. The sample was subjected to a sublimation treatment to remove surface water and expose the polymers before the conductive layer of tungsten was applied. The conductive layer is applied because its heavy atoms emit the secondary electrons necessary for the measurement much better than the low atomic number atoms in polymers.

The pictures from SEM show a large amount of material surrounding the solid particles that resembled a matrix. This matrix was most likely composed of polymer. No particles were observed in other parts of the sample than where this matrix was present. The particles were spherical with diameters between 2 and 8 μm. Smaller sizes may have been present but were difficult to distinguish in the matrix. Some particles were cleaved in half and the interior of the particles was exposed. The smooth surface of these fractures indicated that the particles were solid. The particles were separated from the matrix with 0.5 to 1.5 μm of 'empty' space surrounding the particles (see Figure 5.17b). This matrix is observed under cryogenic conditions for samples that have aged: 48 days for TEM, and 125 days for SEM. The multilayered particles seen in TEM, were not observed in SEM.

The cryo-SEM images resemble that of soy bean oil emulsions in a phosphate buffer with high loading of Na-caseinate as emulsifier.[44] Na-caseinate is a protein that can dissolve in water under basic conditions but precipitates in acidic environment. Droplets of oil were stabilized by aggregates of the caseinate which bridged the droplets together. If similar phenomena are occurring in the PHU dispersion, it indicates that the droplets are formed by a hydrophobic phase and the matrix by a metastable hydrophilic phase.

The length scale of the particles and matrix are such that they were in the size range of optical light microscopy. Therefore, the dispersion has been analyzed using optical microscopy on samples that were 130 days old (see Figure 5.18 and Figure 5.20). Spherical particles were observed in all pictures. The sizes observed range from 1 to 14 μm for figure a and 3 to 60 μm for figure c/d. Particles with diameters larger than 4 μm had a multilayered morphology. In measurements on samples of 1 month old, these multilayered particles were rarely observed. Flow of the liquid between the
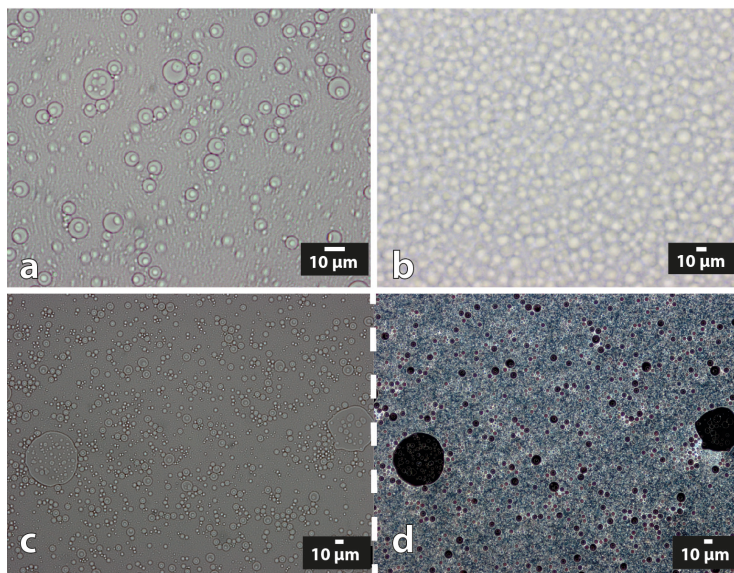
5

Figure 5.18 Optical microscopy of **SDD1** after 130 days: a) free flowing water between particles; b) region of high density of particles; c) bright field; d) dark-field optical microscopy of the same area as c.

particles was observed in live images: the small particles moved freely between the stationary large particles, most likely the large particles were fixated between the glass slide and the cover glass. When the large, multilayered particles were able to move, the inner and outer particle moved as one whole. Therefore, it was confirmed that the inner particle was indeed located inside the larger one. The presence of flow indicated that the matrix observed in cryo-SEM is an artifact of the freezing of the sample. Most likely, the polymer was dissolved in the liquid and could only be observed upon freezing and removal of the water.

In much more dense areas of the sample (b), it was observed that the particles did not fuse together to one homogeneous layer but that the particles remained separate. Comparison between bright- and dark-field images showed that the space between the particles in bright-field contained small scattering particles. The big particles show a dark interior, indicating that these particles did not contain these small particles. The outside layer behaved like a barrier. The smaller particles that resided inside the larger particles were also dark on the inside, indicating that they were hollow vesicles.

Transmission microscopy by both cryo-TEM and optical light microscopy indicated that multilayered hollow particles or vesicles were present in the dispersion.
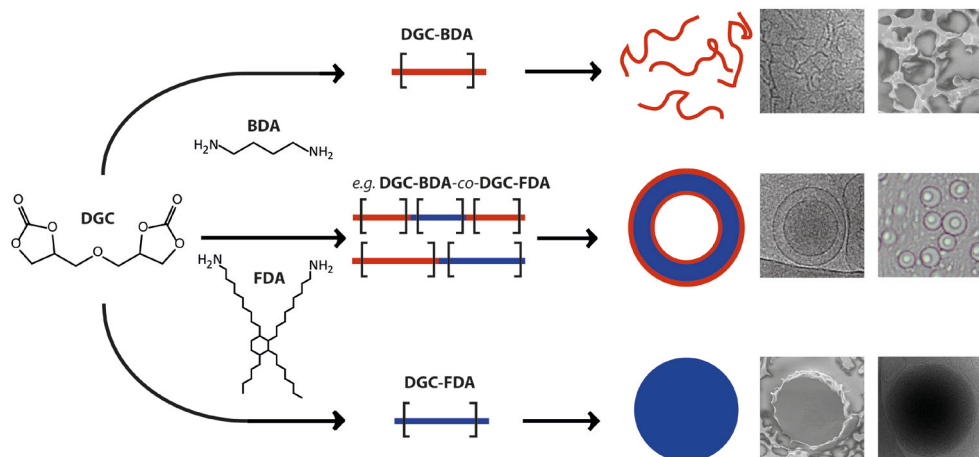
Figure 5.19　　**Graphical explanation for observed structures in cryo-TEM, cryo-SEM, and optical light microscopy.**

Only solid particles were detected in cryo-SEM. Furthermore, cryo-SEM images showed that a significant portion of the polymer was present in the surrounding water. This indicated that these polymers were too hydrophilic to form a dispersion, and dissolved in the continuous phase instead. The phase separation in the polymer as indicated by the presence of two T_g values in DSC, may provide an explanation why a part of the polymer is forming spheres, and a part dissolves in the water phase. Homopolymers of **DGC-BDA** are much more polar than **DGC-FDA** and therefore are more likely to dissolve in water. This may be enhanced by the introduced carboxylic acid groups. In **BDA**-rich segments, these are more closely spaced. This also provides an explanation for the high amount of acids required for stabilization and the low ζ-potentials obtained with this high loading. Only the fraction of acids that are on the **FDA**-rich polymers are required for stabilization of the particles. The rest is lost on the polymers that dissolved and did not add to stabilization. However, it would be expected that the viscosity of the dispersion would be much higher if the polymers dissolved.

　　Polymers that contain large segments rich in **FDA** as well as **BDA** can form structures like the bilayers that were observed. Polymers rich in **BDA** dissolved and PHU rich in **FDA** formed the solid particles. These processes have been summarized in Figure 5.19.

5

5.5 Conclusions

Poly(hydroxy urethane)s (PHU) have been synthesized from diglycerol dicarbonate (**DGC**), butane-1,4-diamine (**BDA**), and dimerized fatty acid diamine (**FDA**) for water-borne dispersion application. Electrostatic stabilization was achieved by reacting part of the hydroxyl groups on the PHU backbone with succinic or citric anhydride and neutralization of the formed carboxylic acids with triethylamine (TEA).

The dispersions were prepared with three different types of dispersing equipment: a toothed rotor-stator, a helical ribbon impeller, and a disperser blade system. The rotor-stator had high material losses in the internal parts. The helical ribbon system could produce stable dispersions with particle sizes between 200 and 5,500 nm, depending on conditions with solids contents up to 17.7 wt%. The ζ-potentials ranged from -23 to -51 mV. All dispersions had broad particle size distributions with *PSD* > 0.1.

A single dispersion was produced using a disc disperser blade at 12.6 wt%. Over time the particle size increased and the ζ-potential decreased significantly towards a neutral dispersion. The loss of ζ-potential is attributed to hydrolysis of the ester bonds. Centrifugation of the dispersion demonstrated that despite the loss of ionic stabilization most of the particles remained stable and only a small part sedimented. Analysis with cryo-TEM, cryo-SEM, and optical microscopy indicated that a large portion of the polymers was not incorporated in the particles, but was present in the water phase. Also many layered particles were observed. These results indicated that **BDA** and **FDA** have a blocky distribution along the polymers, or that there are also polymers with only one diamine incorporated . These observations are in agreement with the phase separation observed in DSC. Polymers and polymer segments that are rich in **BDA** may be hydrophilic enough that they dissolve in the water phase.

This study showed that PHU synthesized from **DGC** can be used to produce water-borne dispersions after introduction of pendent carboxylic acid groups. However, the use of fatty acid diamine and the shorter butane-1,4-diamine resulted in phase separation of hydrophilic and more apolar polymer segments.

5.6 References

(1)   Zhou, H.; Wang, H.; Tian, X.; Zheng, K.; Cheng, Q. Prog. Org. Coatings 2014, 77 (6), 1073–1078.

(2)   Lijie, H.; Yongtao, D.; Zhiliang, Z.; Zhongsheng, S.; Zhihua, S. Colloids Surfaces A Physicochem. Eng. Asp. 2015, 467, 46–56.

(3)   Noble, K.-L. Prog. Org. Coatings 1997, 32 (1-4), 131–136.

(4)   Kim, B. K. Colloid Polym. Sci. 1996, 274 (7), 599–611.

(5)   Manvi, G. N.; Jagtap, R. N. J. Dispers. Sci. Technol. 2010, 31 (10), 1376–1382.

(6)   Nanda, A. K.; Wicks, D. A.; Madbouly, S. A.; Otaigbe, J. U. J. Appl. Polym. Sci. 2005, 98 (6), 2514–2520.

(7)   Hourston, D. J.; Williams, G. D.; Satguru, R.; Padget, J. C.; Pears, D. J. Appl. Polym. Sci. 1999, 74 (3), 556–566.

(8)   Sherman, P. In Industrial rheology with particular reference to foods, pharmaceuticals, and cosmetics.; Academic Press: London, 1970; pp 97–184.

(9)   Hanaor, D.; Michelazzi, M.; Leonelli, C.; Sorrell, C. C. J. Eur. Ceram. Soc. 2012, 32 (1), 235–244.

(10)   Urban, K.; Wagner, G.; Schaffner, D.; Röglin, D.; Ulrich, J. Chem. Eng. Technol. 2006, 29 (1), 24–31.

(11)   Grendele, E.; Galvagni, M. Imatinib mesylate preparation procedure. EP2546247, 2012.

(12)   Athawale, V. D.; Nimbalkar, R. V. J. Am. Oil Chem. Soc. 2010, 88 (2), 159–185.

(13)   Bullermann, J.; Friebel, S.; Salthammer, T.; Spohnholz, R. Prog. Org. Coatings 2013, 76 (4), 609–615.

(14)   Philipp, C.; Eschig, S. Prog. Org. Coatings 2011, 74 (4), 711–705.

(15)   Lu, Y.; Larock, R. C. Biomacromolecules 2008, 9 (11), 3332–3340.

(16)   Athawale, V. D.; Nimbalkar, R. V. J. Dispers. Sci. Technol. 2011, 32 (7), 1014–1022.

(17)   Rix, E.; Ceglia, G.; Bajt, J.; Chollet, G.; Heroguez, V.; Grau, E.; Cramail, H. Polym. Chem. 2015, 6, 213–217.

(18)   Chang, C.-W. W.; Lu, K.-T. T. Prog. Org. Coatings 2012, 75 (4), 435–443.

(19)   Saetung, A.; Kaenhin, L.; Klinpituksa, P.; Rungvichaniwat, A.; Tulyapitak, T.; Munleh, S.; Campistron, I.; Pilard, J.-F. F. J. Appl. Polym. Sci. 2012, 124 (4), 2741–2752.

(20)   Gogoi, S.; Karak, N. ACS Sustain. Chem. Eng. 2014, 141112145942008.

(21)   Li, Y.; Noordover, B. A. J.; van Benthem, R. A. T. M.; Koning, C. E. Eur. Polym. J. 2014, 52, 12–22.

(22)   Li, Y.; Noordover, B. A. J.; van Benthem, R. A. T. M.; Koning, C. E. Eur. Polym. J. 2014, 59, 8–18.

(23)   Chen, R.; Zhang, C.; Kessler, M. R. RSC Adv. 2014, 4 (67), 35476–35483.

(24)   Tramontano, V. J.; Thomas, M. E.; Coughlin, R. D. Technology for Waterborne Coatings; Glass, J. E., Ed.; ACS Symposium Series; American Chemical Society: Washington, DC, 1997; Vol. 663.

(25)   Blank, W. J. Formulating Polyurethane Dispersions; Norwalk, CT, 1996.

(26)   Blank, W. J.; Tramontano, V. J. Prog. Org. Coatings 1996, 27 (1-4), 1–15.

(27)   Blank, W. J. In Proceedings of the 17th Water-Borne and Higher Solids Coatings Symposium; University of Southern Mississippi: New Orleans, LA USA, 1990; pp 279–291.

(28)   Repta, A. J.; Higuchi, T. J. Pharm. Sci. 1969, 58 (9), 1110–1114.

5

(29)   Repta, A. J.; Higuchi, T. J. Pharm. Sci. 1969, 58 (4), 505–506.

(30)   Yoshimura, T.; Matsuo, K.; Fujioka, R. J. Appl. Polym. Sci. 2006, 99 (6), 3251–3256.

(31)   Liu, C. F.; Sun, R. C.; Zhang, A. P.; Ren, J. L.; Wang, X. A.; Qin, M. H.; Chao, Z. N.; Luo, W. Carbohydr. Res. 2007, 342 (7), 919–926.

(32)   Xiao, B.; Sun, X. F.; Sun, R. Polym. Degrad. Stab. 2001, 71 (2), 223–231.

(33)   Chatterjee, S.; Clingenpeel, A.; McKenna, A.; Rios, O.; Johs, A. RSC Adv. 2014, 4 (9), 4743–4753.

(34)   Schroeder, H.; Palmer, D. A. Formation, purification and recovery of phthalic anhydride. US421505, 1980.

(35)   Mahmoud, E.; Lobo, R. F.; Watson, D. Green Chem. 2014, 16 (1), 167–175.

(36)   Zeikus, J. G.; Jain, M. K.; Elankovan, P. Appl. Microbiol. Biotechnol. 1999, 51 (5), 545–552.

(37)   Bechthold, I.; Bretz, K.; Kabasci, S.; Kopitzky, R.; Springer, A. Chem. Eng. Technol. 2008, 31 (5), 647–654.

(38)   Potter, M. J.; Gilson, M. K.; McCammon, J. A. J. Am. Chem. Soc. 1994, 116 (12), 10298–10299.

(39)   Tung, L. A.; King, C. J. Ind. Eng. Chem. Res. 1994, 33 (12), 3217–3223.

(40)   Britton, H.; Robinson, R. J. Chem. Soc. 1931, No. 1456, 1456–1462.

(41)   Ripin, D. H.; Evans, D. A. Evans pKa table http://evans.harvard.edu/pdf/evans_pKa_table.pdf (accessed Apr 10, 2015).

(42)   Tan, H. L.; Feindel, K. W.; McGrath, K. M. Soft Matter. 2010, p 3643.

5

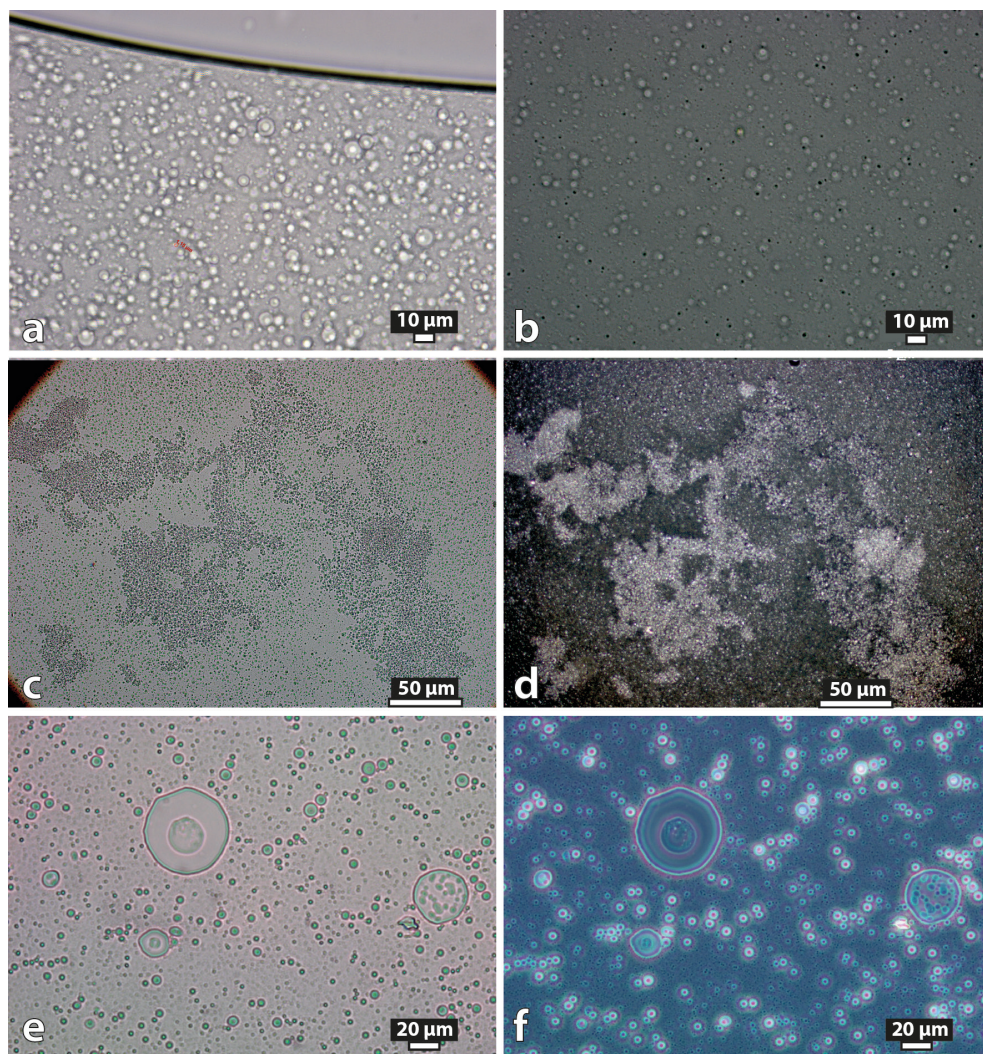## 5.7 Additional figures

Figure 5.20   Optical microscopy of **SDD1** of: a) dispersion after 1 month; b) top layer after 95 days; c) bottom layer after 95 days (bright field); d) bottom layer after 95 days (dark field); e) bright-field of bottom layer after 130 days; f) dark-field optical microscopy of the same area as e.

Chapter 6

Technology assessment

6.1 Introduction

This dissertation focuses on the development of bio-based polyamides and non-isocyanate polyurethanes. The motivation is to provide a bio-based alternative for several polymers that are now produced from petroleum-based sources. Several interesting bio-based diamines are expected to come to the market within a few years and have therefore been included in the study: the short linear diamines butane-1,4-diamine and pentane-1,5-diamine, cyclic sugar-based isoidide and isosorbide diamine, and long-chain dimerized fatty acid diamine (see Figure 1.14). These monomers are suitable to be used in both polyamide and polyurethane synthesis.

The main application area for which the polyamides and polyurethanes have been developed, is the coatings industry as it relies heavily on crude oil as its feedstock. The dominant trend in coating applications the past decades is to reduce volatile organic components. To achieve this, water-borne and solvent-free systems have been developed in the past. The resins used in these types of coatings have to meet requirements, *e.g.* degree of crystallinity and the value of the glass transitions temperature (T_g). Based on these requirements, it is expected that polyamides can perform well in powder coating applications as chain-rigidity is important. The non-isocyanate polyurethanes can be very interesting for water-borne polyurethane dispersions. In this chapter, the usability of these bio-based polymers as coating materials is discussed based on the results described in this dissertation.

6.2 Main conclusions and recommendations

6.2.1 Powder coatings resins from polyamides

The resins presented in this dissertation are based on amorphous polyamides synthesized from bio-based monomers. A series of amorphous polymers based on the fatty acid dimer was made, but the glass transition temperatures of these resins were far too low for powder coating application. The T_g values were found to lie between -10 and 0 °C, a range which is more suitable for *e.g.* adhesives or solvent-borne coatings applications.

The polyamides synthesized from pimelic acid in combination with isoidide diamine and butane-1,4-diamine showed T_g values up to 103 °C, depending on the exact composition, in combination with a low degree of crystallinity. This is suitable for powder coating resins. Some remarks about the synthesis of these isoidide diamine containing polyamides have to be made. Preferably, a salt is produced from the diacid and the diamine. Salts have an equimolar ratio of complementary reactive groups, which is a prerequisite to achieve high molecular weights, and the synthesis of salts adds a purification step of the monomers. However, preparation of the salt of pimelic acid and isoidide diamine proved difficult due to solubility issues. The solubility of the salt was too close to that of the respective monomers. Even prolonged crystallization times at low temperatures didn't produce PA salt crystals with more than 20% yield of the expected amount. Therefore, the salt route was abandoned and the reactants were used as received.

The reaction was started with methanol present to solubilize the monomers and form the salt in-situ upon drying. Dissolving the monomers was also required by the dimensions of the laboratory reactor (see Figure 2.1), the double helical impeller could not be fitted when the monomers were still solid. This is not necessary on industrial scale. The removal of the methanol increased the reaction time.

The reactions were performed in an inert atmosphere because the diamines can react with CO_2, and **IIDA** is oxygen-sensitive when heated. The presence of oxygen leads to severely colored products. The flow of inert gas from the reactor to the condenser setup was optimized to minimize the loss of evaporated monomers. These losses affected the stoichiometric balance and hence the molecular weight of the resulting polymers.

The rheological experiments indicated that curing at 150 °C was insufficient to complete the cross-linking of the polyamides developed in Chapter 2 with both triglycidyl isocyanurate (TGIC) and *N,N,N',N'*-tetrakis(2-hydroxyethyl)adipamide (Primid XL-552). The formulations with TGIC approached industrial cycle times the closest, while Primid showed poor performance in combination with these resins. Reported curing times for Primid-polyester resin mixtures are in the order of ten minutes at 200 °C. Most likely, the removal of water as a condensate from the reaction

6

with Primid was a limiting factor.

Unfortunately, because of the limited availability of the monomers, no powder paint could be produced and tested. Therefore, solvent-borne application was used to produce coatings on aluminum panels. The surfaces of the coatings were very rough due to poor wetting of the substrate. Two coatings showed reasonable wetting. However, cratering was observed. Dewetting and cratering are phenomena leading to defects. These occur when a paint with a high surface tension comes into contact with a surface (dewetting) or particles (cratering) with a low surface tension. When these materials become available in sufficient quantity for powder paint application, the surface tensions of the solvent-borne system and the powder paint have to be determined. If necessary, the molecular composition could be adjusted by replacing **BDA** by other monomers to reduce the surface energy. In contrast to the experiments using the rheometer, compositions with Primid produced the best looking coatings. This is a confirmation that the removal of water affected the experiments with the rheometer.

The hardness, toughness, and solvent-resistance of the coatings depend on the cross-link density and the molecular structure of the resin. Tests of these properties resulted in variable successes. One resin-curing agent combination, *i.e.* **B1** cured with TGIC, could form a sufficiently dense network, while the other combinations of resin and cross-linker were loosely cross-linked. One area that still should be explored to improve the performance is increasing the functionality of these resins. A small amount of a multifunctional monomer, *e.g.* tris(2-aminoethyl)amine or citric acid, should be incorporated in the recipe.[1] Increasing the functionality of the resin will increase the network density in the resulting cured coating. This is essential for the Primid-based formulations as the Primid-based formulations reported in Chapter 3 performed poorly due to insufficient network formation. Primid is the preferred curing agent because of environmental reasons.

Overall, the appearance of the resulting coatings leaves room for improvement. The polymers will require additives to enhance the flow and reduce the surface tension. The formulation of a powder paint to include flow agents is common practice. After increasing the resin functionality, these polymers are still very interesting to

test on a larger scale as resin in powder paint.

6.2.2 Water-borne dispersions of poly(hydroxy urethane)s

The polymers reported in Chapter 4 were amorphous, non-isocyanate poly(hydroxy urethane)s (PHU), prepared from diglycerol dicarbonate (**DGC**). They were produced in bulk conditions at mild temperatures, without a catalyst. The conversion was higher than 95% for all compositions after 5 hours of reaction time at 80 °C. The temperature of the reaction was not very high but still required a lot of energy. This temperature is necessary to melt all the monomers. Catalyzing the reaction with triazabicyclodecene (TBD) could shorten the reaction time and decrease the energy consumed.[2] Note that when carboxylic acid-functional monomers are included to stabilize dispersions, TBD cannot be used as it forms a complex with carboxylic acids. We have used TBD in our laboratory using solution synthesis at room temperature to achieve similar molecular weights as obtained for melt polymerization. No other catalysts have been reported that can compete with TBD. The molecular weights of the poly(hydroxy urethane)s were rather low, compared to values reported in literature.[2–4] Loss of diamine was observed, leading to cyclic carbonate terminated polymers. Therefore, the composition of the reaction mixture should be tuned, or controlled during reaction to achieve higher M_n values.

The choice of diamines allowed for a broad range of T_g values for the resulting polymers. This makes the polymers suitable for more applications besides water-borne coatings. All polymers were amorphous due to the random distribution of segments that had opened to either a primary or a secondary hydroxyl group along the chain. The high hydroxyl value of PHU makes the polymer predominantly polar. This typically results in good adhesion to metal substrates and good compatibility with biomaterials. The large amount of hydroxyl groups can also be used to attach other molecules or perform cross-linking on the material.

Polyurethane dispersions are particles of polyurethane suspended in water. Commercial isocyanate-based polyurethanes contain dimethylolpropionic acid (DMPA) for anionic stabilization. DMPA is not bio-based and its hydroxyl functionality cannot react with the other monomers. Few bio-based diamines that also bear

6

a carboxylic acid group and which can replace DMPA, are available. One of these molecules is *L*-lysine, which has been tested for NIPU synthesis but no polymers could be obtained. The lysine acted as a chain stopper because the amine functionality in the *β*-position showed no reactivity towards cyclic carbonates. Alternatively, anhydrides were reacted with the hydroxyl groups of the PHU. This forms an ester and a carboxylic acid group. The carboxylic acid groups are neutralized with triethylamine. Over time the ester hydrolyzed and the dicarboxylic acid was released from the polymers. Therefore, the use of anhydrides to add carboxylic acid-functionality to the hydroxyl groups on the polymer is not an ideal option for water-borne applications.

The hypothesis at the start of the project was that the hydroxyl groups formed during the polymerization would support the water dispersibility through the increased hydrophilicity. The microscopy study showed that the polymers had become too polar, leading to partial dissolution into the aqueous phase. This was attributed to the use of **BDA** in the polymers. **BDA** is a short diamine which was most likely insufficiently apolar to counteract the polar diglycerol section. The attachment of the acid groups on these polymers increased the polarity even further. The reaction between the anhydrides and the part of the polymers that dissolved upon dispersing, decreased the amount of stabilizing groups available for the apolar polymers and hence the surface charge was lower than expected. In order to produce stable dispersions, the polarity has to be decreased by incorporating longer chain diamines to prevent the polymers from dissolving in the aqueous phase. Furthermore, the degree of ionic stabilization has to be increased. The best approach to enhance stabilization would be the development of a bio-based internal emulsifier that is incorporated into the backbone of the polymer. The bond would not be labile and does not require an additional step during synthesis. An example could be citric acid modified with two glycerol carbonates or with two diamines.

Due to the phase separation caused by **BDA** and **FDA**, polymers with different polarities were obtained. The poly(hydroxy urethane)s rich in **FDA**, *i.e.* **DGC-FDA**, could potentially be used as components in conventional PUDs, or even completely replace the conventional polymers if the stabilization issue is solved. Their increased hydrophilicity could help to stabilize the hydrophobic polyurethanes. Partial cross-

6

linking between the hydroxyl groups and the isocyanates can occur but isocyanates would still preferably react with the diamines for chain extension. Upon drying, the added hydroxyl groups in the PHUs may enhance the adhesion onto polar surfaces like metals.

The amphiphilic polymers with **BDA**- and **FDA**-rich segments can find use in polymersomes. Polymersomes are vesicles that can be loaded with a solute, *e.g.* a medical drug. The membrane formed by the block-copolymers would have to be investigated, particularly in terms of the barrier properties and the thermal stability of the membrane. Toxicity tests may be carried out to test these structures for biomedical applications. In these cases, the use of DMF to prepare the solutions is not an option.

Finally, it is possible to synthesize any of the PHUs of Chapter 4 with amine-functional end-groups. These can potentially be used as chain extenders for conventional PUDs. They would decrease the petroleum-based content and add the enhanced adhesion of the hydroxyl groups. These PHU cannot bear carboxylic acids through anhydride modification as the anhydrides would preferably react with the amines instead of the hydroxyl groups. This is beneficial as the polymers are more likely to enter the particles than to dissolve into the water phase.

6.2.3   Practical considerations

Working with these non-commercial bio-based materials posed some additional challenges. Specifically for these type of polymers, the solubility of the polymers in suitable solvents proved difficult. This affected liquid-based analysis techniques like NMR, as well as the synthesis of polyamide salts, and dissolving the polymers during application of coatings or for dispersing. These issues required the use of harmful and undesirable solvents like DMAc, DMF, NMP, and HFIP.

Another point of attention is the quantity and purity of the monomers available. Unfortunately, some batches of **IIDA** resulted in M_n values of 700 g mol^{-1} while other batches could be polymerized to reach 3,000 g mol^{-1}. This indicated that working in small scale batches can give variations in purity. To avoid these issues, high purity of the monomers is very important. However, this is not always easy because biomass is harvested as a mixture of many compounds. Therefore, separation technology is a

6

crucial first step in the bio-based industry. A second one is the use of catalytic routes with high selectivity, conversion, and yield. These are a necessity to compete with the current highly developed petroleum-based industry. The amount of non-commercial monomer that was available in this project guided the experiments towards an exploratory approach.

In small scale syntheses, effective mixing of a reaction mixture is not trivial. A half-moon stirrer is a commonly used reactor setup. However, on smaller scales this stirrer will not mix the monomers properly but rather spread them onto the reactor wall. Therefore, the helical ribbon impeller was designed and custom made (see Figure 2.1). This stirrer allowed for effective mixing of the reactants. It did have two major drawbacks: the tight-fitting setup did not allow for sampling without losing material, and the steel shaft attached to the impeller removed a significant amount of heat from the reaction mixture. On several occasions, the latter issue resulted in a too viscous reaction melt, upon which the melt retracted into the stirrer and lost contact with the reactor wall. Heating could be improved by using infra-red heating as this removes the necessity for contact. As samples could not be obtained during the reaction, the conversion could not be followed and a possible stoichiometric imbalance could not be corrected for. This led to moderate average molecular weights obtained for the polymers.

The synthetic procedures in this thesis were compared to those of current industrial resins in a study performed within the funding organization, *i.e.* project BPM-181 SUSTAIN.[5] One observation from this project was that the production of poly(hydroxy urethane)s had a comparable environmental impact as common polyurethanes. Furthermore, it was clear that the processes described in this thesis could be further optimized by introducing a catalyst to reduce the energy consumption. This is a promising result for these materials. For the polyamide resins this achievement was unfortunately not matched. The production of the monomers consumes too many resources at this moment. This confirms the need for highly efficient conversion strategies from biomass to monomer, for example through a biorefinery approach.

The results presented in this dissertation show that bio-based alternatives for coating resins in powder coatings can be produced. The developed poly(hydroxy

urethane)s are not yet in a competitive position to function in polyurethane dispersions. To achieve this, an emulsifier will have to be developed that can be incorporated into the polymer chain. In conclusion, this work shows the feasibility of bio-based polyamides and non-isocyanate polyurethanes to function as coating resins.

6.3 References

(1)   Noordover, B. A. J.; Duchateau, R.; van Benthem, R. A. T. M.; Ming, W.; Koning, C. E. Biomacromolecules 2007, 8 (12), 3860–3870.

(2)   Lambeth, R. H.; Henderson, T. J. Polymer 2013, 54 (21), 5568–5573.

(3)   Sheng, X.; Ren, G.; Qin, Y.; Chen, X.; Wang, X.; Wang, F. Green Chem. 2015, 17 (1), 373–379.

(4)   Kihara, N.; Endo, T. J. Polym. Sci. Part A: Polym. Chem. 1993, 31 (11), 2765–2773.

(5)   Haaster, B. van; Shen, L. BPM181 TECHNICAL PROGRESS REPORT 2014; 2014.

6

Curriculum vitae

Juliën van Velthoven attended secondary education at the St.-Odulphuslyceum in Tilburg from which he graduated in 2002.

He did his bachelor's studies in Chemical Engineering and Chemistry at Eindhoven, University of Technology. Subsequently he obtained his MSc. degree in Molecular Engineering from the same university in 2009. During his masters he worked on liposomal MRI contrast agents within Philips Research, and wrote a master's thesis about his research on the supramolecular self-assembly behavior of large chiral disc shaped molecules in the group of prof.dr. E.W. Meijer.

In 2010, he started his doctoral studies in the Laboratory of Polymer Materials at the Eindhoven University of Technology, under the supervision of dr.ir. B.A.J. Noordover and prof.dr. J. Meuldijk. In this project, the development of novel bio-based coating resins for both powder coatings and water-borne coatings was targeted. The results of this work are presented in this dissertation.

Acknowledgements

On these pages I would like to thank everyone that helped me to finish my PhD and that made my stay in SPC, SPM, and again SPC such an enjoyable period in my life. Five years full of memories of coffee and lunch breaks, group trips, the TU/e meerkamp, movie nights, lunch BBQs. They were all really nice. Thank you all!

Bart, heel erg bedankt voor je begeleiding deze jaren. Je hebt er veel aan bijgedragen om dit boekje gereed te krijgen. Ondanks veel organisatorische moeilijkheden door de jaren was je de stabiele factor die ik nodig had om de focus te houden. Ik heb veel van je geleerd in deze tijd.

Beste Jan, je kwam pas later in mijn project. Maar je was heel enthousiast gedurende de jaren. Je wist telkens weer nieuwe motivatie te brengen. Vooral je passie voor organische chemie was erg fijn om te zien. Heel veel dank dat je mijn promotor bent.

I would like to thank prof. Katja Loos, dr. Anja Palmans, prof. Rolf van Benthem, and prof. Henri Cramail for taking part in my reading and defense committee. I also much appreciate your comments to improve this dissertation.

Ik wil Daan van Es graag bedanken voor de goede samenwerking de laatste jaren. Ik ben blij dat je dit wilt afronden door in mijn promotiecommissie plaats te nemen. Veel van de dingen in dit proefschrift waren niet mogelijk zonder de materialen die jullie vanuit Wageningen opstuurden. Ook wil ik Linda Gootjes bedanken voor de moeite die je er elke keer in hebt gestopt om zo goed mogelijke monomeren te sturen.

Ik wil Cor Koning bedanken voor de mogelijkheid in deze groep te starten. Helaas moest je binnen een jaar het project verlaten door je overstap naar DSM. Dat vond ik heel erg jammer maar zo lopen dingen soms. Daarnaast wil ik Alex van Herk bedanken dat hij op wilde treden als nieuwe promotor. En natuurlijk ook bedankt in de tijd dat je mijn huisbaas bent.

I want to thank the BPM consortium and its partners for making this project possible. I also want to thank Gerda, Li Shen, Harald, Pierre, and Richard for the discussions we had about the project.

Of course I want to thank everyone in my office and on the labs for their help and discussions. I've learned a lot and I hope I could also help you. I hope I don't miss a name in this long list of all the people around me: Bahar, Benny, Camille, Chunliang, Cristina, Dirk, Doğan, Donglin, Ece, Elham, Erik, Evgeniy, Fabian, Ferdi, Geert, Gemma, Gijs, Gözde, Hao, Hector, Hemantkumar, Inge, Ioannis, Jack, Jan-Henk, Jerome, Jey, Jing, Joice, Joris, Judith, Karel, Lidia, Lily, Lyazzat, Mark B, Mark P, Martin O, Mischa, Mohammad, Monique, Olessya, Peter, Pim, Pooja, Raf, Seda, Shaneesh, Shuang, Silvia, Stefan, Suguru, Syed, Tamara, Timo, Vamsi, Yanwu, Yingyuan, and Yun.

I also want to thank all the people that kept equipment working and helped me with the analyses of my materials: Anne, Anneke, Carin, Hanneke, Ingeborg, Marco, Martin F, Pauline, and Rinske. Also Pleunie, Caroline, and Leontien deserve a place here. Heel erg bedankt voor alle hulp en gezelligheid en snoepgoed.

Also some people outside of the group helped me throughout the years. Oana, thank you for your help with the press so I could make the rheology samples. Marcel Giesbers took the cryo-SEM pictures. Various people at MST and SyMO-Chem for their help with the NMR. Especially Serge showed me many useful things.

My students Özlem and Joren, thank you for your work. Unfortunately the results didn't end up in this work but I learned a lot from supervising you both. I wish you all the best for the future.

Lily, the past 3 years we've shared an office and lab together and it was a great time. You are kind but you also pushed me when I needed it. I'm grateful for that. And Cristina, the last year you've given me a lot of useful advices on the final experiments and on writing the articles and this thesis. I'm glad that you both will accompany during the defense.

Andrew, Bea, Enikő, Kinga, Kristina, Thaíssa, and Vivian. What would a conference be without you? I had great times in Siófok and Chiang Mai. I hope that we can meet each other again soon.

Then I would like to thank my friends for the good times outside of work. Enjoying the ice, having beers, board games, dinners, weekendjes, and much more. Aleksandra, AnnA en Bram, Anna-Catharina en Matthijs, Arjo, Ivo en Sandra, Joep, Maartje en Rom, Marjolein, Martijn en Tess, Meilof en Marleen, Patrick en Müge, Roderigh, Ron, Sven en Thirsa, Tom, thank you so much for the much needed relaxing.

Ik wil natuurlijk ook mijn familie bedanken voor hun steun de afgelopen jaren. Pap en mam, ik weet dat ik altijd op jullie kan rekenen.

Giulia, I'm so happy that you decided to come to the cold Paesi Bassi and that our paths crossed each other. Spero di poter passare molto del nostro futuro insieme.